8-31-2017

Multiple Modes of Hepcidin Regulation in Breast Cancer

Nicole Farra
University of Connecticut - Storrs, nblanchette@uchc.edu

Multiple Modes of Hepcidin Regulation in Breast Cancer

Nicole Lynne Farra, Ph.D.

University of Connecticut, 2017

Abstract

Iron is an essential nutrient for normal cellular functioning, but excess iron retention is a hallmark of breast cancer, used to fuel cancer cells proliferative demands. Breast cancer cells alter genes that control iron metabolism to promote accumulation of cellular iron. One way breast cancer cells retain iron is through decreased iron export. Breast cancer cells have reduced expression of the iron efflux pump, ferroportin (FPN). FPN is reduced by the iron regulating peptide hepcidin, which binds to FPN and triggers its degradation, resulting in decreased iron export. Hepcidin is elevated in breast cancer to promote accumulation of cellular iron. However, the pathways responsible for elevated hepcidin in breast cancer cells have never been investigated.

In this thesis we utilize several culture methods to examine the full spectrum of hepcidin regulation in breast cancer including two- and three-dimensional culture of established cell lines and primary breast cells, as well as co-culture systems with stromal cells. Ultimately, we reveal a complex hepcidin regulatory network involving protein molecules and spatial cues, consisting of changes at the cellular, dimensional and microenvironmental levels. Specifically, we found regulation of hepcidin by ligands including bone morphogenetic proteins (BMPs), interleukin-6 (IL-6) and growth-differentiation factor-15 (GDF-15) in an autocrine and paracrine fashion, as well as novel regulation by the microenvironment, specifically by contribution of tumor associated fibroblasts and extracellular matrix proteins. Additionally, we reveal global changes in iron metabolism in breast cancer spheroids and that targeting enhanced iron levels present in spheroids results in disaggregation and spheroid cell death. Thus, targeting iron in breast tumors may be an attractive molecular strategy for selective killing of breast cancer cells.

Multiple Modes of Hepcidin Regulation in Breast Cancer

Nicole Lynne Farra

B.S., Hofstra University, 2012

Ph.D., University of Connecticut, 2017

A Dissertation

Submitted in Partial Fulfillment of the

Requirements for the Degree of

Doctor of Philosophy

at the

University of Connecticut

2017

APPROVAL PAGE

Doctor of Philosophy Dissertation

Multiple Modes of Hepcidin Regulation in Breast Cancer

Presented by

Nicole Lynne Farra, B.S.

Major Advisor

_____

Suzy V. Torti

Associate Advisor

_____

Kevin P. Claffey

Associate Advisor

_____

Ann E. Cowan

Associate Advisor

_____

Christopher D. Heinen

University of Connecticut
2017

Acknowledgements

First off, I would like to thank my mentor Dr. Suzy Torti, for giving me the opportunity to work on this thesis project. Suzy gave me the independence and flexibility to mold this project, which ultimately led me down a new and exciting path of understanding iron metabolism in spheroid culture. For the past five years, Suzy has supported me in my work in the lab and beyond. Understanding that my career goals are more geared towards teaching, she allowed me to take some time away from my thesis work to mentor students in the lab as well as outside of the lab in a classroom setting, and for that I am extremely grateful. It is through her consistent support and guidance that I feel prepared to enter the world as an independent scientist and successful teacher.

I would also like to thank Dr. Frank Torti, who has been an additional mentor during my graduate career. During our weekly meetings, Frank always made sure I could take a step back from experiments and see the big picture. This is something that can easily get overlooked with the details of experiments clouding the big picture at hand. Frank taught me how to always have the full story in the back of my mind and not lose sight of the main questions. He was always there providing advice for experiments and how to interpret results when they weren't what I had anticipated. Frank's creativity and passion for science has always inspired me, and I hope to emulate his passion in my career as a scientist and teacher.

In addition to my mentors, I am forever thankful for the members of the lab, both past and present. I would like to thank Lia Tesfay, who took me under her wing when I was rotating in the lab and continued to provide her guidance over the past five years. She is my lab sidekick, always helping me plan and analyze my experiments, and through our years in the lab together, Lia has become one of my dearest friends. I'd also like to thank Dave Lemler and Anna Konstorum for their help with the biostatistics portion of my thesis. They took the time out of their busy schedules and their own work to teach me the basics (and beyond) of microarray

and pathway analyses, a topic that was completely new to me to start. I'd also like to thank Erica Lemler, who was an integral part of our lab for 4 years, making sure our lab was always organized and running smoothly, and is a true friend. Additionally, thanks to Zhiyong Deng, David Manz and Bibbin Paul, who have all been supportive during my time in the lab and offered their help and guidance when needed.

I'd also like to thank my committee members, Dr. Chris Heinen, Dr. Kevin Claffey and Dr. Ann Cowan for their incredible support over the past five years. From my preliminary exam until now, I have always felt like they truly cared about my thesis work and my career goals. They have provided me with endless advice, both experimentally and personally, and I truly enjoyed my yearly committee meetings with them. Although intimidating at first, I really looked forward to the discussions and difference of opinions they had regarding my work or the field, which has taught me how to fight for my work and myself as a scientist. Over the past few years, I went from being insecure in my work, to sticking up for my results and confidently explaining why I thought differently. Taking a step back I now realize that they were preparing me to be a confident and successful scientist, as there will always be critics of your work. I truly thank them for their commitment to my education and thesis throughout the years.

Additionally, there a few others that I'd like to thank from Uconn Health. I'd like to thank Dr. Kim Dodge-Kafka for her continuous support and advice over the years. She's been a true role model and has always given me guidance whenever I needed it. I would also like to acknowledge all MBB faculty for their input and questions during my numerous presentations over the years. Thank you to Jen Gilman, Bridget Clancy-Tenan and Pat Schultz for their administrative help throughout. I'd like to thank Dr. Stephen Crocker, my first rotation mentor, who remained a prominent mentor and friend throughout my graduate studies. Thanks for always giving your honest advice and providing me with a few laughs over the years. I'd also like to give a big shout-out to Lucy and Liz at the Office of Research Safety for the numerous

walks to the basement irradiator until I was finally approved to go unescorted. You've been my entertainment and friends throughout stressful days of experiments.

In addition to everyone at Uconn, I could not have completed my thesis without the tremendous support from my family and friends. I could not thank my parents enough for their continued support and guidance throughout the years. They have been always been engaged throughout my graduate studies, trying to understand the scientific work I do and always so proud even if they don't understand the topics fully. They have always encouraged me to follow my dreams and I'm forever indebted to them for their help, guidance and support.

Additionally, I am forever thankful to my husband, Matt, who has supported me every step of the way. After my first year of graduate school, Matt decided to go to law school part time along side working a full time job. Not only was he working 40 hours a week, but he made the hour drive to Springfield, MA and back three nights a week, returning some nights at 11pm. Anytime that I felt overwhelmed or too busy, I always looked at what he was able to accomplish with work and school and that motivated me to keep up my momentum and push through. We leaned on each other throughout our graduate studies and made quite the team, supporting each other to attain our career goals. With Matt having just graduated from law school, it's nice to see our hard work and dedication paying off and obtaining our graduate degrees together. He's truly my rock and through our mutual understanding and support of one another, I'm excited to see what life has in store for us throughout our journey together.

In addition to my husband and parents, I'd also like to thank my brother, John, my sister-in-law Grace and my nephews Andrew and William, who always provided me with positive words of encouragement or even a few baby pictures and videos to distract me from my studies. Thank you to my grandmother, who has always encouraged me to follow my dreams and is always there to provide me with some laughs. I'd also like to thank my in-laws, Jerry and Donna and my in-law triplet siblings, Jennifer, Eric and Tyler for always supporting me and keeping me grounded. Lastly, thank you to all of my friends, especially Krystina, Kasey, Emily, Jaclyn and

Jenn who continue to be my life-long friends, supporting me on this journey and wherever it takes me next. You all keep me sane and not too serious and I'm so lucky to have such amazing friends to go through life with.

Table of Contents

List of Figures

List of Tables

List of Abbreviations

2D	Two-dimension
3D	Three-dimension
BC	Breast cancer
BMP(s)	Bone morphogenetic protein(s)
rBMP(s)	Recombinant bone morphogenetic protein(s)
BMPRE	Bone morphogenetic protein responsive element
CR	Conditional reprogramming
DCIS	Ductal carcinoma in situ
DCYTB	Duodenal cytochrome B
DMT1	Divalent metal transporter 1
EPO	Erythropoietin
HEPH	Hephaestin
HER2	Human epidermal growth factor receptor 2
HFE	Hemochromatosis protein
HH	Hereditary hemochromatosis
HIF1α	Hypoxia inducible factor 1
HIF2α	Hypoxia inducible factor 2
HJV	Hemojuvelin
HME	Human mammary epithelial cells
ER	Estrogen receptor
FPN	Ferroportin
FT	Ferritin
FTH	Ferritin H
FTL	Ferritin L
IL-6	Interleukin 6

IRE	Iron responsive element
IRP	Iron regulatory protein
LIP	Labile iron pool
mCELL	Methylcellulose
MMP	Matrix metalloproteinase
NAT	Normal adjacent tissue
ND	Not detected
NTC	Non-targeting control
pHEMA	polyHEMA (Poly(2-hydroxyethyl methacrylate))
PR	Progesterone receptor
rIL-6	Recombinant IL-6
SOSDC1	Scelerostin domain containing 1 protein
STAT3	Signal transducers and activators of transcription 3
TAF	Tumor associated fibroblast
TEC	Tumor epithelial cell
TF	Transferrin
TFR	Transferrin receptor
ULA	Ultra-low attachment
UNT	Untreated
UTR	Untranslated region

Chapter I

Introduction and Background

A.) Breast Cancer

Aside from skin cancer, breast cancer is the leading cancer type among American women, with an astounding 1 in 8 females having the chance of invasive breast cancer diagnosis in their lifetime [1]. This year, 252,710 new cases of invasive breast cancer are expected among U.S. women, along with 63,410 new cases of non-invasive ducal carcinoma in situ (DCIS) [1]. Although detection methods and treatments have improved tremendously throughout the past few decades, 40,610 U.S. women are expected to succumb to the disease in 2017 [1]. Besides lung cancer, the predicted number of deaths for breast cancer is higher than those for any other cancer type in women [1].

Depending on the tumor size, molecular sub-type, stage and lymph node involvement, treatment options include surgery (lumpectomy or mastectomy), hormonal therapy, radiation and/or chemotherapy. Although treatments have improved and the 5 year survival rate has reached 91%, the high incidence of breast cancer indicates that more prevention and early detection methods are desired [1]. Interestingly, although it has been praised for its ability to capture breast tumors at their earliest stages, mammography has become a controversial detection method throughout recent years [2]. Improvements in the technology and detection limits have dramatically increased the number of “abnormal” mammograms, leading to sometimes unnecessary and sometimes life-saving biopsies and treatments [3]. The challenge is to determine what abnormalities may progress to invasive carcinomas and what abnormalities will never progress to invasive disease. Therefore, it is imperative to understand the molecular changes that occur during early tumor progression. The propagation of primary patient samples *in vitro*, both normal and tumor from the same patient, allow us to follow the molecular changes that occur and contribute to tumor progression [4]. We will utilize these samples in this thesis among other *in vitro* culture systems to investigate molecular changes that occur during tumorigenesis, specifically with regards to iron metabolism.

In addition to better detection and prevention, for those 40% of women whose cancer was detected after it has spread beyond the breast, 5-year survival rates dip to 85% for disease progression to regional lymph nodes and 26% for progression to distal sites [1]. This drop-off in survival indicates that current traditional treatment strategies are ineffective at treating disease that has spread. Alternative therapies, such as iron chelation and induction of iron dependent cell death, termed ferroptosis, are emerging as innovative ways to halt tumor progression and disease spread, when traditional treatment strategies fail [5, 6].

B.) Iron metabolism

I. Systemic and Cellular Iron Homeostasis

Iron is an essential nutrient and plays a vital role in maintaining proper function at both a systemic and cellular level. Iron is a co-factor in many heme and iron containing enzymes necessary for processes such as DNA synthesis, cell cycle, iron-sulfur cluster biogenesis and energy generation [6]. However, iron must be tightly regulated, as the element has the ability to cycle between reduced and oxidized forms, giving iron the potential to partake in free radical generating reactions and damage cellular DNA. As there is no known mechanism for iron excretion from the body, iron homeostasis is maintained by careful control of iron intake and recycling.

Dietary iron (mainly in the form of ferric (Fe^{3+}) iron) is absorbed in the intestinal enterocytes through cooperative action of a ferric reductase, such as duodenal cytochrome B (DCYTB), and divalent metal transporter 1 (DMT1). Reduced (ferrous (Fe^{2+})) iron is then transported to the basal surface of the duodenal enterocyte, where iron is re-oxidized by hephaestin (HEPH) and exported through the only known mammalian iron exporter, ferroportin (FPN). Ferric iron is loaded onto the carrier protein, transferrin (TF), where it circulates throughout the body destined for areas that require iron, such as peripheral tissues. On peripheral cells, transferrin bound iron is recognized by transferrin receptor (TFR1) where the

binding of the holo-TF to TFR1 triggers endocytosis of the holo-TF-TFR1 complex. In the acidic environment of the endosome, iron is released from TF and is reduced back to its metabolically active state by the ferric reductase, STEAP3. Ferrous iron is transported out of the endosome into the cytosol by DMT1, where it is now part of the metabolically active labile iron pool (LIP). This metabolically active iron is utilized by the cell for processes mentioned above. As metabolically labile iron that is not utilized by the cell can participate in free radical generating reactions, any excess iron is either carefully stored in the iron storage protein Ferritin (FT) or effluxed out of the cell by FPN, where it is loaded back onto TF for further circulation. When systemic iron levels are high, hepcidin is produced by the liver, whose function is to bind to FPN and trigger its degradation, leading to decreased iron efflux from enterocytes into circulation. Hepcidin is also produced locally by peripheral cells, where it also functions to degrade FPN on neighboring cells for decreased iron export and accumulation of intracellular iron [7-9]. An overview of the main players involved in iron absorption and metabolism are shown in Figure 1-1 and detailed in [6, 10].

In addition to hepcidin, intracellular iron levels can be regulated by the iron regulatory proteins 1 and 2 (IRP1 and IRP2) [6]. These proteins control intracellular iron by binding to iron responsive elements (IREs) on promoters of iron related genes such as FT, FPN and TFR1 when iron is low. The IRE can be found at either the 3' untranslated region (UTR) for genes such as TFR1, where binding of IRPs stabilizes mRNA or at the 5' UTR for FT and FPN, where binding of IRP inhibits mRNA translation. Under high iron conditions, IRP2 is degraded and IRP1 gains enzymatic activity as a cytosolic aconitase, rendering neither able to bind to IREs, reducing TFR1 and increasing FT and FPN for overall reduction of cellular iron.

II. Iron and cancer

The relationship between iron and cancer has been widely observed for many years [6, 11]. Large population based studies have all supported a model in which elevated body iron

levels are associated with increased cancer risk. Although each approach has study limitations, four main approaches have been utilized to perceive such a concrete observation. First, studies examined markers of iron stores, such as TF saturation, and found that TF saturation was elevated in men who developed cancer than those men who did not [11, 12]. A second approach examined the association between dietary iron and cancer risk. Numerous studies found higher dietary iron intake to be associated with increased risk of cancer, although the strength of the association varied by study [13-15]. A third epidemiological link between iron and cancer risk utilized a genetic approach, where patients with genetic disorders of iron overload, such as hereditary hemochromatosis, were found to have a 20-200 fold increased incidence of developing hepatocellular carcinoma, and may be at risk for additional cancers such as breast, colorectal and others [16-19]. A final approach examined the effect of reducing body iron stores and cancer risk. Studies found that frequent phlebotomy over about 5 years in elderly men with peripheral artery diseases reduced overall cancer risk as well as cancer-specific death [20]. On the other hand, it is believed that increased breast cancer risk in post-menopausal women is in part due to increased body iron levels as a result of decreased blood loss after menstruation cessation [21]. Taken together, compilation of numerous studies utilizing all four approaches has painted a clear connection between increased body iron and overall cancer risk.

In addition to clinical based studies, which only examine an association between iron and cancer risk, iron retention at the cellular level in cancer cells has also been observed. This has prompted extensive research assessing mis-regulation of iron homeostasis to elucidate a direct role of iron in cancer progression. Iron not only functions to facilitate cell proliferation, but excess iron has the ability to generate free radicals that can result in genome instability and promote transformation [22, 23]. In attempts to determine the connection between excess iron and cancer, investigation into the control of iron metabolism at the molecular level is emerging. It has recently been demonstrated that many iron metabolism proteins, originally studied for

their role in systemic iron homeostasis, are utilized for cellular iron metabolism in peripheral tissues, such as the breast [7, 24].

Many alterations of the proteins that control cellular iron metabolism have been implicated in cancer, including breast cancer, and these cancer-specific protein modifications result in increased intracellular iron, assumed to meet the growth and proliferative demands of cancer cells [6, 25]. Specifically, proteins that control cellular iron uptake and efflux are altered to promote accumulation of intracellular iron. TFR1 is highly expressed in many tumor types, including breast cancer, to promote increased iron import [26] and antibodies against TFR1 have been shown to inhibit tumor growth [27]. Additionally, iron export is deceased in cancer cells, through modulation of the FPN-hepcidin regulatory axis (Figure 1-2) [6]. FPN is reduced on the surface of breast, prostate, ovarian and hepatocellular cancer cells [7, 8, 28, 29]. Interestingly, reduced FPN in breast tumors was associated with reduced metastasis-free survival, suggesting that FPN is predictive of patient outcome [7]. FPN is regulated at the transcriptional, post-transcriptional and post-translational levels. For the basis of this thesis, we will focus on post-translational regulation of FPN by hepcidin, the negative regulator of FPN protein expression, as described above. Hepcidin is also altered in cancer, with elevated expression associated with increased cancer risk. Not only is liver produced systemic hepcidin elevated in multiple cancer types [30-35], but hepcidin is also produced by peripheral cells and elevated in cancer cells compared to normal cells for local targeting of FPN for degradation within tumors [7-9, 28]. As this thesis focuses on hepcidin and the pathways that control its expression in breast cancer, a detailed introduction to hepcidin and its regulation is provided next.

C.) Hepcidin

I. Discovery and role

Hepcidin was first discovered by independent groups in 2000 and 2001 as a small peptide with potent antibacterial activity [36, 37]. Expressed predominantly in the liver, hepcidin is encoded by the HAMP gene where it is synthesized as an 84 amino acid pre-pro-peptide with an N-terminal endoplasmic reticulum target sequence and a C-terminal consensus furin site for cleavage [37]. Cleavage at both sites renders the peptide active where it is rapidly secreted into circulation as a 25 amino acid bioactive hormone [38].

Shortly after its discovery, hepcidin was found to play a central role in systemic iron homeostasis, as well as iron storage in macrophages, and is now commonly referred to the master regulator of iron metabolism [39, 40]. It was determined that hepcidin regulates systemic iron by binding to FPN on intestinal enterocytes and macrophages for control of dietary iron and iron recycling respectively, leading to the internalization and degradation of hepcidin bound FPN in the lysosome [41-43]. Hepcidin levels can be controlled depending on the systemic need for iron. For example, when body iron levels are high, hepcidin is induced and secreted by the liver, where it travels through the circulation for targeting of FPN for degradation, leading to reduced iron uptake from the diet and reduced iron from macrophage stores. When body iron levels are low, hepcidin is reduced, allowing for increased uptake of dietary iron and release of iron from macrophages. Careful control of hepcidin leads to homeostasis of systemic iron levels.

In addition to the role of the hepcidin-FPN axis in control of systemic iron homeostasis, this axis seems to be conserved for control of cellular iron homeostasis in tissues such as the breast, prostate and brain [7-9]. Hepcidin is produced from cells within these peripheral tissues for local control of FPN and intracellular iron levels. As mentioned above, hepcidin has been found to be elevated in serum of breast cancer patients as well as increased in cancer cells of peripheral tissues, suggesting an association between hepcidin and cancer at both the systemic

and local level [7, 8, 28, 30-35, 44]. It is expected that increased hepcidin leads to accumulation of intracellular iron within tumors, resulting in tumor cell growth and progression. Interestingly, the combined expression of ferroportin and hepcidin has been shown to be a powerful predictor of survival in breast cancer patient cohorts [7]. Furthermore, knockdown of hepcidin in breast tumor cells inhibits growth of breast tumor xenografts, indicating that hepcidin produced by tumor cells is an important contributor to tumor growth [28]. Thus, the FPN-hepcidin regulatory axis has significant impact on tumor growth and disease progression in breast cancer patients.

II. Regulation

Due to the key role of hepatic hepcidin in maintenance of systemic iron homeostasis, mechanisms that regulate hepcidin synthesis have been intensively studied in hepatocytes since its discovery. Depending on the requirement for hepatic hepcidin and iron levels, mechanisms have been identified that both positively and negatively regulate the peptide hormone.

a.) Positive Regulation

In order to reduce efflux of iron from intestinal enterocytes and macrophages, hepcidin production must be elevated to reduce iron levels in circulation. In order to achieve this, hepcidin is positively regulated by iron itself through a pathway involving the bone morphogenetic protein (BMP) pathway and downstream signaling components, the Sma and mothers against decapentaplegic vertebrate homologs (SMADs) [45]. The BMPs are a subfamily of the transforming growth factor beta (TGF-β) superfamily, which controls a wide array of growth factor functions, such as bone formation [46]. The connection between the BMP pathway and iron homeostasis was first observed when hepatocyte-specific SMAD4 knock out mice were found to have severe iron overload phenotype [47]. It was discovered that there was a 100-fold reduction in hepatic hepcidin mRNA in the livers of these mice, indicating the role of SMAD4 as an essential transcriptional regulator of hepcidin. Since then, many studies have

found that several BMPs and other ligands of the TGFβ family are capable of inducing hepcidin expression in hepatocytes and other cell types [8, 48]. However, researchers have pinpointed BMP6 as the main ligand for positive regulation of hepcidin transcription by iron *in vivo* [49, 50]. The precise mechanism by which iron induces BMPs as well as the cell type source of BMPs for positive regulation for hepcidin remains unknown.

More recently, other members of the BMP signaling pathway have been shown to regulate hepcidin. These were identified through mutational analysis of hereditary hemochromatosis patients. Specifically, patients with mutations in hemojuvelin (HJV), a BMP co-receptor, were found to have inappropriately low levels of hepcidin, indicating an important role of HJV in hepcidin regulation [51, 52]. Additionally, mutations in additional membrane iron sensors, transferrin receptor 2 (TFR2) or hemochromatosis protein (HFE), result in a subtle decrease in hepcidin production, leading to a less severe form of HH [53, 54]. It is believed that increasing concentrations of TF-bound iron leads to dissociation of HFE from TFR1 (the main iron import protein) at the cell membrane, allowing it to associate with TFR2 [55]. This allows for stabilization of TFR2 to activate the downstream BMP pathway, although the direct connection between TFR2 and BMP-SMAD pathway activation are unknown.

In addition to hepcidin regulation by iron, hepcidin is also greatly regulated by inflammation, as hepcidin was first described as a peptide with antimicrobial properties [37]. It is believed that regulation of hepcidin by inflammation evolved as a host protective mechanism against microbes by reducing body iron levels that microbes require to flourish [56]. A direct connection between iron and inflammation was first demonstrated when treatment of hepatocytes with lipopolysaccharide (LPS) stimulated hepcidin transcription [39]. Further analysis revealed that type II acute phase cytokines, not type I cytokines, induce hepcidin [57]. Specifically, the main and most robust cytokine for hepcidin transcription *in vivo* was found to be IL-6 [57]. IL-6 activates Janus kinase 2 (JAK2) and the corresponding downstream signal transducers and activators of transcription 3 (STAT3) [58]. Upon activation through

phosphorylation, STAT3 translocates to the nucleus and binds to the STAT3 element on the hepcidin promoter for transcriptional induction of hepcidin [58]. It is interesting to note that cross-talk between the BMPs and IL-6 has been observed, for even greater control over hepcidin induction [59].

b.) Negative Regulation

Since hepcidin is the main regulator of systemic iron homeostasis, mechanisms must be in place to suppress its expression when increased body iron levels are needed. One such example is during erythropoiesis. Due to increased demand during red blood cell formation, hepcidin must be suppressed. Although originally thought to be direct negative regulation by erythropoietin (EPO), further studies have suggested erythroferrone or growth differentiation factor 15 (GDF-15) to be the erythroid factor that negatively regulates hepcidin, although some of these studies were conducted in diseased states, such as β-thalassemia [60-63]. A full understanding of erythroid mediated negative regulation of hepcidin remains incomplete.

In parallel to erythropoietic control of hepcidin suppression, hypoxia has been shown to reduce hepcidin levels. Low oxygen conditions stimulate red blood cell production, resulting in increased demand for iron and thus hepcidin suppression [64]. The first molecular connection between hepcidin and oxygen levels was a study in which a hypoxia inducible factor 1 (HIF1α) hepatocyte-specific deletion showed no decrease in hepcidin during hypoxia or iron deficiency, suggesting hypoxic regulation of hepcidin is mediated by HIF1α [65]. The study went on to confirm that HIF1α binds to the hypoxia responsive element on the hepcidin promoter to inhibit gene transcription [65]. However, other studies have suggested negative regulation of hepcidin via hypoxia to involve HIF2α or and indirect mechanism through hypoxia, such as hypoxia leading to increased cleavage of HJV, which sequesters BMPs and inhibits their activation of the downstream signaling pathway [66-68]. Similar to erythropoietic regulation, negative regulation of hepcidin by hypoxia is incompletely understood.

Lastly, another molecular strategy for hepcidin suppression is through inhibition of positive regulators of hepcidin. For example, mutations in the TMPRSS6 gene, which encodes a type II transmembrane serine protease called matriptase-2, results in increased hepcidin levels and severe anemia that does not respond to traditional therapy [69]. It was determined that matriptase-2 cleaves the BMP co-receptor HJV leading to reduced BMP signaling for reduction of hepcidin [70]. Similarly, Scelerostin domain containing 1 protein (SOSTDC1) sequesters BMP ligands resulting in diminished BMP signaling and has been found to be a negative regulator of hepcidin in prostate cancer cells [8, 71].

c.) Additional Regulators

More recently, additional regulators are emerging as supplemental mechanisms for hepcidin regulation, although many of these regulators are limited to one study or have been disputed and have not yet been classified as mainstream regulators of hepcidin. These regulators include hormones, growth factors and other signaling molecules. For example, hormonal control of hepcidin was postulated, based on a need for increased iron during menstruation. Further analysis revealed an estrogen responsive element in the hepcidin promoter, resulting in hepcidin suppression for increased iron in circulation [72]. However other studies found a positive regulation of hepcidin via estrogen [73]. Additionally, Wnt signaling has been suggested to positively regulate hepcidin in prostate cancer cells through a Wnt transcription factor responsive element in the hepcidin promoter [8].

In this thesis, we explore and reveal additional positive and negative regulators of hepcidin that regulate hepcidin locally in breast tissue. Previous studies in prostate cells identified several conserved pathways for both positive (via BMP7, IL-6) and negative (SOSTDC1) regulation of hepcidin [8]. Overall, we identify similar conserved mechanisms as well as additional novel regulators of hepcidin in breast cancer, suggesting a complex regulatory network involving breast cancer cells and the microenvironment.

D.) 3D culture

In order to capture the full spectrum of regulatory pathways that control hepcidin in breast cancer, we utilize a 3D spheroid model for certain chapters of this thesis to better recapitulate the *in vivo* breast tumor architecture [74]. This model has been widely used to better understand cellular process and signaling pathways that 2D culture is unable to fully capture [75, 76]. Literature suggests that signaling pathways in 3D more accurately reflect those present in tumors, compared to 2D culture [76, 77]. Importantly for our studies, 3D spheroid systems also effectively model the metabolic pathways present within tumors [78]. There are many types of 3D culture conditions, but for most of our experiments, we utilize a scaffold and protein free system that allows the same culture conditions as 2D culture. Cells are plated in their normal growth media in 96-well plates coated with Poly(2-hydroxyethyl methacrylate) (commonly referred to as polyHEMA), a polymer that prevents adhesion to the plate and promotes cell aggregation. This widely accepted 3D condition allows us to directly compare 2D to 3D culture without the use of exogenous basement membrane components or scaffolds, to examine potential changes in iron metabolism simply through modifying the cellular architecture and interactions [74, 79]. Additionally, aside from architectural differences that may regulate hepcidin simply by culturing cells in 3D, we can also examine the effects of the microenvironement through utilization of a 3D culture system. These include addition of extracellular matrix (ECM) proteins or stromal cells to breast tumor epithelial spheroids [80]. By utilizing these 3D culture system modifications, it is postulated that we can better mimic breast tumors, including the effect of the microenvironemnt. Ultimately, we believe a 3D model system will capture the full array of regulatory interactions that govern hepcidin expression including contributions of cytokines, extracellular matrix (ECM) and stromal cells, such as tumor associated fibroblasts (TAFs) [81-83].

E.) Primary Patient Samples

Another exciting component of this thesis is our ability to culture primary breast cancer cells from patients. Cell lines are becoming increasingly criticized models in cancer research, as many cell lines are suggested to have evolved over time [84]. Evidence is emerging that the gene expression profiles from established cancer cell lines are markedly different than tumor sample profiles [85]. To make up for these limitations, the use of primary cells isolated directly from patient tumors is becoming increasingly desired for cancer biology research [86]. Unfortunately, attempting to culture primary cells from patients has proven to be difficult, due to limited proliferation and inevitable senescence [87]. However, these limitations can be circumvented through utilization of a technique known as conditional reprogramming (CR) [4]. This technique was developed by the laboratory of Dr. Schlegel, who discovered that with the use of irradiated fibroblasts and Rho kinase (ROCK) inhibitor, primary epithelial cells grow robustly in culture. In addition, after propagation under CR conditions, primary cells retain epithelial characteristics, normal differentiation potential and maintain original karyotypes [4]. It is our belief that, in additional to cell lines, primary breast epithelial cells will enhance our findings and better reflect the transformation process that causes imbalanced iron homeostasis. This system also allows us to have matched normal and tumor breast cells to better understand the mechanisms responsible for increased hepcidin expression in breast cancer cells and follow the iron seeking phenotype as cells transform.

F.) Rationale

As mentioned above, our lab has previously shown that two proteins controlling iron efflux are conserved in breast epithelial cells [7]. Ferroportin (FPN) allows for any excess intracellular iron to be readily exported from cells [88]. Hepcidin regulates FPN protein expression by binding to and inducing its internalization and subsequent degradation, resulting in decreased iron export [41]. Together, FPN and hepcidin comprise a regulatory axis to

maintain tight control of iron efflux. We previously demonstrated that breast cancer cells modulate these proteins to reduce iron efflux, ultimately favoring intracellular iron accumulation. Compared to non-malignant breast epithelial cells, breast cancer cells have increased hepcidin, which controls FPN post-translationally, through degradation [7]. These cancer specific alterations correspond to increased cellular levels of metabolically active iron, known as the labile iron pool (LIP), in breast cancer cells.

In addition, reestablishing iron export by overexpression of FPN in breast cancer cells resulted in decreased growth of tumor xenografts in mice, suggesting that intracellular iron contributes to cellular growth [7]. Further support of modulation of iron export axis in tumor growth was demonstrated when hepcidin depletion in breast tumor xenografts significantly reduced tumor size and progression [28]. Importantly, it was also shown that low tumoral FPN mRNA expression is associated with a significant decrease in metastasis free survival in breast cancer patients [7]. Patients with favorable high FPN expression have a decreased survival rate if they have high tumoral hepcidin mRNA expression [7]. In addition to these modifications of iron proteins in breast cancer, other cancers, including colorectal, renal cell carcinoma and prostate cancer have increased tumoral hepcidin compared to normal samples [8, 44, 89]. FPN is also reduced in multiple tumor types including ovarian and prostate cancer [8, 29].

These findings highlight the importance of FPN and hepcidin in breast cancer progression and prognosis. Determining the mechanisms that regulate hepcidin are of great importance, as hepcidin expression ultimately controls iron efflux by facilitating FPN degradation. Although hepcidin regulation has been well characterized in the liver, regulation of hepcidin in the breast remains poorly understood. Understanding the hepcidin regulatory pathways in breast cancer is of immense importance, as hepcidin and the pathways that control its expression, would be attractive targets to decrease excess cellular iron present in breast cancer cells and reduce the malignant effects that occur as a result of elevated cellular iron levels.

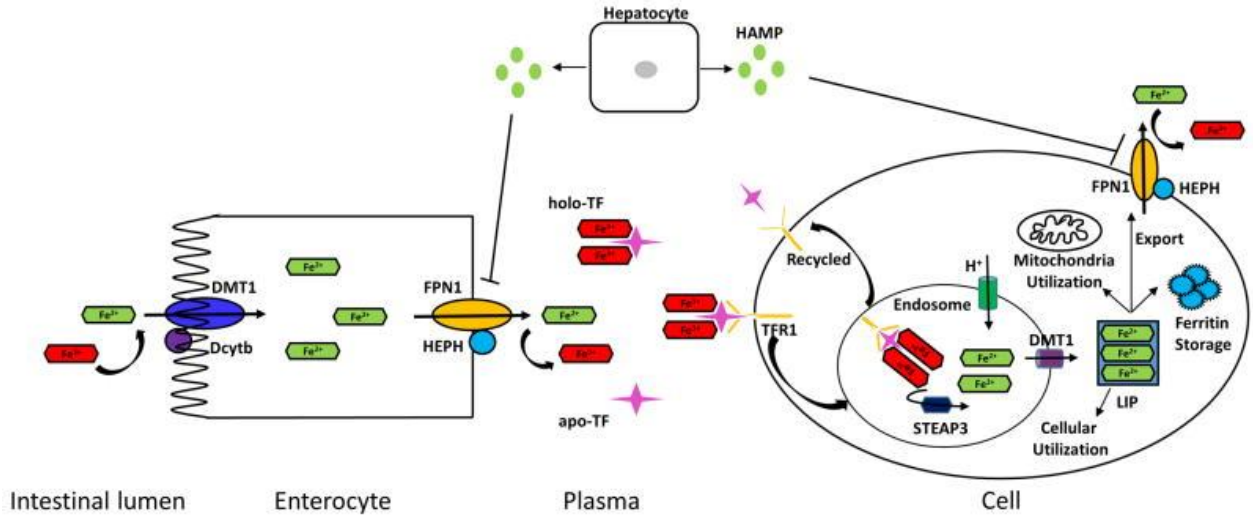

Figure 1-1. An overview of iron absorption and metabolism.
Enterocytes absorb dietary iron through the combined action of ferric reductases, such as Dcytb and divalent metal transporter DMT1. Ferrous iron taken up by enterocytes is exported into the circulation by ferroportin (FPN-1). Concurrently, the Fe^{2+} is oxidized to Fe^{3+} by hephaestin (HEPH), which is functionally associated with FPN-1. Fe^{3+} is loaded on to circulating apo-TF in plasma. Cells take up diferric TF through the cell surface transferrin receptor (TFR1). The TFR1–TF–$(Fe^{+3})_2$ complex is endocytosed, and iron is released from TF. Fe^{3+} is reduced by the ferric reductase STEAP3, and Fe^{2+} is then transported to the cytosol by DMT1, where it enters the cytosolic labile iron pool (LIP). The LIP is utilized by cells for various metabolic needs. Excess iron is stored in ferritin or effluxed to the circulation through FPN-1. Hepatocytes synthesize hepcidin (HAMP) in response to systemic iron levels; the binding of hepcidin to FPN-1 triggers FPN-1 degradation, thus inhibiting iron efflux
(Figure from Manz and Blanchette (2016) Ann N Y Acad Sci. 1368(1): 149–161.

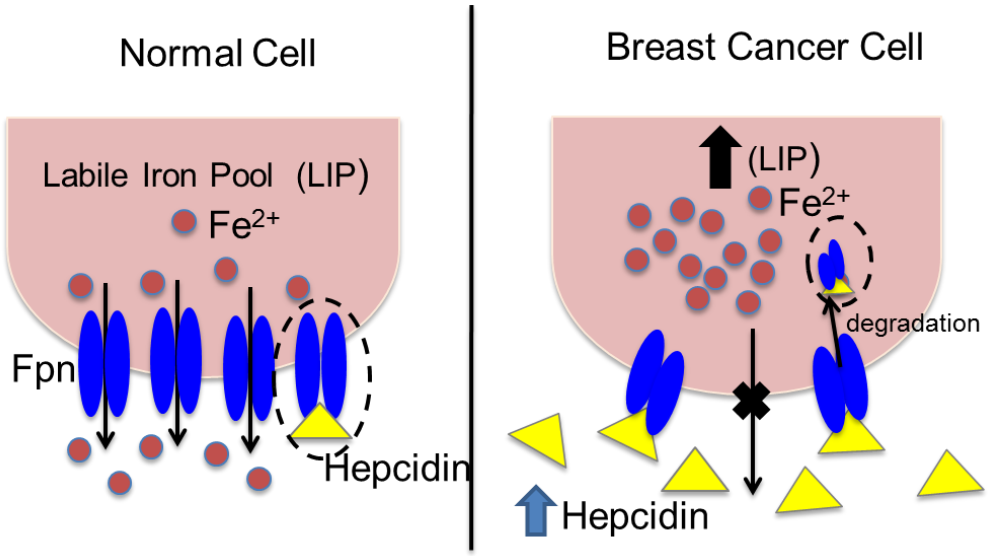

	Normal	Cancer
Hepcidin	Low	High
Ferroportin	High	Low
Labile Iron Pool (LIP)	Low	High

Figure 1-2. Iron export is altered in breast cancer cells.
During breast tumorigenesis, hepcidin expression is increased. Hepcidin functions by binding to ferroportin, which causes its internalization and degradation. This results in decreased iron export and accumulation of intracellular labile iron pool in breast cancer cells.

Chapter II:

Hepcidin Regulation in Breast Cancer Monolayer Cells

(Unpublished Data)

Abstract

Hepcidin is a secreted peptide hormone whose main function is to bind to the iron efflux pump ferroportin (FPN) and trigger its degradation, resulting in decreased iron export from intestinal enterocytes, macrophages and peripheral tissues. Hepcidin is produced by breast epithelial cells for local control of iron metabolism and is elevated in breast cancer to promote accumulation of intracellular iron cancer cells need to proliferate. Here, we investigate the pathways that control increased hepcidin in breast cancer cell monolayers. A conserved pathway of canonical BMPs and/or IL-6 signaling for induction of hepcidin in breast cancer cells was revealed and preference of these ligands for regulation of hepcidin seems to be breast cell-line specific. Hepcidin can also be increased in normal breast epithelial cells through exogenous stimulation with IL-6, suggesting that iron homeostasis can be altered in normal cells through paracrine stimulation by exogenous sources. Additionally, hepcidin induced by BMPs or IL-6 is functionally capable of FPN degradation, suggestive of a fully functional hepcidin-FPN regulatory axis upon induction with BMPs/IL-6. Thus, targeting of these molecular regulators of hepcidin may represent a promising therapeutic strategy to decrease hepcidin levels. Decreased hepcidin would restore intracellular iron back to normal levels, which would ultimately be detrimental to rapidly dividing cancer cells and halt tumor growth.

Introduction

Since its initial discovery in the liver, hepcidin is now referred to as the master regulator of systemic iron homeostasis [37, 39]. As a secreted hormone peptide, hepcidin, and the pathways that control its expression, are considered attractive molecular targets for controlling some forms of anemia, where overproduction of hepcidin results in decreased iron absorption from duodenal enterocytes to the blood for absorption [90]. It was previously determined that iron levels and inflammatory pathways positively regulate hepcidin transcription in the liver [91]. In response to increased body iron levels, bone morphogenetic proteins (BMPs) are activated

and upon binding to their receptors, trigger a downstream SMAD signaling cascade that leads to induction of hepcidin transcription in liver cells [92]. Synthesis of hepcidin was also found to be induced by inflammatory signals, mediated by Interleukin 6 (IL-6) and its downstream signaling mediator STAT3[93]. Both SMADs and STAT3 act on the human hepcidin promoter through direct binding to the corresponding BMP-responsive elements (BREs) and the STAT3 binding sites on the hepcidin promoter respectively [94].

Although these pathways have been widely investigated in the liver, the mechanisms that control hepcidin transcription in breast cancer cells are not completely known. One study, published in parallel to this thesis, suggested that serum hepcidin is elevated in breast cancer patients and that this increase is also regulated by increased iron, BMPs and IL-6 present in serum from BC patients [28]. Furthermore, they showed that reduction of hepatic hepcidin levels resulted in suppression of breast cancer progression, suggesting that circulating hepcidin is able to act locally on breast cancer cell ferroportin to reduce tumor iron and tumor growth. However, although this study shows conserved mechanisms for increased hepatic hepcidin for systemic effect on breast cancer cells, it does not examine local regulation of hepcidin produced by breast cancer cells themselves. Additionally, as previously mentioned, hepcidin is also elevated in breast cancer cells cultured *in vitro* compared to normal breast epithelial cells [7]. Thus, without systemic stimulation from exogenous sources, breast cancer cells must have some form of autocrine regulation of hepcidin, potentially through conserved mechanisms utilizing BMPs and/or IL-6.

It was previously shown that liver cells endogenously produce BMP ligands, which contributes to basal hepcidin expression via an autocrine signaling mechanism [92]. Additionally, our lab has previously shown that prostate cancer cells endogenously produce BMPs and IL-6 for autocrine regulation of hepcidin, where hepcidin is also elevated compared to normal prostate cells [8]. Several studies have shown that breast cancer cells also have the ability to endogenously produce several cytokines, including BMPs and IL-6 [95, 96].

Endogenous BMP production in breast cancer cells has been suggested to play a role in disease progression [97, 98]. In addition, IL-6 was shown to be locally produced by some breast cancer cells, such as the highly aggressive MDA-MB-231 triple negative breast cancer cell line, and is thought to contribute to breast cancer growth and metastasis [99, 100]. Endogenous production of these cytokines may act via autocrine signaling to stimulate downstream signaling targets for the local induction of hepcidin in breast cancer cells (Figure 2-1). In this chapter, we aim to elucidate the molecular pathways that control hepcidin expression in breast monolayer cells.

Results

IL-6 and BMPs positively regulate hepcidin in R5 and MDA-MB-231 breast cancer cells

Due to the fact that hepcidin is induced in the liver by the BMPs and IL-6, we first wondered if increased expression of hepcidin through autocrine regulation by these ligands was conserved in breast cancer cells. To test this, we examined basal mRNA expression of IL-6 and several BMPs known to induce hepcidin expression. We found moderate expression of BMP6 and prominent IL-6 expression in the R5 breast cancer cell line, a genetically transformed cell line derived from normal human mammary epithelial (HME) cells with the catalytic subunit of telomerase, SV40 T antigen, and high levels of oncogenic H-*ras* [101] (Figure 2-2A). Compared to normal HME cells, R5 breast cancer cells have significantly elevated IL-6 transcript, suggesting the IL-6 could be responsible for increased hepcidin expression in these breast cancer cells (Figure 2-2B). To confirm secretion of IL-6 for potential functional autocrine regulation of hepcidin, we examined IL-6 levels by ELISA and confirmed that R5 breast cancer cells secrete increased IL-6 compared to HME breast cells (Figure 2-2C). This suggests that IL-6 could be increased in R5 breast cancer cells for autocrine regulation of hepcidin.

To further confirm if IL-6 can induce hepcidin in R5 breast cancer cells, we treated R5 cells with recombinant IL-6 (rIL-6) and examined activation of its downstream signal protein

(STAT3) as well as hepcidin expression following treatment. After 24 hours of rIL-6 treatment, we saw activation (phosphorylation) of STAT3 at three increasing concentrations of rIL-6 (Figure 2-3A). Additionally, we saw ~2-fold increase in hepcidin precursor protein and increasing hepcidin secretion (up to ~3-fold), as detected by ELISA, with increasing concentration of rIL-6 (Figure 2-3A and B). Thus, we concluded that R5 breast cancer cells are able to respond to IL-6 for induction of hepcidin. This further supports the hypothesis that IL-6 may be a conserved mechanism in breast cancer cells for induction of hepcidin.

We also wondered if, despite modest (BMP6) or no detectable (BMP4, BMP7) production of BMPs, R5 breast cancer cells could respond to exogenous treatment of BMPs for paracrine induction of hepcidin via a conserved BMP signaling pathway (Figure 2-4A). To test this, we treated R5 breast cancer cells with recombinant BMPs (rBMPs) for BMP4, BMP6 and BMP7. After 24 hours of rBMP treatment, we saw increased activation (phosphorylation) of SMAD1-5-8, the downstream signaling molecule of BMP ligands, compared to untreated cells (Figure 2-4B). Additionally, we saw a 2-fold increase in hepcidin protein expression with rBMP6, and a modest increase with BMP4 and BMP7 (Figure 2-4B). It's interesting to note that despite BMP4 activating pSMAD1-5-8 the most, it was BMP6 that seemed to have the most robust effect for inducing hepcidin. BMP6 is also the most potent BMP for induction of hepcidin in the liver, and thus, seems to be conserved as the most potent BMP inducer of hepcidin in breast cancer cells. Taken together, these data suggest that both IL-6 and BMPs are conserved in R5 breast cancer cells for positive regulation of hepcidin.

Next, we wanted to confirm that regulation of hepcidin by BMPs and IL-6 could be replicated in another breast cancer cell line that has not been genetically transformed. Thus, we tested the effect of BMPs and IL-6 on inducing hepcidin utilizing a commonly used, aggressive, triple negative subtype cell line, the MDA-MB-231 cells. Despite activation of the downstream pathways of IL-6 and BMPs, we found a very modest effect on further stimulation of hepcidin mRNA and protein with BMPs and IL-6 (Figure 2-5A and B). However, we observed that MDA-

MB-231 have the highest basal hepcidin expression compared to all cell lines tested, and thus saturated receptors from endogenous production of BMPs and/or IL-6 may inhibit further exogenous stimulation (Figure 2-6A). Since MDA-MB-231 cells have been previously characterized for their production of pro-inflammatory cytokines, such as IL-6, we compared IL-6 levels across all cell lines. We confirmed this, as MDA-MB-231 cells had very high levels of IL-6, with ~7 fold and ~2.5 fold increase compared to R5 cells at the transcript and secreted protein levels respectively (Figure 2-6B and C). Due to high endogenous production of IL-6, we depleted IL-6 levels with neutralizing antibody and found a significant reduction in hepcidin protein when IL-6 was reduced (Figure 2-6D). This supports the hypothesis that IL-6 may be regulating hepcidin through an autocrine signaling loop in MDA-MB-231 breast cancer cells.

BMPs, but not IL-6, regulate hepcidin expression MCF-7 BC cells

We next wanted to determine the regulation of hepcidin in a breast cancer cell line that does not produce endogenous IL-6. Thus, we examined endogenous production of BMPs and IL-6 in an addition breast cancer cell line, the MCF-7 cells. MCF-7 cells do not produce detectable levels of IL-6, unlike the R5 and MDA-MB-231 breast cancer cells, suggesting that something else may be responsible for increased hepcidin expression in MCF-7 breast cancer cells (Figure 2-7A). Instead, we found that MCF-7 cells transcriptionally produce high levels of BMP4, 6 and 7, compared to MCF-10A, suggesting that a conserved BMP signaling mechanism may be responsible for increased hepcidin in these MCF-7 breast cancer cells (Figure 2-7A). To test this, we treated MCF-7 cells with rBMPs, and found that despite activation of SMAD1-5-8, we found no further increase in hepcidin protein expression compared to untreated cells (Figure 2-7B). However, since these cells are producing their own ligands, similar to MDA-MB-231 producing high basal IL-6, we postulated additional exogenous stimulation with BMPs has a minimal effect on further elevating hepcidin expression. Therefore, instead of exogenous addition, we reduced basal production of BMPs in MCF-7 cells, to determine if depleting BMPs

would result in a decrease in hepcidin expression. (Please refer to chapter 3 figures where the subsequent data on MCF-7 is also used for a submitted manuscript). To test this, we treated MCF-7 cells with neutralizing antibodies against BMP4, 6, 7 or an isotope matched IgG and found that depleting BMPs resulted in decreased hepcidin expression, most prominently by inhibiting BMP4 and BMP6 (Figure 3-1D). This supports the hypothesis that BMPs may be regulating hepcidin through an autocrine signaling loop in MCF-7 breast cancer cells. To confirm this effect of BMP depletion on hepcidin expression, we utilized siRNA as an additional approach to reduce endogenous BMP4, 6 and 7. Similarly, we found that inhibition of BMPs by knock-down (KD), resulted in decreased hepcidin expression in MCF-7 breast cancer cells, most significantly with BMP4 and BMP6KD (~40% and ~60% respectively at the protein level) (Figure 3-1B and C). KD efficiencies were confirmed (Figure 3-S1D-F). Taken together this suggests that the BMP pathway is conserved for positive regulation of hepcidin in MCF-7 breast cancer cells.

Despite MCF-7 lack of IL-6 production, we wanted to examine the potential role of IL-6 from exogenous sources for paracrine induction of hepcidin via a conserved IL-6 signaling pathway. MCF-7 cells express IL-6 receptor (IL-6R), although at lower levels compared to the BMP receptors (Figure 3-S1C). Thus, we treated MCF-7 cells with recombinant IL-6 at three increasing concentrations and despite activation of STAT3 (Figure 3-1D), we observed a very slight increase of hepcidin expression (Figure 3-1D). Therefore, we concluded that BMPs seem to predominately regulate hepcidin expression in MCF-7 breast cancer cells. Taken together, this suggests that induction of hepcidin, both autocrine and paracrine levels, seem to be cell line specific. Yet, it appears that overall the IL-6 and/or BMP pathways may be conserved in the breast for regulation of hepcidin in a cell type specific manner.

Normal breast epithelial cells are able to respond to IL-6 stimulation for increased hepcidin expression

We next wondered if IL-6 regulates hepcidin expression in normal breast epithelial cells. Despite the fact that human mammary epithelial (HME) cells produce negligible IL-6, we postulated that they may respond to exogenous IL-6, as IL-6 derived from adipocytes or fibroblasts has been observed in breast tissue [102-104]. To test this, we treated HME cells with two concentrations of rIL-6 and found that STAT3 was activated, and hepcidin was elevated (~3 fold precursor protein; ~2 fold secreted protein) (Figure 2-8A and B). This suggests that hepcidin can be induced in normal breast epithelial cells via a conserved IL-6 signaling pathway, if an exogenous source of IL-6 is present.

BMPs and IL-6 stimulate hepcidin induction that is functionally capable of FPN degradation

In order to determine if hepcidin induced by exogenous sources was functionally capable of FPN degradation, we used a fourth breast cancer cell line, the T47-D cells, which have high basal levels of FPN. Thus, to determine if hepcidin was functional in these cells, we first confirmed that exogenous addition of BMPs and IL-6 was capable of hepcidin induction. Although modest, we found that treatment with all exogenous proteins resulted in increased hepcidin expression (Figure 2-10A). Thus, compared to untreated cells, those with exogenous treatment of BMPs or IL-6 should have less FPN as a result of increased hepcidin. As a positive control, we first treated T47-D cells with recombinant hepcidin and found that FPN expression, which normally localizes to the cell surface of T47-D cells, as analyzed by FPN immunofluorescence, was now internalized and punctate, suggestive of FPN degradation by hepcidin (Figure 2-10B). To determine if the increased hepcidin production as a result of BMPs or IL-6 was functional in degrading FPN, we re-treated T47-D cells with recombinant BMPs or IL-6 and examined FPN by immunofluorescence. Although not as dramatic as with recombinant hepcidin, stimulation of hepcidin by BMPs or IL-6 resulted in reduced FPN membrane staining and increased intracellular localization, suggestive of FPN degradation (Figure 2-10C). Overall,

this suggests that stimulation of breast cancer cells with BMPs or IL-6 increases expression of hepcidin, which is functionally capable of FPN degradation.

Discussion

Overall, we observed that the BMP and IL-6 pathways are conserved pathways in the breast for induction of hepcidin. First, we observed that R5 breast cancer cells have the ability to respond to exogenous stimulation of IL-6 and BMPs (most robustly with BMP6 of the three BMPs tested; Figure 2-3 and 2-4) for further increased hepcidin expression, which is already elevated compared to normal breast epithelial cells to start. This paracrine regulation may be extremely interesting in the context of a tumor microenvironment. It demonstrates the possibility of further induction of hepcidin by exogenous sources, potentially through exogenous production and paracrine stimulation by stromal cells, which we investigate in chapter three. Although this stimulation mimics a paracrine signaling mechanism, it would be interesting to determine if either IL-6 or BMPs regulate the basal increased hepcidin expression present in R5 cells through an autocrine fashion, via production and signaling from the tumor cells themselves. R5 cells predominantly produce IL-6, with low endogenous production of BMPs, thus one may expect that IL-6 could be responsible for increased basal hepcidin expression in these cells compared to their HME normal counterparts (who produce negligible endogenous IL-6). By depleting levels of endogenous IL-6, either with neutralizing antibodies or siRNA, we would expect for basal hepcidin expression to be reduced. This would allow us to determine if IL-6 is regulating increased basal hepcidin expression in R5 breast cancer cells.

Next, we confirmed the role of IL-6 in autocrine regulation of hepcidin in the MDA-MB-231 breast cancer cells. Since these cells have high levels of basal hepcidin and high endogenous production of IL-6 (Figure 2-6), we decided to reduce basal IL-6 levels to determine the effect on hepcidin. We found that depletion of IL-6 with neutralizing antibodies resulted in a reduction in basal hepcidin level (Figure 2-6), although our IgG isotope matched control had a slight effect on hepcidin as well. This confirms that IL-6 is positively regulating hepcidin in an

autocrine fashion in the MDA-MB-231 breast cancer cells. Additionally, we would want to investigate the role of BMPs in regulation of hepcidin in these cells. Although we did not observe an effect with exogenous stimulation with BMPs, perhaps depletion of endogenous BMPs would also result in a decrease in basal hepcidin, similar to IL-6, as MDA-MB-231 cells produce endogenous BMPs in addition to IL-6.

In the MCF-7 breast cancer cells, we found a similar, yet overall different pattern of hepcidin regulation in these cells, suggesting that hepcidin regulation may be cell-type specific in breast cancer cells. We found that in contrast to R5 and MDA-MB-231 breast cancer cells, MCF-7 cells do not produce IL-6, but instead produce high levels of endogenous BMPs (Figure 2-7 and Figure 3-1). Thus, we thought that BMPs may be regulating basal expression of hepcidin in MCF-7 cells. We first tried to stimulate MCF-7 cells with exogenous BMPs, but realized that no further increase in hepcidin could be observed, perhaps due to saturated BMP receptors, as BMPs seem to regulate basal hepcidin expression in these cells (Figure 2-7). Instead, due to the fact that endogenous BMP and hepcidin expression are high basally, we used two separate methods, neutralizing antibodies and siRNA to deplete endogenous BMPs and found a reduction in hepcidin, most prominently with reduction in BMP6 (Figure 3-1). This suggests that BMP signaling is at least partially responsible for increased basal hepcidin expression present in MCF-7 cells. Interestingly, unlike the R5 cells, which produce low levels of BMPs but respond to exogenous BMP for hepcidin induction, MCF-7 cells respond very modestly to exogenous IL-6, despite having low endogenous levels (Figure 3-1). This led us to hypothesize that MCF-7 cells may have low IL-6 receptor expression, which was confirmed by examining basal IL-6R expression in MCF-7 cells (Supplementary Figure 3-S1). Ultimately, this low expression could limit the robustness of a response for induction of hepcidin. However, it is interesting to note that we did see activation in the downstream mediator via phosphorylated STAT3, suggesting that MCF-7 cells were able to respond, at least in part, to IL-6 stimulation, despite low receptor expression. It is also possible that levels of hepcidin in MCF-7 cells are

relatively high to start (and higher than R5 cells at basal level), thus activating other known regulatory pathways of hepcidin may not result in any further increase in hepcidin expression, as the promoter may not respond to further stimulation by other transcription factors. However, some studies in the liver have found a synergistic effect from stimulating the promoter with both BMPs and IL-6 [105]. It would be interesting to first deplete endogenous BMPs in MCF-7 cells and subsequently treat BMP depleted cells with IL-6 to see if the response to IL-6 could be more robust in this context. This would enable us to determine if BMPs and IL-6 could compensate for one another for induction of hepcidin in breast cancer cells or hint that minimal IL-6R expression is limiting a significant effect on hepcidin by IL-6 stimulation.

Another interesting finding was that normal breast epithelial cells are also able to respond to exogenous stimulation by IL-6 (Figure 2-8). Human mammary epithelial cells produce low levels of BMPs and IL-6 and have basally low levels of hepcidin. However, upon exogenous stimulation with IL-6, we observed a significant increase in hepcidin expression (Figure 2-8). It would be interesting if exogenous stimulation by BMPs, specifically BMP6, would also result in similar hepcidin induction, as this would suggest that normal breast cells are able to respond to exogenous stimulation of BMPs and/or IL-6 for resulting increase in hepcidin expression. It would also be of importance to determine if this increase hepcidin from exogenous IL-6 stimulation is functional. One may expect FPN expression to be reduced and labile iron pool (LIP) to be increased as a result of increased hepcidin expression in stimulated HME cells. If the LIP is increased, it would be interesting to see if the growth rate of these cells would be increased as a result of increased intracellular iron. This would demonstrate that proliferation rates in normal cells could be increased directly as a result of stimulating hepcidin expression via IL-6 (and possibly BMPs).

We also examined the functionality of hepcidin induced by BMPs or IL-6. To do this, we used the T47-D breast cancer cells, a cell line that has prominent expression of FPN. Although induction of hepcidin in T47-D cells by BMPs or IL-6 wasn't robust, there was still enough of an

increase to see an effect on FPN (Figure 2-9). Although FPN degradation was not as dramatic as with recombinant hepcidin, there seemed to be a definite change in localization of FPN when hepcidin was stimulated with BMPs or IL-6, from cell surface, to more intracellular and punctate staining when hepcidin was induced exogenously. It would be interesting to see if this effect could be more enhanced if the experiment was carried out for a longer period of time, or if the addition of BMPs and IL-6 together could enhance the effect on FPN degradation.

Overall, we examined the role of BMPs and IL-6 in regulation of hepcidin in four separate breast cancer cell lines. We observed that different breast cancer cell lines have varying basal expression of BMPs and IL-6 and respond to exogenous BMP and IL-6 differently. It would be worth examining the role of BMPs and IL-6 in additional breast cancer lines of different molecular subtypes (ER, PR, HER2 status) to determine if a pattern of preferential regulation by BMPs or IL-6 exists by subtype or if it may be selective in a more random fashion. Ultimately, by understanding the mechanisms responsible for increased hepcidin in breast cancer, we hope to unveil molecular targets in hopes of reducing hepcidin expression in breast cancer cells. By targeting molecular regulators with the goal of depleting hepcidin, we hope that excess intracellular iron will be exported from cells and proliferation of breast cancer cells will be reduced.

Materials and Methods

Cell Line Culture

MCF-7, MCF-10A and MDA-MB-231 cells were obtained from the Wake Forest University Comprehensive Cancer Center Tissue Culture Core facility. MCF-10A and MCF-7 were verified by ATCC cell authentication testing service. HME cells were purchased from Lonza. HME cells transduced with h-TERT, SV40 T antigen, and high levels of H-ras are termed R5 cells here and were a gift from the laboratory of R. Weinberg [101]. T47-D cells were obtained from ATCC. MCF-7 and MDA-MB-231 cells were cultured in Dulbecco's minimal essential medium (DMEM)–

F12 (Gibco) supplemented with 10% FBS (Benchmark). MCF-10A and HME cells were cultured in Mammary Epithelial Growth medium (MEGM) bullet kit (Lonza catalog #CC-3150). MCF-10A media was supplemented with 100ug/ml cholera toxin (Sigma). T47-D cells were cultured in RPMI-1640 supplemented with 10% FBS and 10µg/mL human insulin (Life Technologies). All cells were maintained at 37°C in a humidified atmosphere containing 5% CO2.

Neutralizing antibody and recombinant protein treatments

All treatments were added to corresponding normal growth media (without serum) for 24 hours. Neutralizing antibodies (R&D systems) against IL-6 or isotope-matched IgG were used at 1 or 3 ug/mL. Human recombinant IL-6, BMP4, BMP6 or BMP7 (R&D systems) were used at 50, 100 or 200ng/mL. Human recombinant Hepcidin (Peptides International) was used at 800nM.

Real-time qPCR.

RNA was isolated and purified from cells using High Pure RNA Isolation Kit (Roche Diagnostics) following the manufacturer's instructions. Oligo(dT) primer was used in cDNA synthesis. Briefly, 200–400 ng of RNA was reverse transcribed in a total volume of 50 µl with a reverse transcription reagents kit (Applied Biosystems). To make a standard curve, serial dilutions of RNA from one sample were added to the RT reaction. Aliquots (2 µl) of cDNA were added to a 18 µl reaction mixture containing 10 µlof 2× SYBR® Green PCR Master Mix (BioRad) and 400 nm primers. The reaction included primer sequences specific to IL-6, BMP2, BMP4, BMP6, BMP7, hepcidin, ferroportin or β-actin depending on the experiments described. See Supplemental Table 3-S2 for primer sequences. Absence of DNA contamination was confirmed by performing PCR from cDNA without reverse transcriptase.

Western Blots

Samples were lysed in 1X RIPA buffer in the presence of protease and phosphatase inhibitors (Roche Diagnostics, Basel, Switzerland), were reduced with 10 mM β-mercaptoethanol and

proteins separated by SDS-PAGE. Western blots were probed with antibodies to phospho-Smad-1/5/8 (Cell Signaling), total Smad-5 (Cell signaling), Phospho-Smad2/3 (Cell Signaling), total-Smad2 (Cell Signaling), Phospho-STAT3 (Cell Signaling), Total STAT3 (Cell Signaling), hepcidin (Fitzgerald) or β-actin (Abcam). Western blots were quantified with Image J. Phosphorylated blots were quantified by normalization to corresponding total protein. Hepcidin blots were quantified by normalization to β-actin.

ELISA analysis for secreted IL-6 and Hepcidin

Secreted IL-6 was measured in conditioned growth media from HME and R5 cells using an IL-6 Human ELISA kit from R&D systems and following manufacturers' protocol. Secreted hepcidin was measured in conditioned growth media following 24 hours of IL-6, BMP4, BMP6 or BMP7 recombinant protein treatment using a Hepcidin-25 ELISA kit from Bachem Americas, Inc. and following manufacturers' protocol.

Immunofluorescence

T47-D cells were plated in 8-chamber slides and upon exogenous stimulation with BMPs or IL-6 for 24 hours, cells were fixed with 4% formaldehyde for 15 minutes and blocked with 5% BSA at 4°C overnight. Anti-human ferroportin (Amgen-38C8) was applied for one hour followed by 1:800 dilutions of rhodamine-green conjugated goat anti-human secondary antibody (Jackson ImmunoResearch). Slides were mounted with ProLong Gold anti-fade reagent (Invitrogen, Carlsbad, CA, USA). Images were acquired using a fluorescent inverted microscope (Zeiss Axio Vert.A1).

Statistical analysis

Statistical analyses were performed using Excel and are reported as the mean ± standard deviation. Error bars represent standard deviation. Unless otherwise noted, significant differences between control and treatment groups were determined using two-tailed unpaired Student's t tests.

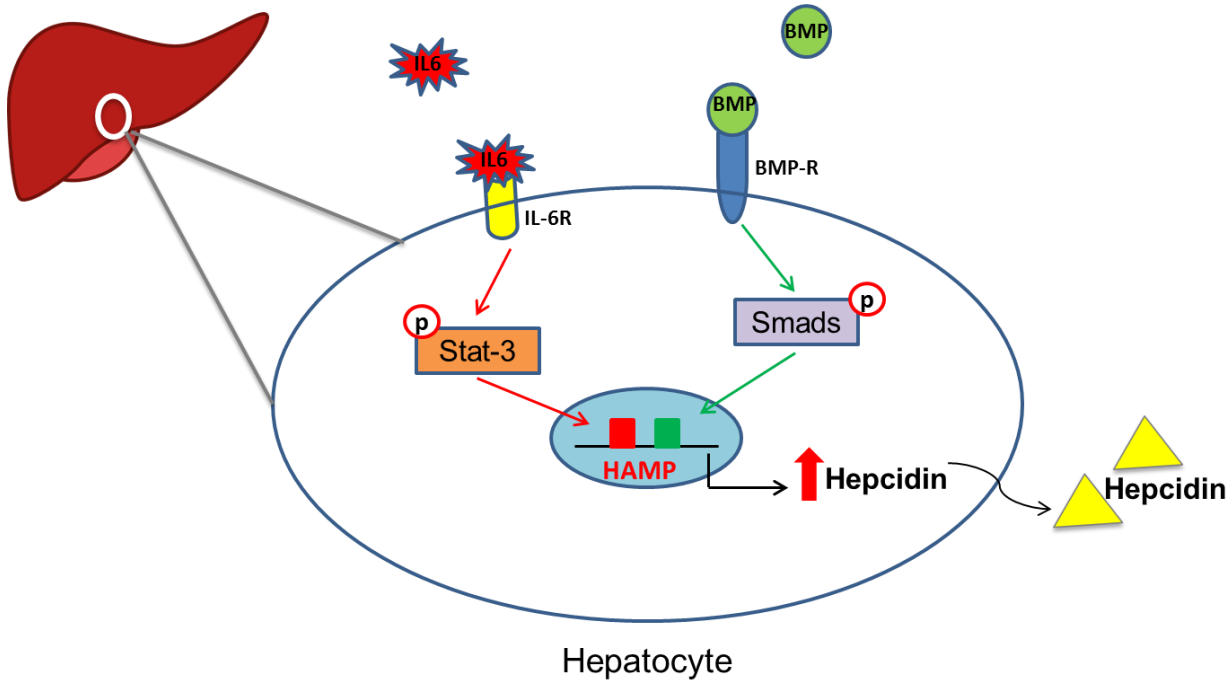

Figure 2-1. Regulation of hepcidin in the liver via BMPs and IL-6.
Previous studies have demonstrated that hepcidin is regulated in the liver transcriptionally by BMPs and IL-6. Each ligand binds to their respective receptor activating its corresponding downstream signal cascade leading to activation by phosphorylation of STAT3 and/or SMAD1-5-8/SMAD4 for IL-6 or BMP respectively. These transcription factors translocate to the nucleus where they bind to their respective responsive elements on the hepcidin promoter to trigger transcriptional activation of the hepcidin gene.

A

Transcript	BMP4	BMP6	BMP7	IL-6	Ferroportin	Hepcidin
R5	-	+	-	++	+	++

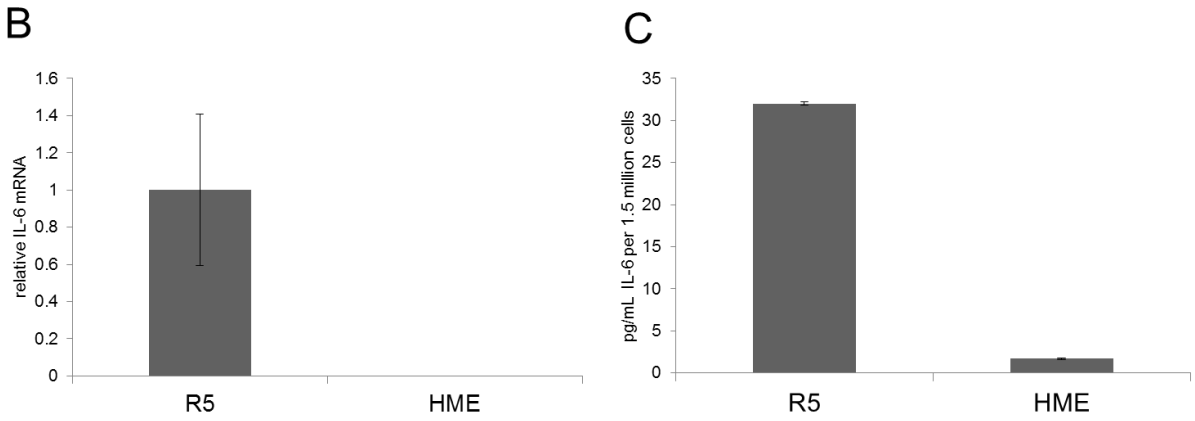

Figure 2-2. R5 breast cancer cells have increased IL-6 expression compared to normal human mammary epithelial cells. (A) Chart summary from RT-qPCR analysis of BMP4, BMP6, BMP7, IL-6, Ferroportin and Hepcidin mRNA (normalized to β-actin) in R5 breast cancer cells. (-) denotes no detectable expression, (+) denotes minimal transcript levels, (++) denotes moderate/high expression levels. (B) RT-qPCR of IL-6 (normalized to β-actin) comparing basal levels of IL-6 in R5 breast cancer cells and HME normal breast cells. (C) IL-6 ELISA for R5 and HME cells after 48 hours of secretion in normal growth media.

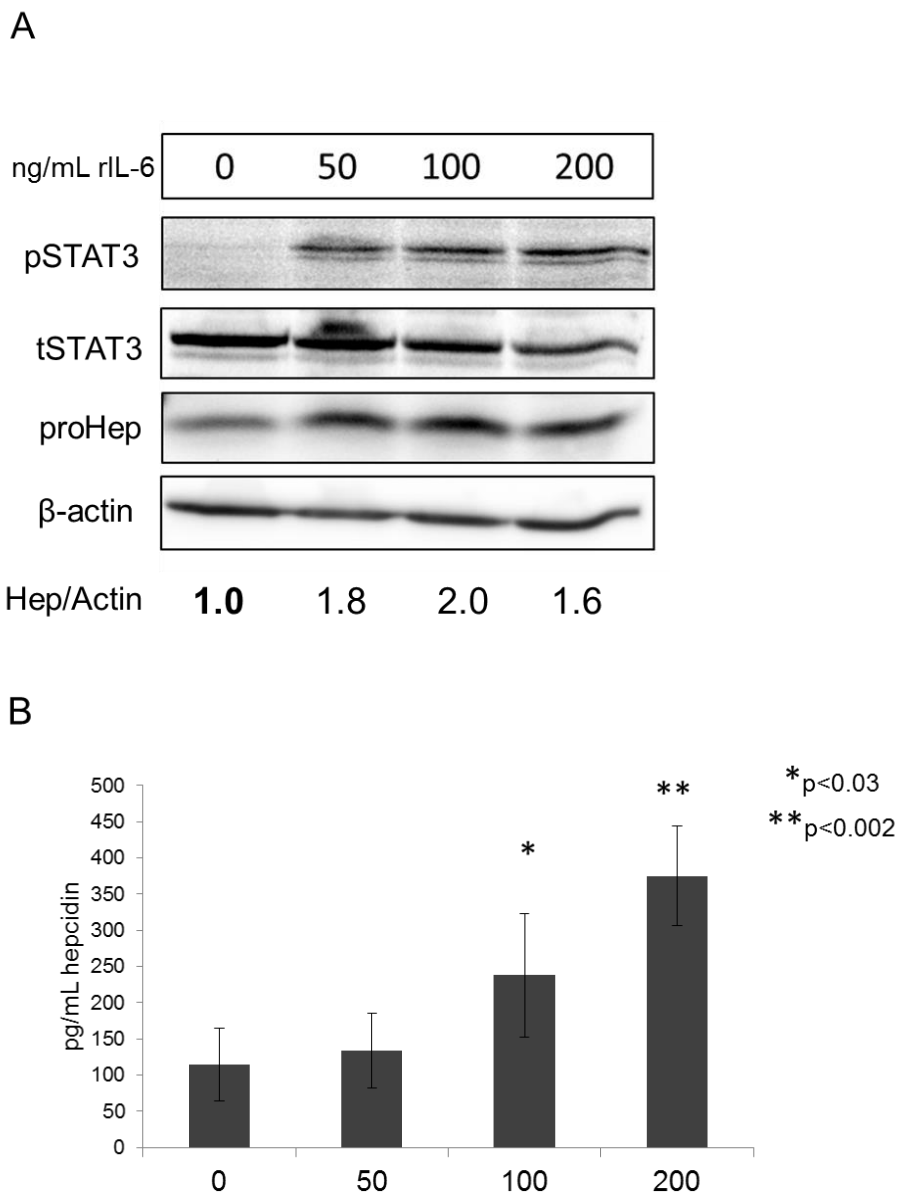

Figure 2-3. Hepcidin expression and secretion is increased and STAT3 is activated with exogenous IL-6 treatment in R5 Breast Cancer Cells.
(A) Western blot analysis of phosphorylated STAT3 (pSTAT3), total STAT3 (tSTAT3), pro-hepcidin and β-actin after 24 hours of rIL-6 treatment in R5 breast cancer cells. (B) Secreted Hepcidin, as detected by ELISA (Bachem) 24 hours following rIL-6 treatment in R5 breast cancer cells.

A

Transcript	BMP2	BMP4	BMP6	BMP7	IL-6	Ferroportin	Hepcidin
R5	++	-	+	-	++	+	++

B

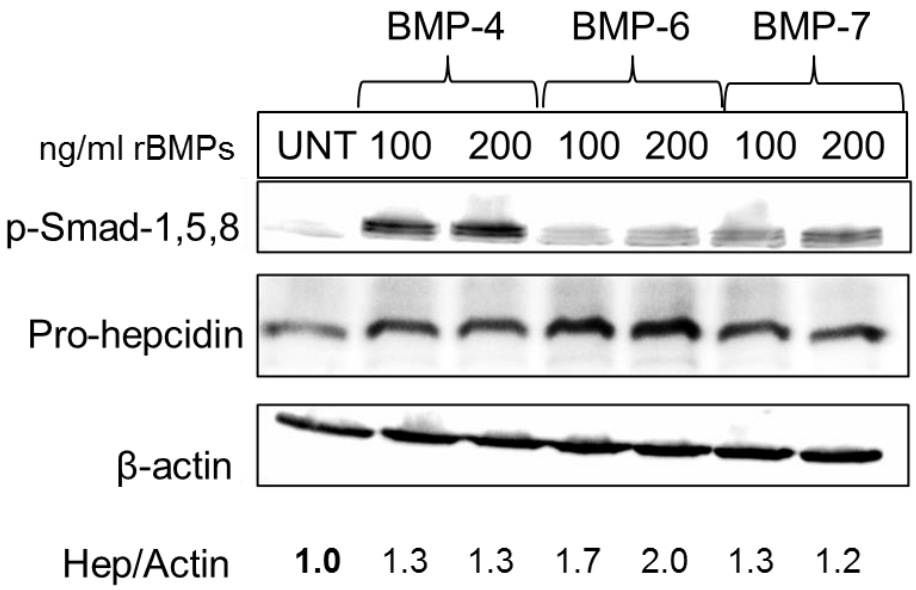

Figure 2-4. Exogenous BMPs positively regulate hepcidin expression in R5 BC cells. (A) Chart summary from RT-qPCR analysis of BMP2, BMP4, BMP6, BMP7, IL-6, Ferroportin and Hepcidin (normalized to β-actin) in R5 breast cancer cells. (-) denotes no detectable expression, (+) denotes minimal transcript levels, (++) denotes moderate/high expression levels. (B) Western blot analysis of phosphorylated SMAD1-5-8, pro-hepcidin and β-actin following treatment with recombinant BMP-4, -6 or -7 for 24 hours in R5 breast cancer cells.

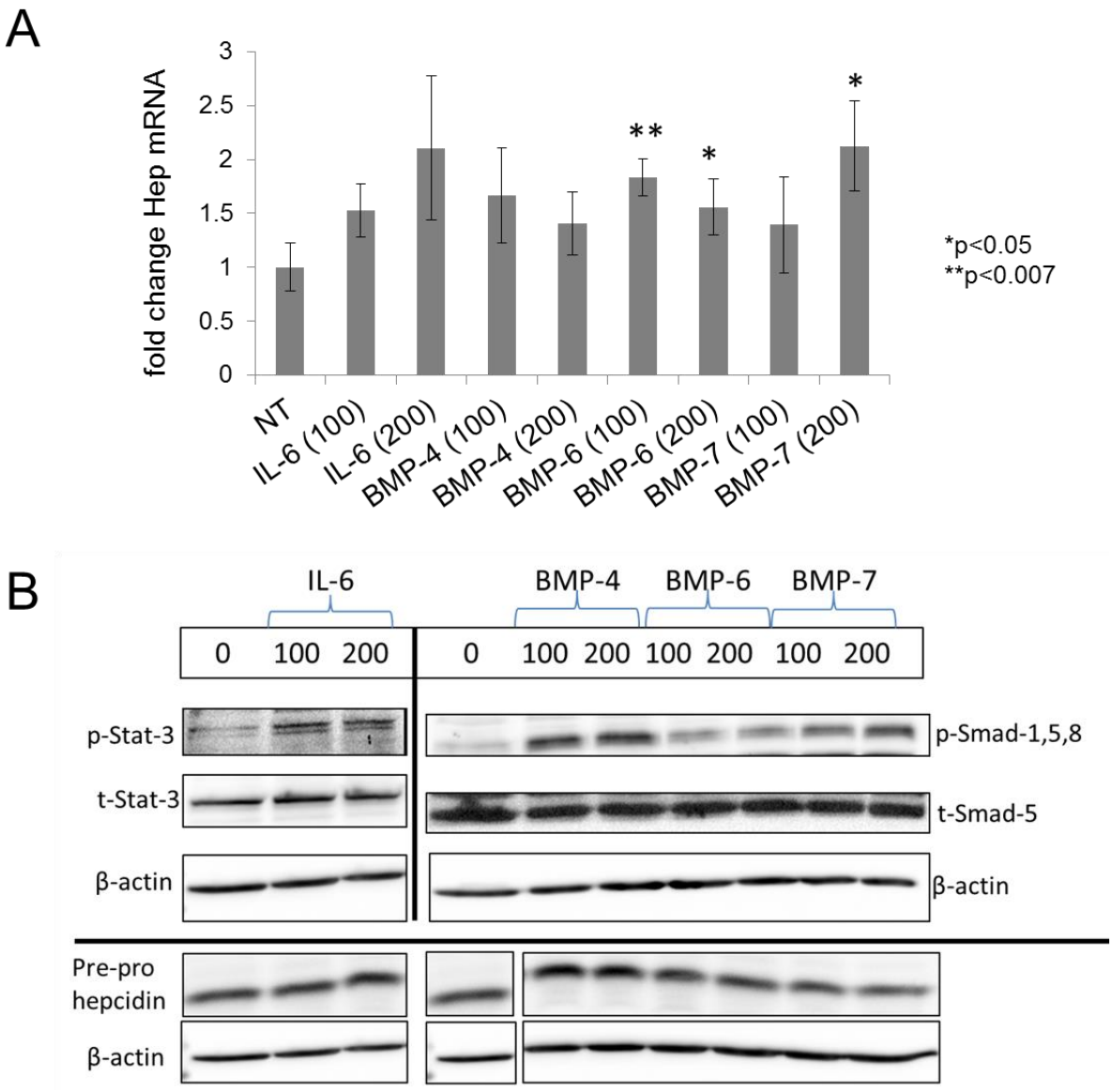

Figure 2-5. Exogenous BMPs and IL-6 have a limited effect on induction of hepcidin in MDA-MB-231 breast cancer cells.

(A) RT-qPCR of hepcidin (normalized to β-actin) and (B) Western blot of phosphorylated STAT3, total STAT3, pro-hepcidin and β-actin following recombinant BMP and IL-6 treatment for 24 hours in MDA-MB-231 cells.

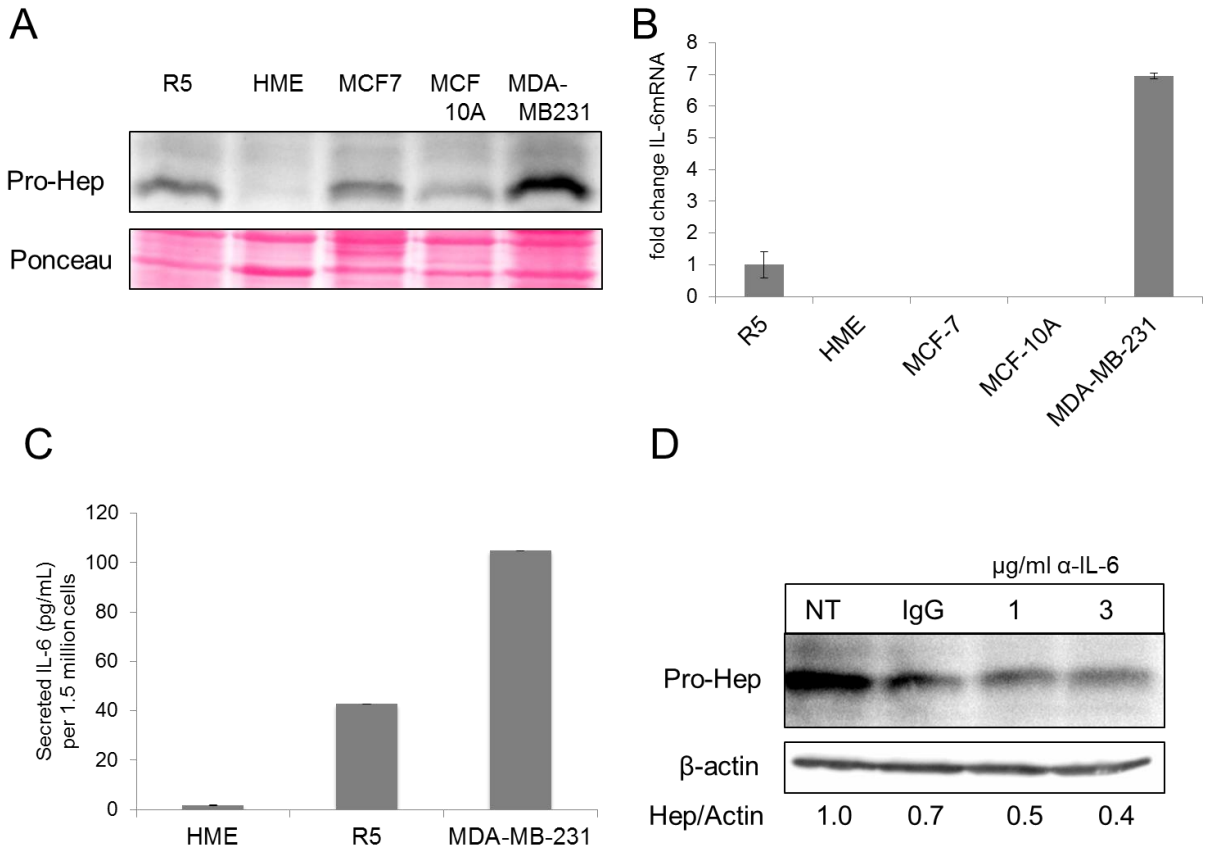

Figure 2-6. Depletion of endogenous IL-6 results in decreased hepcidin expression in MDA-MB-231 breast cancer cells.

(A) Western blot analysis of basal pro-hepcidin and Ponceau stain from R5, HME, MCF7, MCF-10A, MDA-MB-231 breast cells. (B) RT-qPCR of endogenous IL-6 mRNA (normalized to β-actin) from R5, HME, MCF7, MCF-10A, MDA-MB-231 breast cells. (C) ELISA analysis for secreted IL-6 levels in HME, R5 and MDA-MB-231 breast cells. (D) Western blot analysis of pro-hepcidin and β-actin following treatment with neutralizing antibodies against IL-6 (1=1µg/ml and 3=3µg/ml), IgG control (3µg/ml) or no treatment (NT) for 24 hours in MDA-MB-231 breast cancer cells.

A

Transcript	BMP4	BMP6	BMP7	IL-6	Hepcidin
MCF7	++	++	++	-	++

B

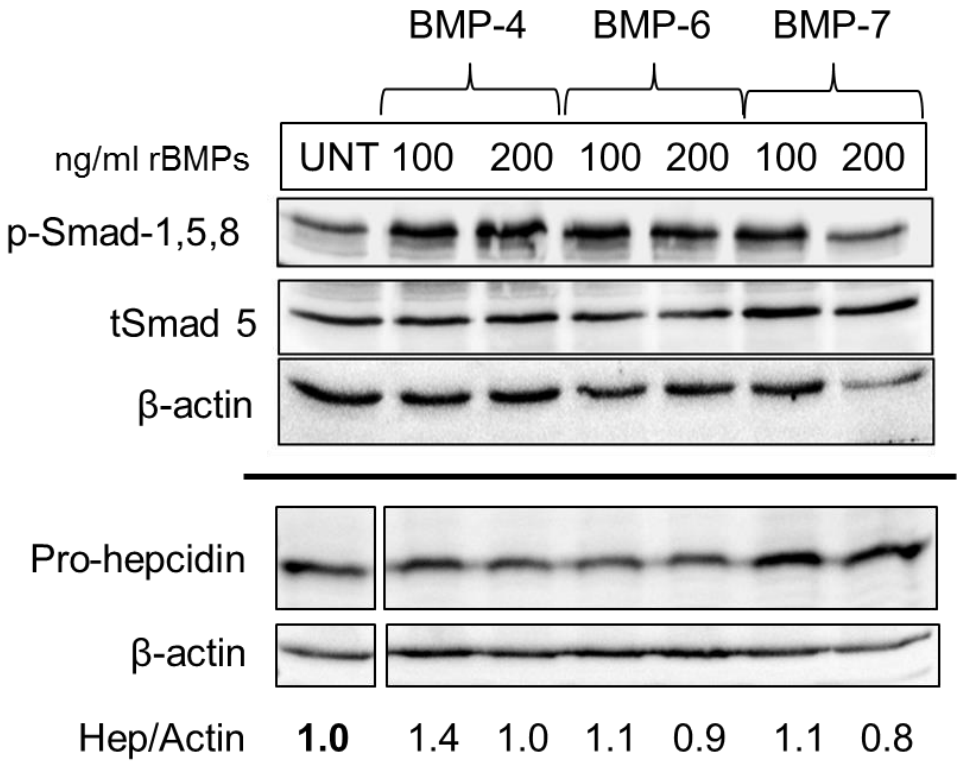

Figure 2-7. MCF-7 BC cells have no further induction of hepcidin with exogenous BMP treatment.

(A) Chart summary from RT-qPCR analysis of BMP4, BMP6, BMP7, IL-6 and Hepcidin mRNA (normalized to β-actin) in MCF-7 breast cancer cells. (-) denotes no detectable expression, (+) denotes minimal transcript levels, (++) denotes moderate/high expression levels. (B) Western blot analysis of phosphorylated SMAD1-5-8, total SMAD5, pro-hepcidin and β-actin following treatment with recombinant BMP-4, -6 or -7 for 24 hours in MCF-7 breast cancer cells.

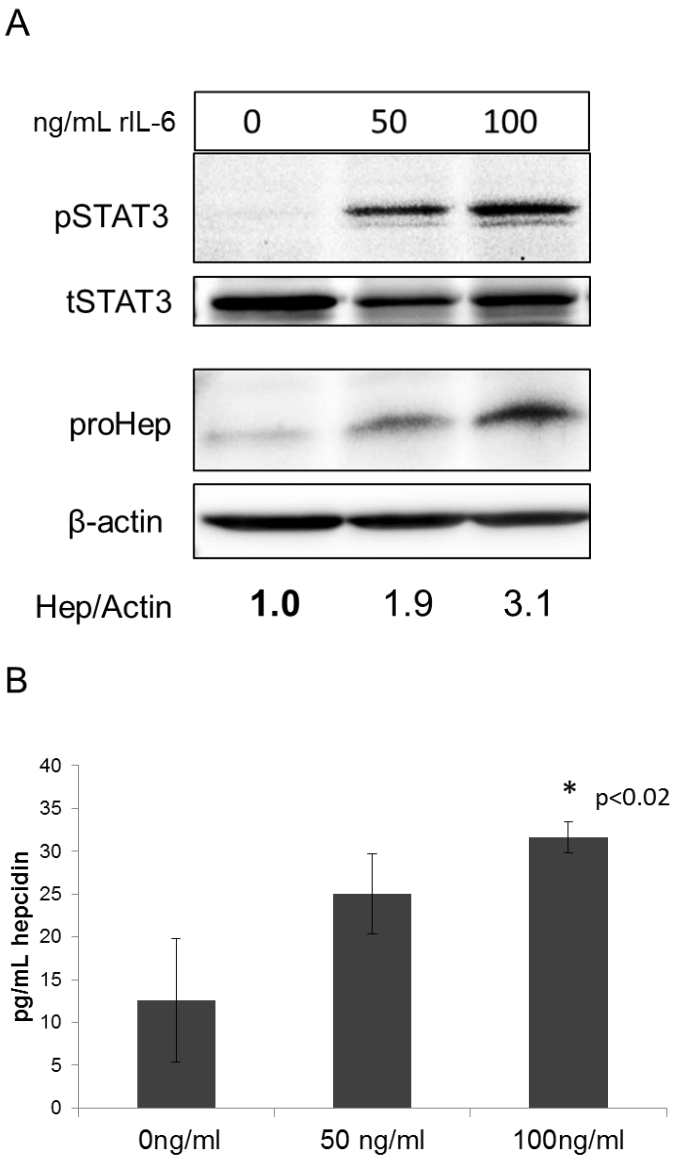

Figure 2-8. Normal breast epithelial cells (HME) can be stimulated exogenously with IL-6 for induction of Hepcidin.

(A) Western blot analysis of phosphorylated STAT3, total STAT3, pro-hepcidin and β-actin after 24 hours of rIL-6 treatment in HME normal breast cells. (B) Secreted Hepcidin, as detected by ELISA (Bachem) 24 hours following rIL-6 treatment in HME cells.

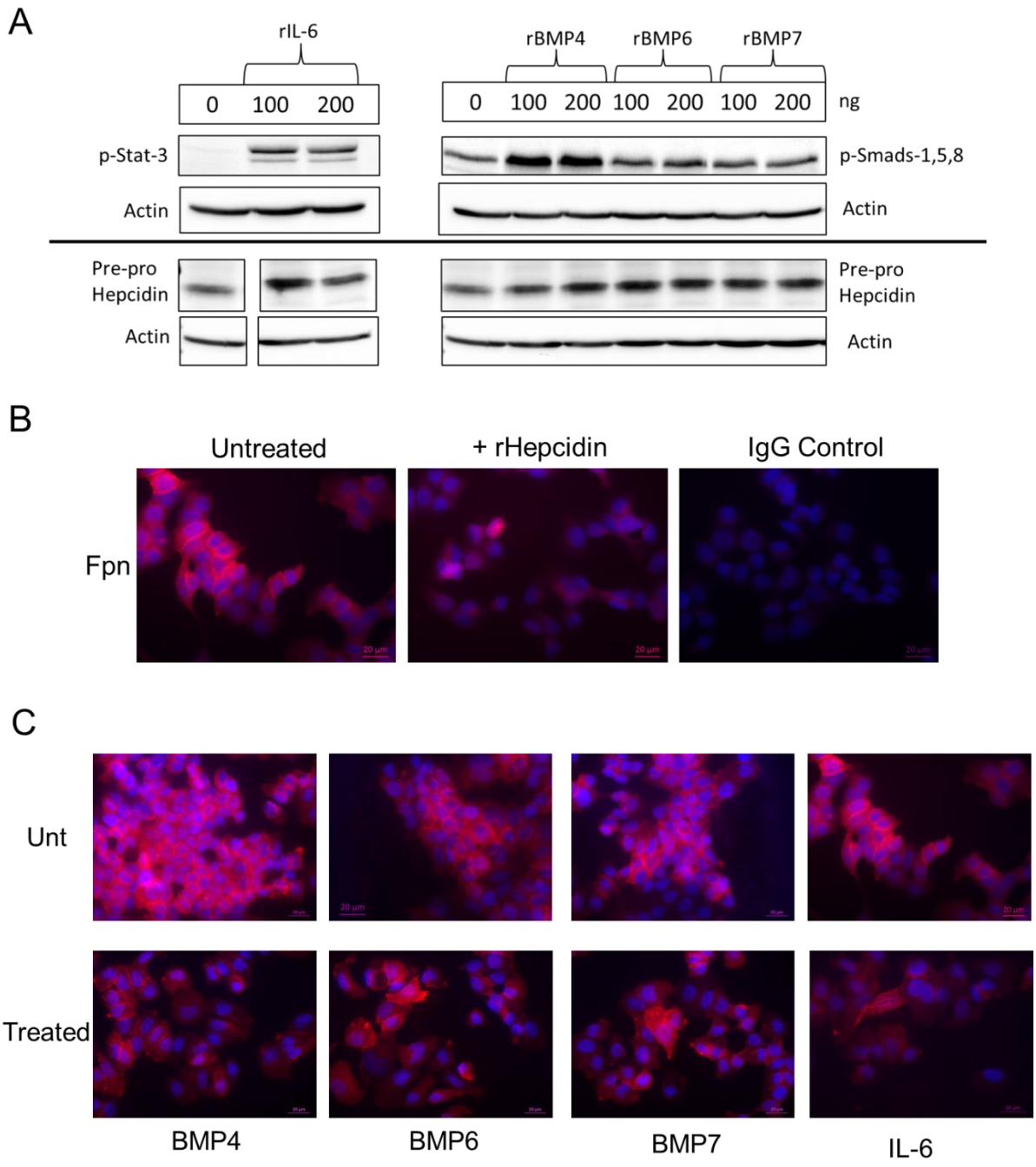

Figure 2-9. T47-D breast cancer cells respond to exogenous BMPs and IL-6 for induction of hepcidin that is functional.

(A) Western blot of phosphorylated STAT3 (pSTAT3), phosphorylated SMAD1-5-8, pro-hepcidin and β-actin following recombinant IL-6 treatment (0, 100, 200ng/mL) or recombinant BMP4, 6, or 7 treatment (0, 100, 200ng/mL) respectively in T47-D cells for 24 hours. (B) Immunofluorescence of FPN following 24 hours of 800nM recombinant Hepcidin treatment. (C) Immunofluorescence of FPN following 24 hours of 200ng/mL of rBMP4, rBMP6, rBMP7 or rIL-6.

Chapter III:

Contribution of three dimensional architecture and tumor-associated fibroblasts to hepcidin regulation in breast cancer

(Submitted to Oncogene)

Nicole Blanchette-Farra[1], Daniel Kita[2,6], Anna Konstorum[3], Lia Tesfay[1], David Lemler[1,7], Poornima Hegde[4], Xiaohong Wang[4], Kevin P. Claffey[2], Frank M. Torti[5], Suzy V. Torti[1]

[1]Department of Molecular Biology and Biophysics, University of Connecticut Health Center, Farmington, CT, USA
[2]Department of Cell Biology, University of Connecticut Health Center, Farmington, CT, USA
[3]Center for Quantitative Medicine, University of Connecticut Health Center, Farmington, CT, USA
[4] Department of Pathology, University of Connecticut Health Center, Farmington, CT, USA
[5]Department of Medicine, University of Connecticut Health Center, Farmington, CT, USA

[6]Current address: Alexion Pharmaceuticals, New Haven, CT, USA
[7]Current address: Department of Molecular Biomedical Sciences, North Carolina State University, Raleigh, NC, USA

Abstract

Hepcidin is a peptide hormone that negatively regulates iron efflux and plays an important role in controlling the growth of breast tumors. In patients with breast cancer, the combined expression of hepcidin and its receptor, ferroportin, predict disease outcome. However, mechanisms that control hepcidin expression in breast cancer cells remain largely unknown. Here we use three-dimensional breast cancer spheroids derived from cell lines and breast cancer patients to probe mechanisms of hepcidin regulation in breast cancer. We observe that the extent of hepcidin induction and pathways of its regulation are markedly changed in breast cancer cells grown in three dimensions. In monolayer culture, BMPs, particularly BMP6, regulate hepcidin transcription. When breast cancer cells are grown as spheroids, there is a 10-22 fold induction in hepcidin. Microarray analysis, combined with knockdown experiments, reveal that GDF-15 is the primary mediator of this change. This increase in hepcidin as breast cells develop a three-dimensional architecture increases intracellular iron, as indicated by an increase in the iron storage protein ferritin and a decrease in expression of ferroportin. Immunohistochemical staining of human breast tumors confirms that both GDF-15 and hepcidin are expressed in breast cancer specimens. Further, levels of GDF-15 are significantly correlated with levels of hepcidin at both the mRNA and protein level in patient samples, consistent with a role for GDF-15 in control of hepcidin in human breast tumors. Inclusion of tumor-associated fibroblasts in breast cancer spheroids leads to a further induction of hepcidin. This induction is mediated by fibroblast-dependent secretion of IL6. Breast cancer cells grown as spheroids are uniquely receptive to IL-6-dependent induction of hepcidin by tumor-associated fibroblasts, since IL-6 does not induce hepcidin in cells grown as monolayers. Collectively, our results suggest a new paradigm for tumor-mediated control of iron through the control of hepcidin by tumor architecture and the breast tumor microenvironment.

Introduction

Enhanced acquisition and retention of iron is a hallmark of breast cancer. This metabolic alteration results from changes in proteins of iron metabolism that increase iron uptake, alter iron storage, and/or reduce iron efflux: for example, transferrin receptor 1 (TfR1), the receptor that mediates uptake of transferrin-bound iron and the major iron importer cells, is frequently upregulated in breast cancer [1-3], as is IRP2, a master regulator of intracellular iron [4]. Conversely, ferroportin, an iron efflux pump, is downregulated in breast cancer cells and patient tissues. [5, 6].

Hepcidin, a peptide hormone that binds to ferroportin and triggers its degradation [7], plays an important role in breast cancer. Whereas the expression of ferroportin is down-regulated in breast cancer, expression of hepcidin is upregulated [5, 6]. Hepcidin secreted by breast cancer cells binds to ferroportin and initiates ferroportin degradation, thus blocking iron efflux and increasing iron retention [5, 6]. Knockdown of hepcidin in breast tumor cells inhibits growth of breast tumor xenografts, indicating that hepcidin produced by tumor cells makes an important contribution to tumor growth through an autocrine/paracrine loop [6]. Further, the combined expression profile of ferroportin and hepcidin is a powerful predictor of survival after mastectomy for women with breast cancer [5]. Thus, the ferroportin/hepcidin regulatory axis has significant impact on tumor growth and disease progression in breast cancer patients.
In addition to its role in breast cancer, hepcidin is involved in systemic iron homeostasis: hepcidin synthesized in the liver plays a critical role in controlling systemic iron trafficking by regulating ferroportin in intestinal cells, macrophages, and hepatocytes, and thus determining the delivery of iron to the circulation [8-10]). In the liver, numerous laboratories have shown that hepcidin is controlled transcriptionally by BMPs, principally BMP6 [11, 12], as well as by inflammatory cytokines such as IL-6 that increase transcription of hepcidin through a STAT3-mediated pathway [13].

In breast cancer, however, the pathways of hepcidin regulation are poorly understood. Here, we probe mechanisms of hepcidin regulation in breast tumors using both two-dimensional and, to better recapitulate tissue architecture, three-dimensional (3D) cell culture [14, 15] [16-18]. We also include tumor-associated fibroblasts in these three dimensional structures to facilitate study of the interactions that occur between the different cell types that are constituents of the tumor microenvironment. Further, in addition to breast cancer established cell lines, we use patient-derived cells that have been conditionally reprogrammed [19] to enable us to use breast cancer epithelial cells isolated directly from patients ([20]; see Materials and Methods). We report three major new findings. First, that three-dimensional culture of breast cancer cells uncovers a novel mechanism of hepcidin regulation involving GDF-15 secreted by breast epithelial cells. Second, that IL-6 derived from tumor fibroblasts further augments hepcidin secretion from breast cancer cells, implicating the tumor stroma in hepcidin regulation. Third, that the spatial organization of tumor cells alters responses to extracellular cues and activates additional pathways of hepcidin induction. These studies suggest a new paradigm for tumor-mediated control of iron through the control of hepcidin by tumor architecture and the breast tumor microenvironment.

Results

BMP6 plays a major role in hepcidin induction in MCF7 breast cancer cells

To investigate pathways that control hepcidin expression in breast cancer (BC), we initially examined MCF-7 cells, a well-studied breast cancer cell line [106]. We confirmed that as previously described [7], MCF-7 cells grown under conventional tissue culture conditions exhibited increased hepcidin compared to non-tumorigenic MCF-10A breast epithelial cells (Supplementary Figure 3-S1A and B), thus modeling the increased hepcidin seen in breast cancer.

We first considered the contribution of bone morphogenetic proteins (BMPs) and interleukin 6 (IL-6) to hepcidin regulation in breast cancer cells, since these pathways regulate hepcidin transcription in the liver through activation of SMAD and STAT3 signaling pathways, respectively [92, 93]. Measurement of endogenous transcript levels revealed that MCF-7 cells had higher expression of several BMPs implicated in control of hepcidin than MCF-10A cells, particularly BMPs-4, 6 and 7 (Figure 3-1A and Supplementary Table 3-S1). Additionally, MCF-7 cells expressed BMP receptors required for downstream BMP signaling (Supplementary Figure 3-S1C).

To directly test the role of BMPs in hepcidin regulation, we depleted endogenous BMPs with siRNA and assessed the effect on hepcidin. Knockdown of BMPs was efficient (60-95%) (Supplementary Figure 3-S1 D-F). Although depletion of all three BMPs reduced hepcidin (Figure 3-1B and C), knockdown of BMP6 resulted in a more pronounced decrease in hepcidin than knockdown of BMP4 or BMP7 when assessed at both the transcript and protein level (Figure 3-1B and C). siRNA-mediated inhibition of BMP6 decreased hepcidin to approximately the level seen in MCF10A cells. Antibodies directed at BMPs were also effective at reducing hepcidin, particularly anti-BMP-6, and to a lesser extent, anti-BMP4 (Figure 3-1D). We next investigated the role of IL-6 and the STAT3 signal transduction pathway to regulation of hepcidin in MCF7 cells. Although IL-6 transcripts were non-detectable (Supplementary Table 3-S1), MCF-7 cells expressed IL-6 receptor (Supplemental Figure 3-S1C). Further, alternative activators of STAT3 signaling such as IL-1, IL-5, interferons or epidermal growth factor (EGF) have been described [107-110], and it was possible that these might trigger STAT3 activation and increase hepcidin synthesis. We therefore treated MCF-7 cells with recombinant IL-6 and measured effects on activation of STAT3 and hepcidin. Although STAT3 was successfully activated by IL-6 under these conditions, there was no corresponding induction of hepcidin (Figure 3-1E). Taken together, these results suggest that among previously identified regulators of hepcidin, BMPs, particularly BMP6, play a predominant role in MCF-7 breast cancer cells.

Hepcidin is dramatically induced in breast cancer spheroids

Recent results have suggested that three-dimensional (3D) culture may be useful for studying metabolic changes in cancer, particularly breast cancer [111, 112]. To test whether additional pathways regulating hepcidin might be uncovered using three-dimensional culture, we grew MCF-7 breast cancer cells and the non-tumorigenic MCF-10A breast cell line as three-dimensional spheroids. Cells were plated in wells coated with poly(2-hydroxy-ethyl methacrylate)(polyHEMA), which prevents cell adhesion and fosters the spontaneous aggregation of cells into multicellular spheroids, as previously described [113]. As shown in Figure 3-2A, under these conditions both MCF-10A non-tumor and MCF-7 tumor cells formed viable spheroids as demonstrated by calcein-AM staining.

We measured hepcidin levels in MCF-10A and MCF-7 cells grown under these 3D culture conditions and compared them to hepcidin synthesized by cells grown in monolayers. As expected, hepcidin expression was increased in MCF-7 spheroids when compared to MCF-10A spheroids (Figure 3-2B and E). Strikingly, when levels of expression of hepcidin in cells grown under two and three dimensional culture conditions were compared, there was a 15 fold increase in hepcidin mRNA and 6-7 fold induction of hepcidin protein in MCF-7 cells grown in 3D (Figure 3-2C and F). This difference was not seen in MCF-10A cells, which exhibited similar levels of hepcidin under both two and three dimensional culture conditions (Figure 3-2D and G). Normal mammary epithelial cells (HME) similarly exhibited no increase in hepcidin when grown under 3D culture conditions (Supplemental Figure 3-S1G).

Hepcidin is induced in breast cancer spheroids prepared from patient cells

To confirm the selective induction of hepcidin in breast cancer spheroids, we next turned to primary breast epithelial cells. Breast cancer cells were isolated directly from breast tumors. At the same time, non-malignant breast epithelial cells were obtained from normal adjacent tissue to serve as patient-matched controls. Both malignant and non-malignant epithelial cells

were expanded on irradiated fibroblast feeder layers and re-plated in the absence of feeder layers prior to initiating experiments (detailed methodology is provided in Materials and Methods [114]). Cells exhibited typical epithelial markers, including E-cadherin and pan-cytokeratin (Supplementary Figure 3-S2A and B). Vimentin, a mesenchymal marker, was not expressed (Supplementary Figure 3-S2A). Tumor cells expressed higher levels of N-cadherin, a protein associated with breast cancer cell motility and invasion [115], than non-cancer epithelial cells isolated from the same patient (Supplementary Figure 3-S2A).

We then measured hepcidin levels in these patient-derived normal and tumor cells. Tumor cells expressed increased levels of hepcidin transcripts when compared to normal cells under both monolayer and 3D culture conditions (Supplementary Figure 3-2C and D). As we had observed in MCF-10A and MCF-7 cells, the difference in hepcidin expression was particularly pronounced in cells grown as spheroids. We also examined the expression of hepcidin using immunofluorescent staining. Consistent with changes observed at the mRNA level, there was a substantial increase in hepcidin in tumor cells (Figure 3-3A). This was accompanied by a decrease in ferroportin in tumor spheroids compared to spheroids from normal cells (Figure 3-3A), suggesting that hepcidin produced by spheroids is functional in targeting ferroportin for degradation. To confirm the functionality of hepcidin in breast tumor spheroids, we treated cells with two different anti-hepcidin antibodies and assessed the consequences of this treatment on levels of ferroportin. As expected, blockade of hepcidin by anti-hepcidin antibodies increased ferroportin, indicating that hepcidin synthesized by these cells exerts its expected biological activity (Figure 3-3B).

Next, we compared the effects of 3D culture on hepcidin in breast cancer and normal cells. Using primary breast tumor spheroids derived from four separate breast cancer patients (Table 3-1), we observed a marked hepcidin induction in 3D culture compared to 2D (Figure 3-3C and Supplementary Figure 3-S2 E-H), with increases in transcript levels ranging from 10 to 22 fold. In contrast to MCF10A cells, which did not increase synthesis of hepcidin when

cultured in 3D (Figure 3-2D and G), hepcidin was also induced in spheroids from normal cells, albeit at lower levels than in tumor cells (~3.5 fold transcriptionally) (Figure 3-3C).

To assess whether the increase in hepcidin observed in 3D cultures of tumor cells was associated with changes in intracellular iron, we measured levels of ferritin. Ferritin is an iron storage protein composed of H and L subunit types [116]. Because levels of ferritin are post-transcriptionally increased by iron [117-119], it is frequently used as a surrogate marker for intracellular iron [41, 120]. We anticipated that increased hepcidin would lead to decreased ferroportin, thus reducing iron efflux and increasing intracellular iron and ferritin. As shown in Figure 3-3E, expression of both ferritin H and L subunits was indeed increased from 2D to 3D culture in patient tumor cells, suggesting that the increased levels of hepcidin seen in tumor spheroids contributes to a phenotype of iron retention.

BMPs and IL-6 make modest contributions to hepcidin induction in breast cancer spheroids

We next sought to determine the regulatory pathways responsible for hepcidin induction in breast cancer spheroids. As seen with monolayer cells, measurement of transcript levels revealed that BMPs, particularly BMP-4, 6 and 7, were basally expressed in MCF-7 spheroids and expression was increased compared to MCF-10A spheroids (Supplementary Figure 3-S3 A-D). Additionally, MCF-7 spheroids expressed BMP receptors, and BMP receptor expression was enhanced in 3D culture compared to monolayer culture (Supplementary Figure 3-S3E). In contrast, and consistent with monolayer cells, expression of IL-6 was not observed in MCF-7 spheroids (Supplementary Figure 3-S3D).

To test the contribution of BMPs and IL-6 in regulation of hepcidin synthesis in spheroids, we first reduced levels of endogenous BMPs 4, 6 and 7 using siRNA (Supplementary Fig 3-S3 F-H) and assessed effects on hepcidin expression. Depletion of BMPs reduced hepcidin expression in MCF-7 spheroids (Figure 3-4A and 3-4B); depletion of BMP6 had the most pronounced effect, resulting in an approximate reduction of 30-35% in hepcidin transcripts

and protein compared to non-targeting control (NTC). Similar to what we had observed in 2D, there was no detectable expression of IL-6 or phosphorylation of STAT3 in MCF-7 spheroids (Figure 3-4C), and knockdown of STAT3 using siRNA only modestly reduced hepcidin transcripts (~20%) (Figure 3-4D).

Growth Differentiation Factor 15 (GDF-15) induces hepcidin expression in BC spheroids through activation of SMAD 1-5-8

Since none of the classical regulators of hepcidin explained the 10-22 fold transcriptional increase in hepcidin expression seen in spheroids (Figure 3-2C and Supplemental Figure 3-S2 E-H), we next examined differences in global gene expression between MCF-7 cells grown as monolayers and spheroids to search for non-canonical mechanisms that might underlie the induction of hepcidin in spheroids. To assure that differences we observed were independent of the specific method used to induce spheroid formation, we compared gene expression profiles from cells grown using three different methods of 3D culture: (1) spheroids cultured in polyHEMA-coated 96-well plates; (2) spheroids cultured in ultra-low attachment 96-well plates; and (3) spheroids cultured in 0.24% methylcellulose [78]. Hepcidin was upregulated to a similar extent using all three of these methods when compared to monolayer culture (Supplementary Figure 3-S4A).

Overall, from 1809 to 2117 genes were significantly differentially expressed in MCF-7 spheroids, depending on the 3D culture condition (Supplementary Table 3-S2). Specific gene expression changes observed between 2D and 3D were remarkably similar using each of the 3 methods of 3D cell culture (Table 3-2). GAGE Pathway analysis revealed that global differences in gene expression profiles induced by 3D culture were similar to those previously described, including cell cycle, DNA replication and mismatch repair (Table 3-3) [121-123]. Nine of the top 10 perturbed pathways were the same in all three 3D cases, although there were differences in their rank order (Table 3-3).

To search for inducers of hepcidin, we examined genes that were most significantly upregulated under all three 3D culture conditions (Table 3-2). Notable among these was GDF-15: induction of GDF-15 ranged from 16.07 to 21.9 fold (FDR p-value $p<0.009$) (Table 3-2). Expression (Bi-weight average signal (log2)) of GDF-15 was robust, with an average expression level roughly equivalent to the mean of all other genes expressed in these cells (Supplementary Figure 3-S4 B-D).

Growth differentiation factor-15 (GDF-15; also called MIC-1 [124]) is a member of the TGF-β superfamily that is up regulated in many cancers, including breast cancer [124, 125]. GDF-15 has previously been shown to correlate with and potentially regulate hepcidin, although in some contexts GDF-15 may act as an inhibitor rather than an activator of hepcidin (see Discussion and [63, 126-128]). We observed that GDF-15 was increased in our breast cancer cell models when compared to non-cancer cells: MCF-7 spheroids had increased GDF-15 compared to MCF-10A spheroids, as did patient tumor spheroids compared to spheroids derived from normal adjacent cells (Figure 3-5A and B). To confirm the induction of GDF-15 seen in the microarray analysis, we measured GDF-15 mRNA using RT-qPCR and GDF-15 protein using an ELISA assay in MCF-7 cells grown as monolayers or spheroids. As anticipated, MCF-7 spheroids exhibited increased GDF-15 expression (transcript and secreted protein) relative to monolayer cultures (Figure 3-5C and D). Increased expression of GDF-15 was correlated with increased hepcidin expression in 3D spheroids (Figure 3-5E and F). To confirm the generality of these findings, we also examined GDF-15 in patient-derived breast cancer cells. Similar to MCF-7 cells, primary tumor cells also exhibited a pattern of increased GDF-15 expression from 2D to 3D culture (Supplementary Figure 3-S5 A and B).

To directly test whether GDF-15 induced hepcidin, we used siRNA to reduce levels of GDF-15 in BC spheroids. We observed that efficient knock-down of GDF-15 (~85%; Supplementary Figure 3-S5 C and D) significantly reduced hepcidin expression at both at the transcript and protein levels (~70% and 40% respectively) (Figure 3-6A and B and

supplementary Figure 3-S5E). Although GDF15 knockdown did not completely abrogate the induction of hepcidin seen in spheroids (Figure 3-6A), reducing GDF-15 had a greater inhibitory effect than blocking either BMP6 or STAT3 (Figure 3-4).

GDF15 dependent hepcidin induction in spheroids is mediated by SMAD 1-5-8

Our next goal was to assess the signaling pathway linking GDF-15 to hepcidin production. Although GDF-15 downstream signaling is incompletely understood, there is evidence that GDF-15 may utilize the SMAD pathway [44, 45]. SMAD signaling proceeds via two divergent pathways: pSMAD2-3 (TGFβ signaling) and pSMAD1-5-8 (BMP signaling) [46]. We assessed the activity of both these pathways in 2D versus 3D culture using a western blot for activated (phosphorylated) SMAD2-3 and SMAD1-5-8. As shown in Figure 3-6C, only SMAD1-5-8 was activated from 2D to 3D culture of MCF-7 cells. Further, reduction of GDF-15 in MCF-7 spheroids using siRNA simultaneously reduced SMAD 1-5-8 activity (Figure 3-6D) and hepcidin synthesis (Figure 3-6A), supporting a role for SMAD 1-5-8 signaling in GDF-15-mediated control of hepcidin transcription in spheroids. This result prompted us to examine a role for GDF-15 in control of hepcidin in 2D. As shown in Figure 3-6, hepcidin levels did not change following either knockdown of GDF-15 (Figure 3-6E and F and Supplementary Figure 3-S6 A-D) or addition of exogenous GDF-15 (Supplementary Figure 3-S6E) in 2D cultures. Together, these data suggest that GDF-15 regulates hepcidin induction breast cancer spheroids selectively, and does so through the activation of a SMAD 1-5-8-dependent pathway.

Expression of GDF-15 and hepcidin are correlated in breast cancer tissue

To test whether an association between GDF-15 and hepcidin was also present in breast cancer tissue, we first analyzed hepcidin (gene symbol HAMP) and GDF-15 (gene symbol GDF15) transcripts in the publicly available TCGA breast cancer dataset [47]. Levels of both transcripts were significantly increased in cancer tissue (n=526) compared to normal

adjacent tissue (n= 61) ($p<2x10-12$ for GDF15, $p<0.002$ for HAMP) (Figure 3-7A and B). We divided tumors into two groups based on hepcidin expression (above or below the mean) and assessed GDF-15 expression in these two groups. GDF-15 expression was significantly different among the high and low subdivisions of HAMP ($p<0.01$), with high HAMP associated with high GDF-15 expression (Figure 3-7C). Similarly, when tumors were divided into two groups based on GDF-15 expression, high GDF-15 was significantly associated with high HAMP ($p<0.04$) (Figure 3-7D).

To explore the relationship between GDF-15 and hepcidin at the protein level and to assess whether both proteins were expressed in breast epithelial cells, we performed immunohistochemical analysis of tumor sections from 56 breast cancer patients. As shown in Figure 3-7E, expression of both GDF-15 and hepcidin was evident in breast cancer tissue. Staining with pan-cytokeratin confirmed the expression of both proteins in epithelial cells. Expression of GDF-15 and hepcidin were also faintly evident in some surrounding stromal cells (Figure 3-7E). Further, as shown in Figure 3-7E and 3-7F, there was a strong positive correlation between GDF-15 and hepcidin in epithelial cells ($R2=0.44$, $p<3x10-8$), consistent with a role for GDF-15 in regulation of hepcidin in human breast tumors *in vivo*.

Tumor Associated Fibroblasts Contribute to hepcidin induction via paracrine IL-6 signaling

In addition to autocrine regulation of hepcidin by tumor epithelial cells themselves, we asked whether other cell types in the tumor microenvironment might contribute to hepcidin induction. In particular, we focused on tumor associated fibroblasts (TAFs), since these cells are known to support tumor growth through secretion of pro-inflammatory cytokines and growth factors [48]. TAFs isolated from patient tumor tissue were fibroblastic in shape and expressed vimentin, a mesenchymal marker (Supplementary Figure 3-S7A). When TAFs were co-cultured

with tumor epithelial cells (TECs), we observed a significant increase in hepcidin (Figure 3-8A and B).

We then explored the mechanism of TAF-dependent induction of hepcidin. To test whether the induction of hepcidin by TAFs required direct cell contact or was mediated by a secreted factor, we prepared conditioned medium from TAFs and cultured TEC spheroids in this medium. As shown in Figure 3-8C, an increase in hepcidin was detected when TEC spheroids were exposed to conditioned media (CM) from TAFs, supporting the role of a secreted factor in hepcidin induction. We then measured levels of known hepcidin agonists in TAFs. We found that TAFs produced copious IL-6, with no detectable levels of BMP6 or GDF-15 (Supplementary Figure 3-S6B). Additionally, primary tumor epithelial cell (TEC) spheroids expressed IL-6 receptor (IL-6R), suggesting their potential ability to respond to paracrine IL-6 signaling (Supplementary Figure 3-S7C).

We therefore tested whether the TAF factor that induced hepcidin was IL-6. TEC were cultured in the presence of either TAFs or TAF CM and pSTAT3, the downstream signal activator of IL-6, was measured. As shown in Figure 3-8D, both TAFs and TAF conditioned medium activated STAT3. We then directly evaluated the role of IL-6 in stimulating hepcidin by incubating the conditioned medium with neutralizing anti-IL-6 antibody before addition to TEC spheroid culture. We found that depletion of IL-6 from CM (Supplementary Figure 3-S7D) significantly reduced hepcidin levels (Figure 3-8E and F). Consistent with these results, the addition of recombinant IL-6 to TEC cultures stimulated hepcidin synthesis (Supplementary Figure 3-S7 E and F). These results suggest that TAFs in the tumor microenvironment contribute to the synthesis of hepcidin in breast cancer epithelial cells through secretion of IL-6. A model of hepcidin regulation in breast cancer is shown in Figure 3-9.

Discussion

The significant association between iron efflux pathways and breast cancer patient outcome [7], as well as the role of hepcidin in breast cancer tumor growth *in vivo* [28] prompted us to investigate mechanisms of hepcidin control in breast cancer. We used 3D culture of both breast cancer cell lines and patient-derived breast tumor cells to more fully explore mechanisms controlling hepcidin synthesis *in vivo*.

Three dimensional culture is an important tool in the study of breast cancer growth and metabolism that can provide unique biological insights not evident in cells grown in 2D [129]. It has been suggested that 3D culture may more successfully predict tumor cell behavior in vivo than 2D models, since breast cancer cells grown in 3D exhibit a gene expression profile that more closely mimics human tumors than cells grown in 2D [76, 77]. 3D culture is a promising tool for drug screening that may more accurately predict clinical success of anti-cancer drugs [130, 131]. In the present study, we found that BMPs, particularly BMP6, were important regulators of hepcidin synthesis in breast cancer cells grown in both 2D and 3D (Figure 3-1 B,C and Figure 3-4 A,B). However the growth of breast cells in 3D allowed additional regulatory mechanisms to become evident.

The first novel pathway of hepcidin regulation that we observed in cells grown in 3D was mediated by GDF-15. GDF-15 is a member of the TGF-β superfamily that plays a broad role in tissue homeostasis and repair [124]. GDF-15 is induced in response to inflammation, acute injury or malignancy [125, 132, 133]. Serum levels of both GDF-15 and hepcidin are increased in patients with breast cancer [28, 125] and other malignancies [126-128]. GDF-15 may play multiple roles in cancer; however, studies in breast cancer cells have suggested a role of GDF-15 in enhanced invasion as well as in maintenance of breast cancer stem cells [134, 135]. We observed that GDF-15 and hepcidin mRNA were both elevated in primary cells from breast tumor tissue compared to normal adjacent tissue (Figure 3-3 and Figure 3-5). Further, immunohistochemical staining of breast cancer tissue arrays (Figure 3-7E) as well as

interrogation of publicly available microarray datasets from breast cancer patients (Figure 3-7 A-D) indicated that there was a positive correlation between GDF-15 and hepcidin in breast tissue. Our work thus extends the known functions of GDF-15 to the local regulation of hepcidin in tumor tissue, representing a new role for GDF-15 in tumorigenesis. Specifically, the upregulation of GDF-15 and consequent increase in hepcidin in tumor tissue may foster tumor growth by enhancing tumor iron retention. The decrease in ferroportin and increase in ferritin we observed in tumor spheroids (Figure 3-3) is consistent with this interpretation.

GDF-15 has previously been described as a negative regulator of hepcidin, since high serum levels of GDF-15 in patients with β-thalassemia were associated with suppression of hepatic hepcidin [63]. However, in this same study, the response of hepatoma cells to GDF-15 in vitro was shown to be biphasic, with lower levels of GDF-15 stimulating hepcidin synthesis, and higher levels (≥ 10,000 pg/ml) inhibiting hepcidin [63] . We observed that the level of GDF-15 produced by breast cancer spheroids ranged from 100-500 pg/ml, consistent with an inductive effect of GDF-15 on hepcidin.

GDF-15 and the BMPs are both members of the TGF-β superfamily. Previous work has identified SMAD-1,5,8 as the regulatory pathway that mediates induction of hepcidin by BMPs in hepatocytes [50]. Although the receptor(s) and signaling pathways activated by GDF-15 have been less well studied than those that mediate BMP activity, experiments presented here suggest that GDF-15 and BMP6 may converge on the same downstream signaling pathway to induce hepcidin. Thus we observed that pSMAD-1,5,8 was elevated from 2D to 3D culture of breast cancer cells, and that both hepcidin and activated SMAD-1,5, 8 were abrogated when GDF-15 was decreased with siRNA (Figure 3-6).

The second major observation to emerge from this study is that stromal cells in the tumor microenvironment can contribute to regulation of hepcidin synthesis in breast tumor cells. Stromal cells play a significant role in breast tumorigenesis and secrete factors such as TGF-β and IGF-1 that can directly activate pathways in tumor epithelial cells (TECs)[136] (reviewed in

[136], [104]). For example, TAFs have been found to secrete CXCL12 for promotion of proliferation, migration and invasion of breast tumor epithelial cells [137]. We found that IL6 secreted by TAFs significantly contributes to hepcidin synthesis (Figure 3-8). TAFs grown in the absence of TECs showed minimal hepcidin expression (Figure 3-8A and B), suggesting that co-culture induces hepcidin primarily in TECs rather than in the TAFs themselves. Consistent with this interpretation, conditioned media from TAFs induced hepcidin in TECs to a similar extent as co-culture with TAF cells (Figure 3-8C).

Since IL-6 was the only ligand previously associated with induction of hepcidin that was produced by TAFs, and TAF-mediated induction of hepcidin could be blocked by anti-IL-6 antibody (Figure 3-8), our experiments suggest that IL-6 is the major and perhaps only factor secreted by TAFs that influences hepcidin synthesis. However a limitation of our studies is that we were unable to isolate TAFs from multiple patient samples. In addition, multiple additional cell types populate the tumor microenvironment, including immune cells of multiple lineages [138]; thus, more extensive analyses may uncover additional regulators that contribute to fine-tuning hepcidin synthesis in the tumor microenvironment. Interestingly, although we did not observe secretion of GDF-15 in breast cancer TAFs (Supplementary Figure 3-S7B), GDF-15 is secreted by TAFs isolated from prostate tumors and promotes prostate tumorigenesis [139]. Since hepcidin is also upregulated in prostate tumors [8], it is possible that prostate cancer, TAFs may contribute to hepcidin synthesis through secretion of GDF-15.

A third observation to emerge from our studies is that an alteration in the spatial configuration of tumor cells is sufficient to alter responses to extracellular cues and activate additional pathways of hepcidin induction. Thus, although cells grown in 2D displayed receptors rendering them potentially responsive to IL-6, hepcidin synthesis was not triggered by treatment with exogenous IL-6 in cells grown in 2D (Figure 3-1E). In contrast, breast cancer cells grown in 3D induced hepcidin when exposed to IL-6 (Figure 3-8 and Supplemental Figure 3-S7 E and F).

This result underscores the importance of spatial organization in the activation of tumor signaling pathways, including those that regulate iron metabolism.

Collectively, the experiments presented here demonstrate the existence of multiple mechanisms that coordinately control hepcidin synthesis in breast tumor spheroids. Studies of mechanisms through which tumor cells and cells in the tumor microenvironment regulate synthesis of hepcidin may not only uncover new pathways through which hepcidin is controlled, but may ultimately suggest new strategies for inhibiting local synthesis of hepcidin that can be used to target the metabolic dependence of tumor cells on iron.

Materials & Methods

Cell Line Culture

MCF-7 and MCF-10A cells were obtained from the Wake Forest University Comprehensive Cancer Center Tissue Culture Core facility and verified by ATCC cell authentication testing service. HME cells were purchased from Lonza. MCF-7 cells were cultured in Dulbecco's minimal essential medium (DMEM)–F12 (Gibco) supplemented with 10% FBS (Benchmark). MCF-10A and HME cells were cultured in Mammary Epithelial Growth medium (MEGM) bullet kit (Lonza catalog #CC-3150). MCF-10A media was supplemented with 100ug/ml cholera toxin (Sigma). All cells were maintained at 37°C in a humidified atmosphere containing 5% CO2.

Patient Sample Isolation

Tumor and adjacent non-tumor human mammary tissue was obtained under the approval of the Institutional Review Board of UConn Health and was de-identified. Fresh specimens were put into F media [4] [3:1 v/v Ham's F12 Nutrient Mix: Dulbecco's Modified Eagle Medium (Life Technologies), 5% fetal bovine serum (Gemini Bio-Products), 0.4 µg/mL hydrocortisone (Stemcell Technologies), 5 µg/mL human insulin (Life Technologies), 8.4 ng/mL cholera toxin (Sigma), 10 ng/mL epidermal growth factor (Life Technologies), 24 µg/mL adenine

(Sigma), penicillin-streptomycin (Life Technologies), and 10 µmol/L Y-27632 (Tocris)], and placed immediately on ice.

Primary Cell Culture

Primary cell culture was performed using conditional reprogramming technique previously described [114]. Briefly, specimens were removed of excess fat, minced, and then digested in 0.1 U/mL collagenase and 0.8 U/mL dispase (Roche) for approximately 1-2 hrs at 37˚C. The cell suspension was passed through a 100 µm nylon filter and centrifuged at 400 x g. The cell pellet was resuspended in F media and washed three more times to ensure removal of the proteases. For tumor associated fibroblast (TAF) culture propagation (when applicable), half of the resuspended cell pellet was directly plated in dishes overnight in F-media and re-fed the next day with F-media minus cholera toxin. TAFs were cultured in a 37˚C humidified incubator with 5% CO2 and 7% O2. Expanded cells were trypsinized with 0.05% trypsin and replated up to five passages before freezing as stocks. For tumor/adjacent normal epithelial cells, the remaining resuspended cell pellet was plated onto irradiated (4000 Rad) mouse NIH 3T3 fibroblasts in the presence of 10 µmol/L Y-27632 (Tocris) and cultured in F-media at 37˚C humidified incubator with 5% CO2 and 7% O2. Cells were passaged by differential trypsinization; when approximately 90% confluent, the cells were incubated with 0.05% trypsin (Life Technologies) to first remove the feeder fibroblast cells. The detached fibroblasts were aspirated and the remaining epithelial cells were incubated with 0.25% trypsin until detached. The cells were neutralized with equal volume F media, gently triturated to generate a single cell suspension, and centrifuged at 400 x g. The cells were resuspended in F media and passaged at 1:2 – 1:4 ratios onto irradiated feeder cultures. NIH 3T3 fibroblasts were maintained in DMEM supplemented with 10% FBS and 1% Pen-Step for initial culturing before use as a feeder layer. For use in all experiments, primary cells were passaged directly from conditional reprogrammed

conditions and plated as monolayers or spheroids without 3T3 fibroblasts in F-media without Y-27632 to re-differentiate cells for at least 2 days.

Spheroid Culture

24 hours before spheroid plating, U-bottom 96-Well Polystyrene Round Bottom Microwell Plates (Fischer Scientific) were coated with Poly(2-hydroxyethyl methacrylate) (polyHEMA) (Sigma). Briefly, 2.4g of polyHEMA (Sigma) was dissolved in 20mL of 70% EtOH to make a 10X stock. A 1X solution was prepared with 70%EtOH and 30ul per well was added. Plates were left in laminar flow hood overnight to ensure EtOH evaporation. To generate spheroids, cells were passaged from monolayer cultures and cells were seeded at 8,000 cells/well in polyHEMA coated plates in corresponding normal growth media. In some experiments, spheroids were plated in basal growth media containing no serum. To examine spheroid viability, 2uM calcein-AM was added to spheroid wells and live spheroids were imaged using a fluorescent inverted microscope (Zeiss Axio Vert.A1). For microarray analysis only, additional spheroid techniques were used, including plating 8000 cells in ultra-low attachment 96-well plates (Corning) or the addition of methylcellulose (0.24% total) as an aggregating agent, as previously described by Longati et al. [78].

Tumor Associated Fibroblast (TAF) and Tumor Epithelial Cell (TEC) Co-Culture & Conditioned Media Treatments

Tumor associated fibroblasts (TAFs) were propagated in F-media. For conditioned media (CM) experiments, 90% confluent cultures were replenished with fresh F-media and allowed to secrete for 48 hours before removal of CM and subsequent addition of CM to TEC cultures (8000 cells/spheroid). For direct co-cultures, TECs were trypsinized and TAFs were trypsinized and irradiated (4000 rad). For co-culture spheroid generation, co-cultures were produced by mixing 80% TEC/20% TAF (6400/1600) or 100% TEC/20% TAF (8000/1600) in F-media immediately before plating as spheroids.

Neutralizing antibody and recombinant protein treatments

For neutralization of BMPs, cells were treated with 1 or 3 μg/mL anti-BMP4, anti-BMP6, anti-BMP7, (R&D Systems) or 3 μg/mL isotope-matched anti-IgG (R&D systems). For neutralization of hepcidin, spheroids were treated during time of plating with 1 or 3ug/mL of anti-Hepcidin-25 (Amgen-19D12[140]; referred to as αHep#1), anti-Hepcidin-25 (Abcam; referred to as αHep#2) or anti-IgG (R&D systems) for 48 hours. For neutralization of IL-6 in TAF conditioned media, TAF conditioned media was collected as described above and pre-treated with 1 or 5 μg/mL anti-IL-6 or isotope-matched anti-IgG neutralizing antibodies (R&D Systems) for one hour before addition of CM to TEC spheroids. Human recombinant IL-6 (R&D Systems) was used at 2 and 200 ng/mL. Human recombinant GDF-15 (R&D Systems) was used a 0.1, 1, 10, 100 and 200 ng/mL.

Real-time qPCR.

RNA was isolated and purified from cells using High Pure RNA Isolation Kit (Roche Diagnostics) following the manufacturer's instructions. Oligo(dT) primer was used in cDNA synthesis. Briefly, 200 – 400 ng of RNA was reverse transcribed in a total volume of 50 μl with a reverse transcription reagents kit (Applied Biosystems, Foster City, CA, USA). To make a standard curve, serial dilutions of RNA from one sample were added to the RT reaction. Aliquots (2 μl) of cDNA were added to a 18 μl reaction mixture containing 10 μl of 2× SYBR® Green PCR Master Mix (Bio-Rad, Hercules, CA, USA) and 400 nm primers. See Supplemental Table 3-S2 for primer sequences. Absence of DNA contamination was confirmed by performing PCR from cDNA without reverse transcriptase.

Western Blots

Samples were lysed in 1X RIPA buffer in the presence of protease and phosphatase inhibitors (Roche Diagnostics, Basel, Switzerland), were reduced with 10 mM β-mercaptoethanol and

proteins separated by SDS-PAGE. Western blots were probed with antibodies to phospho-Smad-1/5/8 (Cell Signaling), total Smad-1 (Cell signaling), Phospho-Smad2/3 (Cell Signaling), total-Smad2 (Cell Signaling), Phospho-STAT3 (Cell Signaling), Total STAT3 (Cell Signaling), hepcidin (Fitzgerald), Ferroportin (Novus Biologicals) Ferritin H [141], Ferritin L (Abcam), E-Cadherin (Cell Signaling), N Cadherin (Cell Signaling), Vimentin (Cell Signaling), Cyclophilin B (Abcam) or β-actin (Abcam). Western blots were quantified with Image J normalized to loading control (β -actin or Cyclophilin B).

Immunofluorescence

Primary patient spheroids were embedded in OCT, sectioned and fixed with 4% formaldehyde for 15 minutes and blocked with 5% BSA at 4°C overnight. Anti-human ferroportin (Amgen-38C8) and anti-rabbit Hepcidin (Fitzgerald) were applied for one hour followed 1:800 dilutions of rhodamine-green conjugated goat anti-human secondary antibody (Jackson ImmunoResearch) for ferroportin and Alexa-fluor 555 conjugated goat anti-rabbit IgG secondary antibody (Invitrogen) for hepcidin. Slides were mounted with ProLong Gold anti-fade reagent (Invitrogen, Carlsbad, CA, USA). Images were acquired using a fluorescent inverted microscope (Zeiss Axio Vert.A1).

Immunohistochemistry

Primary patient spheroids were embedded in OCT, sectioned and stored in -80° until IHC procedure. Breast tissue microarray slides were obtained from US Biomax, Inc., (Rockville, MD, USA; cat# BR1503e). For both specimen types, antigen retrieval was performed using 0.05% citraconic anhydride (Acros Organics, Geel, Belgium) at pH 7.4 prior to immunostaining. For primary patient spheroids, slides were stained with Hematoxylin and eosin or pan-cytokeratin (AE 1/3) (Cell Signaling Technology) with hematoxylin counterstain. Images were acquired using a Zeiss Axio Vert.A1 microscope with color Axio Vert.A1 camera (Carl Zeiss Microscopy

GmbH., Jena, Germany). For breast tissue microarrays, slides were stained with a rabbit anti-GDF-15 antibody (Sigma-Aldrich) or rabbit anti-Hepcidin antibody (Fitzgerald). An isotype matched rabbit anti-IgG was used for negative control and anti-pan keratin (Cell Signaling) was used to distinguish epithelial from stromal cells. Slides were counterstained with hematoxylin (Poly Scientific R&D Corp., Bay Shore, NY, USA). Images were acquired using a Zeiss Axio Scan Z1 (Carl Zeiss Microscopy GmbH., Jena, Germany). To quantify Hepcidin and GDF-15 expression, stained microarray images were analyzed with Fiji software using reciprocal intensity as previously described[142]. Briefly, diaminobenzidine (DAB) signal was isolated from images by color deconvolution. Regions of interest were drawn around epithelial tissue throughout the entire tissue core. Mean DAB intensity/area was then measured in the regions of interest (breast epithelia). Reciprocal intensity (expressed in arbitrary units) was derived by subtracting the maximum intensity value from measured mean DAB intensity/area values. Two cores per patient were used (n=56) and one value was established per patient by normalization with respect to total epithelial cell area. Patients with one or both tissue cores that were negative for anti-pan keratin staining were excluded from quantification analysis. For correlation of staining intensities between Hepcidin and GDF-15, a regression analysis was performed.

siRNA Knock-down

All reagents were obtained from GE Dharmacon (Lafayette, CO, USA). ON-TARGETplus human SMARTpools were used for siBMP4 (652; cat#: L-011221-00), siBMP6 (654; cat#; L-021475-00), siBMP7 (655; cat#: L-011592-00), STAT3siSTAT3(6774; cat #: L-003544-00), siGDF-15 (9518; cat#: L-019875-00) (referred to as KD#1) and siNTC (cat#: D-001810-10-05) were used for knockdown experiments. ON-TARGETplus individual siRNA human siGDF-15 was used for GDF-15 KD #2 (cat:J-019875-05). siGENOME Control siRNA was used for GAPDH (cat#: D-001140-01-05). Transfections were performed according to the manufacturer's recommendations using Dharmafect #1 (T-2001) transfection reagent. For monolayer cells,

knock-down was performed for 24, 48 or 72 hours before harvesting. For spheroids, knock-down was performed in monolayer culture for 24 hours before trypsanization of cells and subsequent spheroid plating. Spheroids were harvested after 3 days, 4 days after initial siRNA transfection. KD efficiencies were confirmed at time of harvest by RT-qPCR and/or by ELISA methods described.

ELISA analysis for secreted GDF-15, BMP-6 and IL-6

GDF-15 and IL-6 were measured in conditioned growth media using a GDF-15 or IL-6 Human ELISA kit from R&D systems and following manufacturers' protocol.. For siRNA knock-down efficiency, GDF-15 was measured in serum free growth media. BMP-6 was measured in conditioned normal growth media using a Human BMP-6 ELISA kit from Thermo Scientific and following manufacturers' protocol.

Microarray analysis

MCF-7 cells (monolayer and 3 different 3D culture techniques; pHEMA, mCELL and ULA explained above) were harvested at the day 3 time point and used as samples for microarray analysis. RNA was collected and purified from cell culture lysate using High Pure RNA Isolation Kit (Roche Diagnostics). High quality RNA was submitted to the Yale Center for Genome Analysis (West Haven, CT) for Affymetrix GeneChip analysis of gene expression. Three biological replicates from each condition were hybridized onto the Affymetrix Human Transcriptome Array 2.0 (HTA-2.0). Raw CEL files were checked for quality and RMA normalized using Affymetrix Expression Console Software (version 1.4.1.46). Three separate differential expression (DE) analyses were performed for each of the three spheroid culture techniques against monolayer culture using Affymetrix Transcriptome Analysis Software (version 3.0.0.466) with Probeset Annotations release 36 based on UCSC hg19. Significant DE up-regulated genes were generated based on transcript cluster ID's (probesets) with criteria of ANOVA p value of <0.05 and a fold change greater or less than 2 fold. For compilation of top 10

up-regulated genes, transcript cluster ID's were checked for uniqueness with respect to gene annotation. Additionally, transcript cluster ID's without a corresponding gene symbol or containing _hap (haplotype chromosomes) were discarded. For compilation of top 10 up-regulated genes, transcript cluster ID's without a corresponding gene symbol or containing _hap (haplotype chromosomes) were discarded.

GAGE Analysis

The transcript cluster ID with the highest average expression per gene in each dataset was selected to represent the expression of that gene. Significantly perturbed KEGG (Kyoto Encyclopedia of Genes and Genomes, [1]) pathways within each dataset were found using the Gene Set Analysis method Generally Applicable Gene-set Enrichment (GAGE), since it is optimized for use with both small and large datasets [2], using the bidirectional option (same.dir=F) and unpaired sample setting (compare="unpaired").

TCGA analysis

Lowess-normalized gene-level mRNA expression data from Agilent custom whole genome microarrays (TCGA, BRCA, 2012; PMID: 23000897) of primary breast cancer samples were uploaded on 10-24-16 from the Broad Firehose (https://gdac.broadinstitute.org/), along with clinical and biospeciman supporting data [143]. For each sample, GDF-15 and HAMP expression was extracted. Samples were classified as 'cancer' if the 'Sample' identifier of the sample barcode was 01a or 01b and samples were classified as 'normal' if the 'sample' identifier of the sample barcode was 11a or 11b, based on identification between the sample identifier and the sample type in the biospecimen data. All statistical analyses were performed in Prism 6. For comparison of GDF-15 and HAMP expression, respectively, between the normal and cancer samples, and of GDF-15 expression between low and high HAMP cancer samples, an independent two-tailed t test was used.

Statistical analysis

All experiments were performed at least three times using a minimum of three replicates/condition in each experiment. Results of representative experiments are shown in the figures. Statistical analyses were performed using Excel or Prism 6 (Graphpad software) and are reported as the mean ± standard deviation. Error bars represent standard deviation. Unless otherwise noted, significant differences between control and treatment groups were determined using two-tailed unpaired Student's t tests.

Acknowledgements

This work was supported in part by NCI R01CA188025 (SVT) and NCI R01CA171101 (FMT). We thank Li Chen and Drs. Nathaniel Dyment and David Rowe for assistance in image acquisition, as well as Tara L Arvedson (Amgen, Thousand Oaks, CA) for a generous gift of anti-ferroportin antibody.

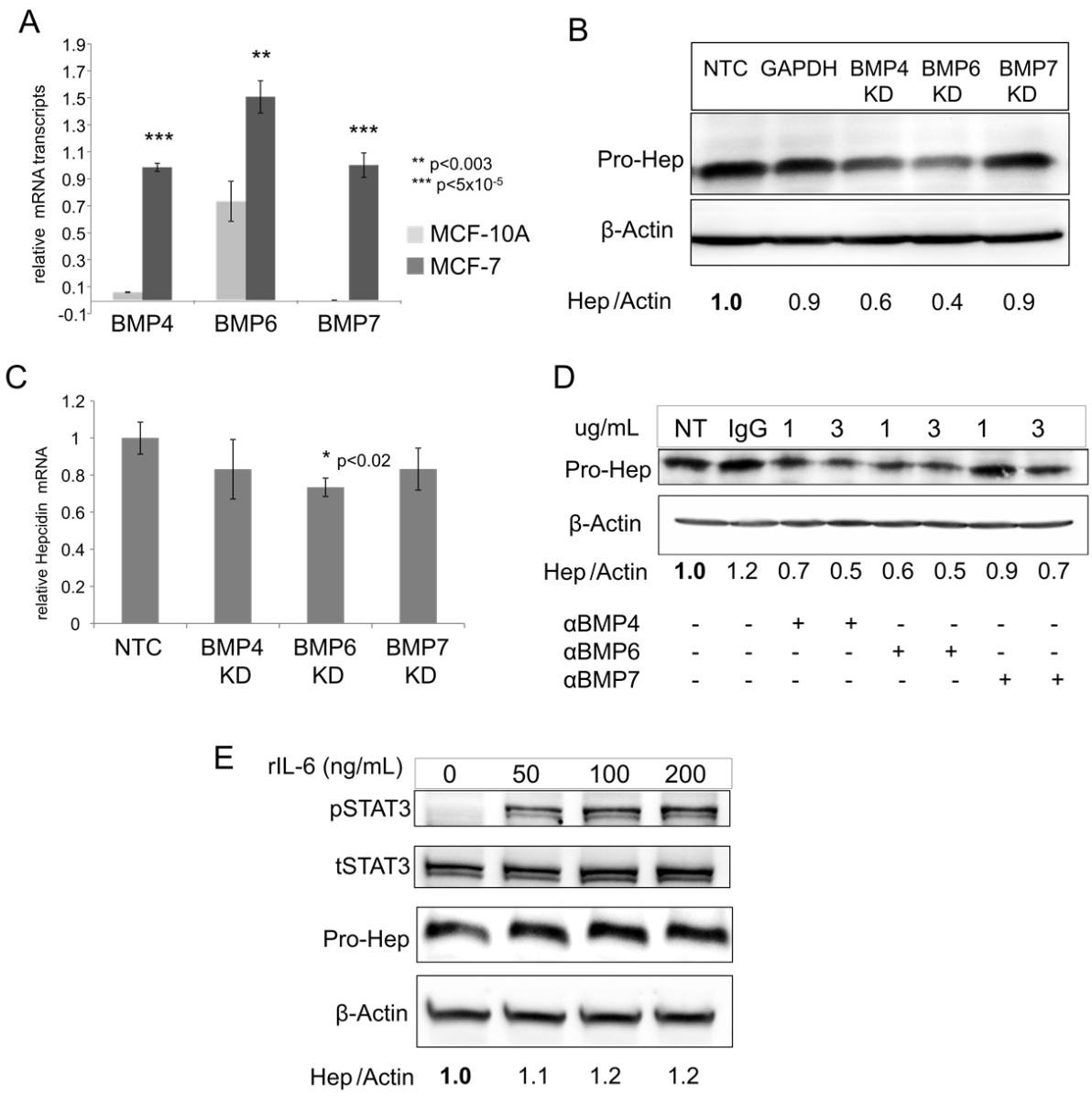

Figure 3-1. BMPs regulate hepcidin expression in MCF-7 breast cancer cells.
(A) RT-qPCR of BMP4, BMP6 or BMP7 mRNA (normalized to β-actin) in MCF-7 and MCF-10A monolayer cells. (B) Western blot analysis of pro-hepcidin and β-actin and (C) RT-qPCR of hepcidin mRNA (normalized to β-actin) following siRNA knock-down of non-target control (NTC), BMP4, BMP6, and BMP7 for 48 hours in MCF-7 cells. For statistical analysis and quantification samples were compared to NTC. GAPDH siRNA was used as an additional control in western blot analysis. (D) Western blot analysis of pro-hepcidin and β-actin after the addition of 1 and 3 μg/mL neutralizing antibodies against BMP4, BMP6, BMP7 or IgG (3μg/ml) isotope control for 48 hrs in MCF-7 cells. (E) Western blot analysis of phosporylated-STAT3 (pSTAT3), total STAT3 (tSTAT3), pro-hepcidin, and β-actin following the addition of recombinant IL-6 for 24 hours in MCF-7 cells.

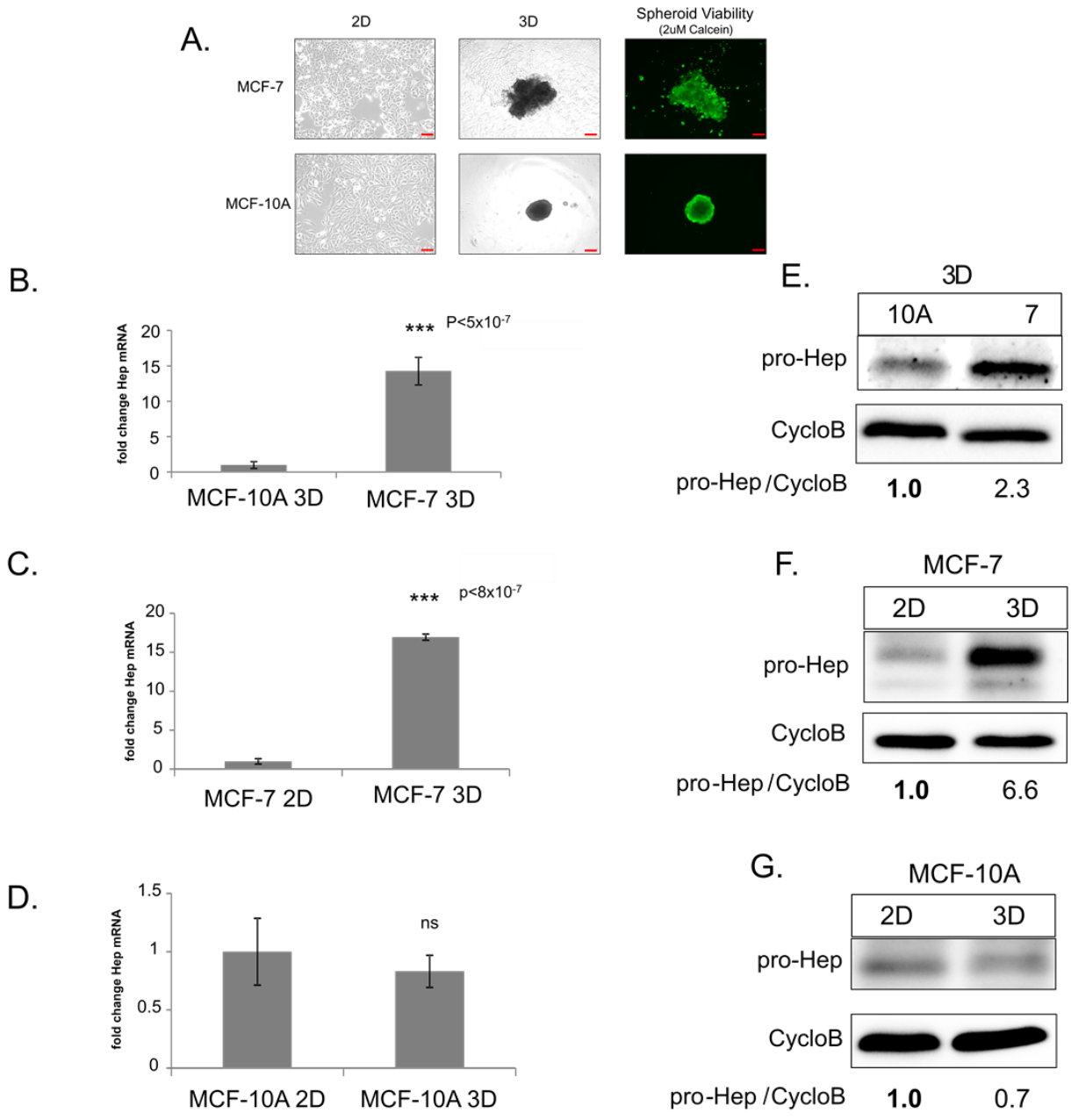

Figure 3-2. Hepcidin is increased in MCF-7 breast cancer spheroids compared to non-tumor spheroids and is induced from 2D to 3D culture of breast cancer cells.
(A) Phase-contrast imaging of MCF-7 and MCF-10A cells grown in 2D and 3D and fluorescent imaging of spheroids stained with 2μM calcein. (B-D) RT-qPCR of hepcidin mRNA (normalized to cyclophilin A) in MCF-7 and MCF-10A cells grown in 2D and 3D. (E-G) Western blot of pro-hepcidin using Cyclophilin B as internal control. Scale bar: 10μm (2D), 200μm (3D)

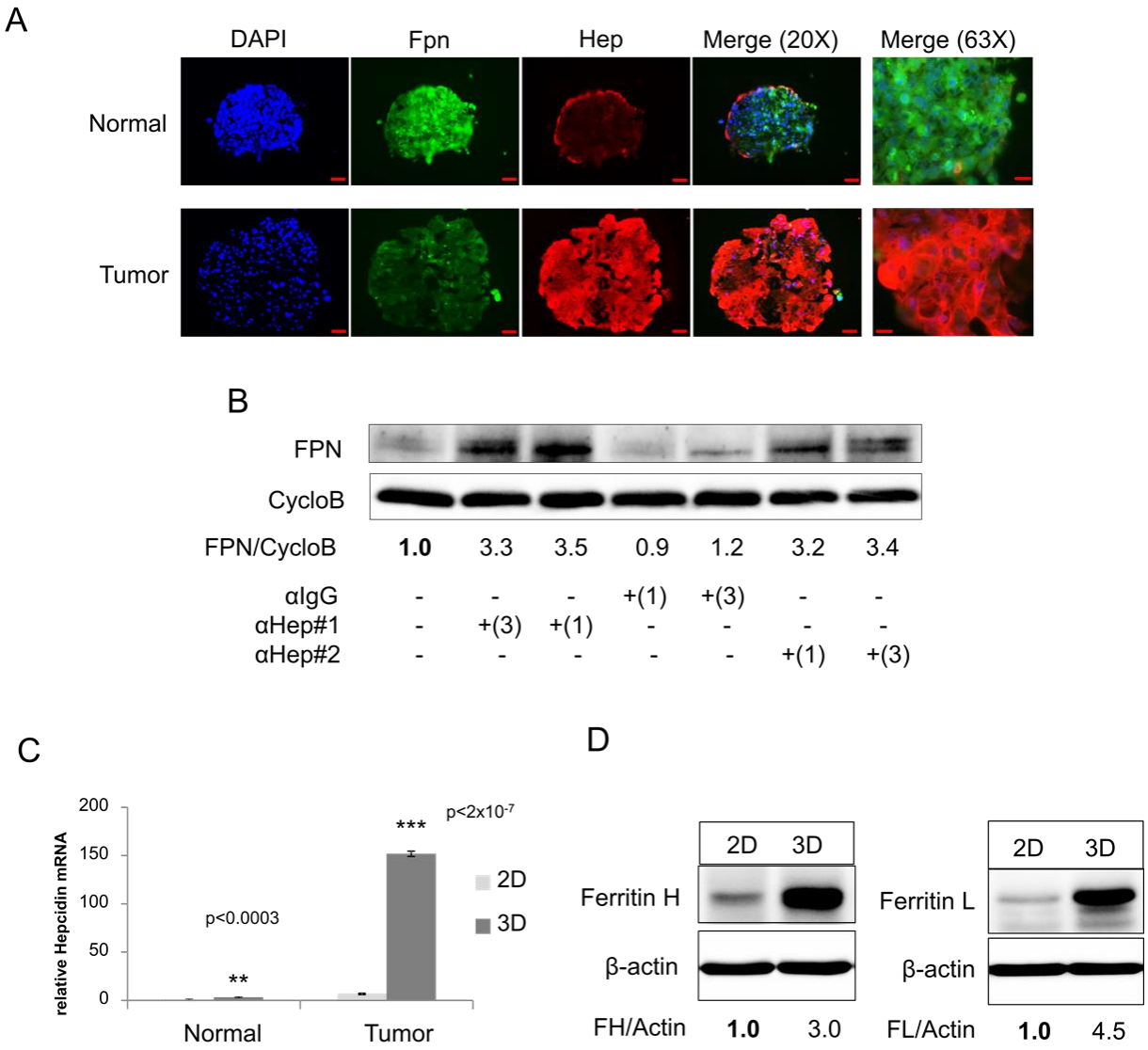

Figure 3-3. Hepcidin is increased in primary patient breast cancer spheroids, degrades FPN and is associated with an increase in the iron storage protein ferritin.
(A) Immunofluorescence staining of FPN (green) Hep (red) and DAPI (blue) in primary breast spheroid sections from patient 107 normal and tumor. (B) Western blot analysis of Ferroportin (FPN) and Cyclophilin B (CycloB) following 48 hours of treatment with 1 or 3 μg/mL anti-hepcidin antibody (#1 Amgen, #2 Abcam) or isotope-matched IgG control in patient 107 spheroids. (C) RT-qPCR of Hepcidin mRNA (normalized to Cyclophilin A) of normal adjacent and tumor patient breast cell monolayer vs. spheroids. (D) Western blot analysis of Ferritin H, Ferritin L and β-actin of patient 107 monolayer and spheroids. Scale bar 50μM (20X); 20μM (63X).

Table 3-1. Clinical characteristics of primary breast tumor samples.

Patient #	Patient Age	Tumor Type	Tumor Grade (Nottingham)	Tumor Size (I/P)	ER Status	PR Status	Her-2 Status	Nodal Status	TNM
107	57	Ductal	I	1.5x1.0x0.5	0/8	0/8	0	0	pT1cN0MX
109	80	Ductal Colloid	II	2.8 x 1.1	8/8	4/8	0	0	pT2NXMX
113	53	Ductal (Left)	I	8.5x8.0x3.8	5/8	0/8	0	0	pTisN0MX
		Lobular (Right)	II	5cm	8/8	8/8	0	0	pT3N0MX
129	65	Ductal	II	2.1cm	8/8	7/8	2/3	Pos (0.56mm) micro FISH 1.3	pTpN1micpMX

All tumor samples were de-identified at time of obtainment. Clinical pathology was performed and recorded for each patient.
(ER) estrogen receptor, (PR) progesterone receptor, (Her-2) human epidermal growth factor receptor 2, TNM tumor node metastasis

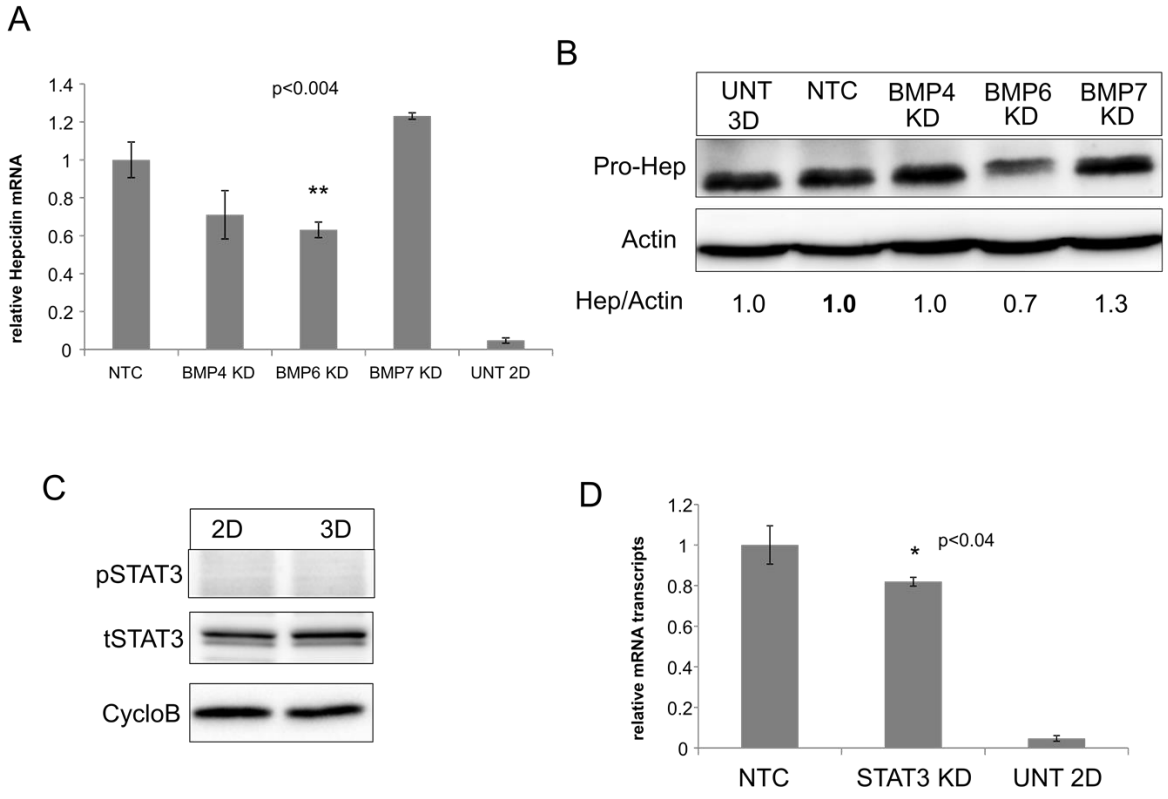

Figure 3-4. Known regulators of hepcidin have a modest effect on regulation of hepcidin in breast cancer spheroids. (A) RT-qPCR of Hepcidin mRNA (normalized to Cyclophilin A) and (B) western blot analysis of pro-hepcidin and β-actin following siRNA knock-down of non-target control (NTC), BMP4, BMP6, and BMP7 in MCF-7 spheroids. Untreated MCF-7 cells grown in 2D (A) or 3D (B) were used as controls. Statistical analysis and quantification was normalized to non-targeting control siRNA. (C) Western blot analysis of p-STAT3, total STAT-3 and Cyclophilin B in MCF-7 monolayer versus spheroids cultured for 3 days. (D) RT-qPCR of hepcidin mRNA (normalized to Cyclophilin A) following siRNA knock-down of NTC and STAT3 in MCF-7 spheroids. For statistical analysis samples were compared to non-targeting control. Untreated MCF-7 2D was used as a control.

Table 3-2. Top 10 upregulated genes in 3D culture from monolayer vs. each of the 3 spheroid conditions from microarray analysis.

Rank	Fold Change (linear)	ANOVA p-value	FDR p-value	Gene Symbol	Description	Fold Change (linear)	ANOVA p-value	FDR p-value	Gene Symbol	Description	Fold Change (linear)	ANOVA p-value	FDR p-value	Gene Symbol	Description
1	47.93	1.79E-07	0.001206	UGT2B15	UDP glucuronosyltransferase 2 family, polypeptide B15	46.69	2.92E-07	5.08E-04	UGT2B15	UDP glucuronosyltransferase 2 family, polypeptide B15	41.34	4.39E-08	0.000355	UGT2B15	UDP glucuronosyltransferase 2 family, polypeptide B15
2	40.23	1.12E-07	0.000949	UGT2B17	UDP glucuronosyltransferase 2 family, polypeptide B17	38.24	1.71E-07	4.81E-04	UGT2B17	UDP glucuronosyltransferase 2 family, polypeptide B17	31.38	2.14E-07	0.000534	UGT2B17	UDP glucuronosyltransferase 2 family, polypeptide B17
3	24.63	0.000015	0.003028	MIR21	microRNA 21	27.78	0.000004	1.10E-03	MIR21	microRNA 21	24.11	0.000018	0.002121	TNFSF10	tumor necrosis factor (ligand) superfamily, member 10
4	19.67	0.00003	0.003846	TNFSF10	tumor necrosis factor (ligand) superfamily, member 10	25.41	0.000018	1.77E-03	TNFSF10	tumor necrosis factor (ligand) superfamily, member 10	21.9	0.000079	0.004237	GDF15	growth differentiation factor 15
5	16.55	0.000161	0.008027	GDF15	growth differentiation factor 15	16.07	0.000002	3.41E-03	GDF15	growth differentiation factor 15	16.46	0.000001	0.000775	MIR21	microRNA 21
6	15.18	0.00007	0.001521	MSMB	microseminoprotein, beta-	15.63	0.000046	4.23E-04	CMAHP (non-coding)	cytidine monophospho-N-acetylneuraminic acid hydroxylase, pseudogene	16.24	8.50E-07	0.000534	MSMB	microseminoprotein, beta-
7	15.12	0.00009	0.000525	CMAHP (non-coding)	cytidine monophospho-N-acetylneuraminic acid hydroxylase, pseudogene	15.48	0.000078	5.88E-04	MSMB	microseminoprotein, beta-	15.86	2.97E-07	0.000601	CMAHP (non-coding)	cytidine monophospho-N-acetylneuraminic acid hydroxylase, pseudogene
8	13.48	6.64E-07	0.000496	CMAHP (coding)	cytidine monophospho-N-acetylneuraminic acid hydroxylase, pseudogene	14.39	5.02E-08	3.02E-04	CMAHP (coding)	cytidine monophospho-N-acetylneuraminic acid hydroxylase, pseudogene	15.25	0.000023	0.000534	CMAHP (coding)	cytidine monophospho-N-acetylneuraminic acid hydroxylase, pseudogene
9	11.78	3.21E-08	0.003542	LINC01087	long intergenic non-protein coding RNA 1087	13.88	5.14E-07	1.10E-03	TNFAIP3	tumor necrosis factor, alpha-induced protein 3	12.69	3.92E-07	0.002055	TNFAIP3	tumor necrosis factor, alpha-induced protein 3
10	11.38	0.00001	0.005684	TNFAIP3	tumor necrosis factor, alpha-induced protein 3	13.75	0.000023	0.003158	LINC01087	long intergenic non-protein coding RNA 1087	10.96	2.32E-07	0.001067	CAPN9	calpain 9

Significant DE up-regulated genes were generated based on transcript cluster ID's (probesets) with criteria of ANOVA p value of <0.05 and a fold change greater or less than 2 fold. (pHEMA: 1809 DE, 942 up-regulated in 3D; ULA: 2117 DE, 904 up-regulated in 3D; mCELL: 1822 DE, 809 up-regulated in 3D)

Transcript cluster IDs that were not annotated with a gene symbol or containing _hap (haplotype chromosomes) were excluded from top-10 and were as follows: TC05000962.hg.1, TC02000102.hg.1, TC10002067.hg.1, TC4_ctg9_hap1000004.hg.1

Table 3-3. GAGE pathway analysis for top-10 perturbed pathways from monolayer to spheroid culture of MCF-7 cells.

	PolyHEMA		Ultra-low Attachment		Methylcellulose	
Rank	**Pathway**	**q-value**	**Pathway**	**q-value**	**Pathway**	**q-value**
1	hsa04110 Cell cycle	1.40E-31	hsa04110 Cell cycle	1.74E-31	hsa04110 Cell cycle	9.33E-31
2	hsa03030 DNA replication	2.34E-22	hsa03030 DNA replication	4.08E-21	hsa03030 DNA replication	1.01E-20
3	hsa03013 RNA transport	1.39E-10	hsa03013 RNA transport	1.83E-11	hsa03460 Fanconi anemia pathway	2.12E-09
4	hsa00240 Pyrimidine metabolism	2.74E-10	hsa00240 Pyrimidine metabolism	3.85E-10	hsa03013 RNA transport	2.12E-09
5	hsa03460 Fanconi anemia pathway	3.86E-10	hsa03460 Fanconi anemia pathway	1.35E-09	hsa04068 FoxO signaling pathway	2.23E-09
6	hsa03040 Spliceosome	9.00E-10	hsa04068 FoxO signaling pathway	2.16E-09	hsa00240 Pyrimidine metabolism	2.96E-09
7	hsa04114 Oocyte meiosis	4.86E-09	hsa04114 Oocyte meiosis	1.80E-08	hsa04114 Oocyte meiosis	6.24E-08
8	hsa03430 Mismatch repair	7.32E-09	hsa03430 Mismatch repair	2.03E-08	hsa03430 Mismatch repair	6.24E-08
9	hsa04068 FoxO signaling pathway	2.17E-08	hsa03050 Proteasome	4.41E-08	hsa04115 p53 signaling pathway	2.09E-07
10	hsa04115 p53 signaling pathway	1.67E-07	hsa04115 p53 signaling pathway	6.36E-08	hsa03410 Base excision repair	5.53E-07

The transcript cluster ID from differential expression analysis with the highest average expression per gene in each dataset was selected to represent the expression of that gene. Significantly perturbed KEGG (Kyoto Encyclopedia of Genes and Genomes, [1]) pathways within each dataset were found using the Gene Set Analysis method Generally Applicable Gene-set Enrichment (GAGE). Top 10 pathways and corresponding q-value are displayed for each 3D condition.

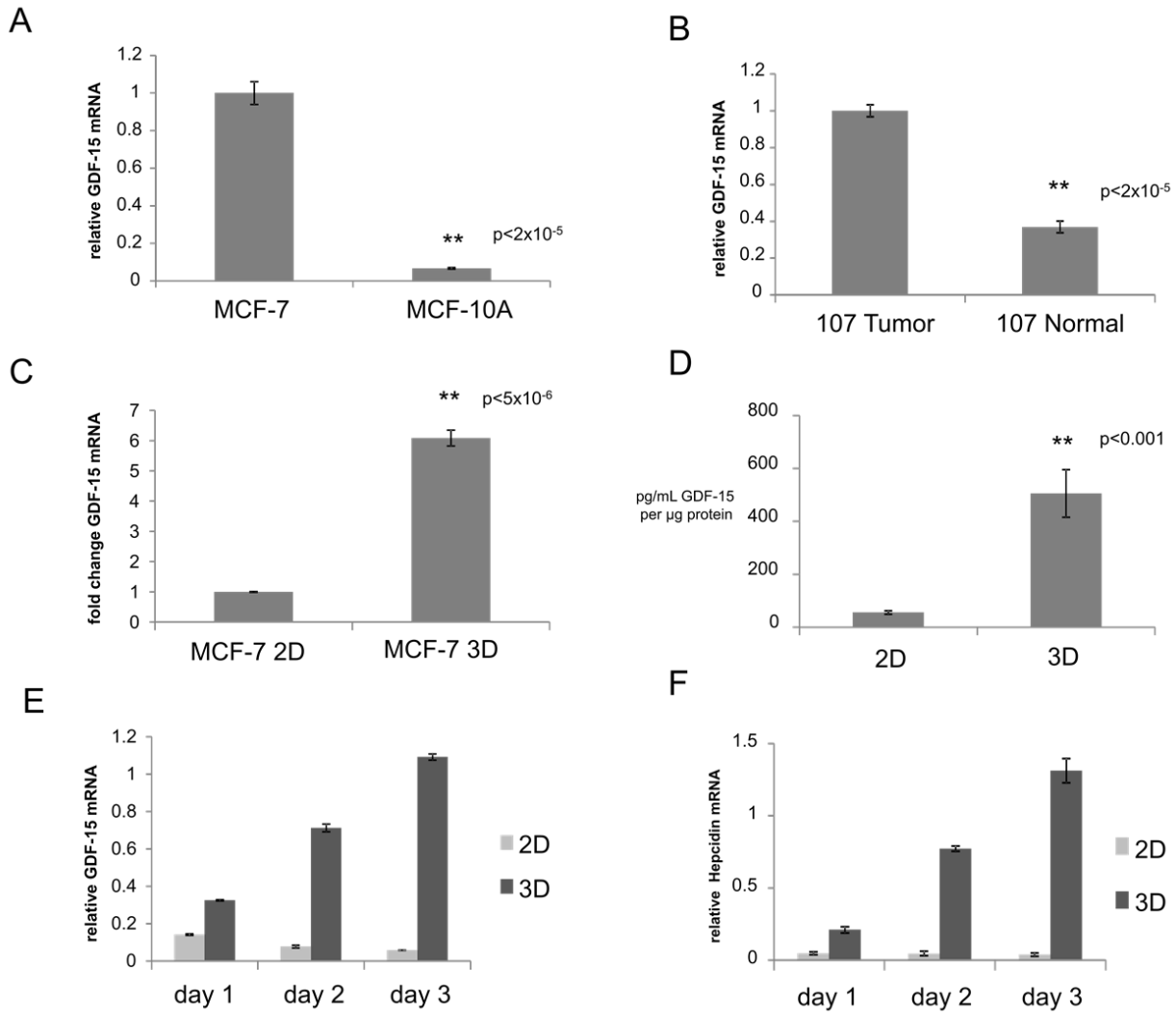

Figure 3-5. GDF-15 is induced in breast cancer spheroids and correlates with hepcidin expression. (A-C) RT-qPCR of GDF-15 mRNA (normalized to Cyclophilin A) between (A) MCF-7 and MCF-10A spheroids, (B) patient 107 Tumor vs. normal adjacent tumor (normal) spheroids and (C) MCF-7 monolayer vs. MCF-7 spheroids. (D) Secreted GDF-15 from conditioned media of MCF-7 monolayer and spheroids. (E-F) RT-qPCR of (E) GDF-15 mRNA (normalized to Cyclophilin A) and (F) hepcidin mRNA (normalized to Cyclophilin A) in MCF-7 monolayer (2D) and spheroids (3D) over time.

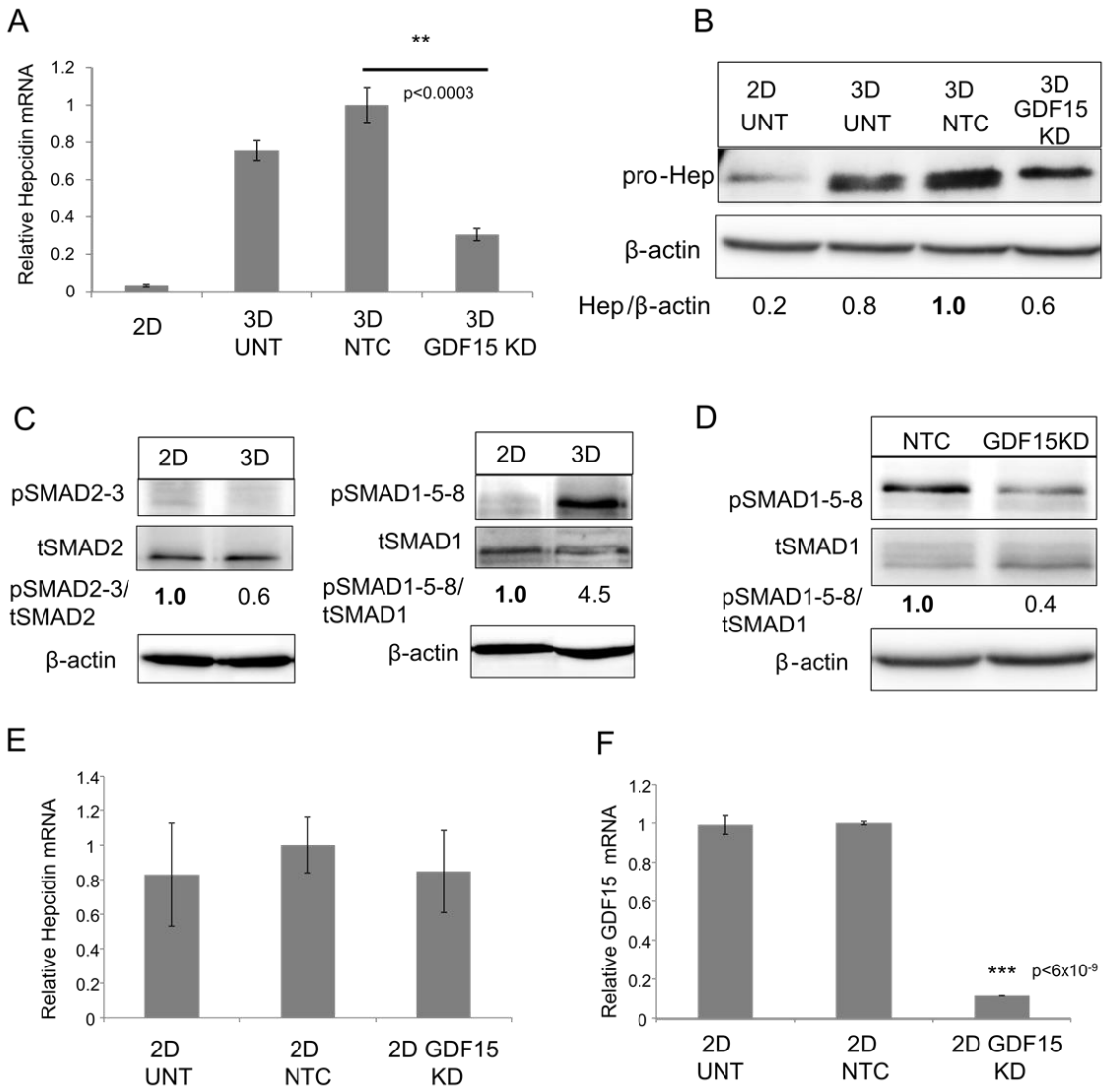

Figure 3-6. GDF-15 positively regulates hepcidin via a conserved pSMAD1-5-8 pathway. (A) RT-qPCR of Hepcidin mRNA (normalized to Cyclophilin A) and (B) western blot analysis of pro-hepcidin and β-actin following knock-down using non targeting control (NTC) siRNA and GDF-15 siRNA (KD#1) in MCF-7 spheroids. Untreated MCF-7 cells grown in 2D or 3D were used as controls. For statistical analysis, samples were compared to non-targeting control. (C) Western blot analysis of phosphorylated SMAD2-3, total SMAD2, phosphorylated SMAD1-5-8, total SMAD-1, and β-actin in MCF-7 monolayers and spheroids. (D) Western blot analysis of pSMAD1-5-8, tSMAD-1 and β-actin following siRNA knock-down of NTC and GDF-15 knock-down #1. (E-F) RT-qPCR of (E) hepcidin mRNA (normalized to Cyclophilin A) and (F)GDF-15 mRNA (normalized to Cyclophiin A) following siRNA knock-down of NTC and GDF-15 knock-down #1 for 3 days in MCF-7 monolayer. For statistical analysis, samples were compared to non-targeting control.

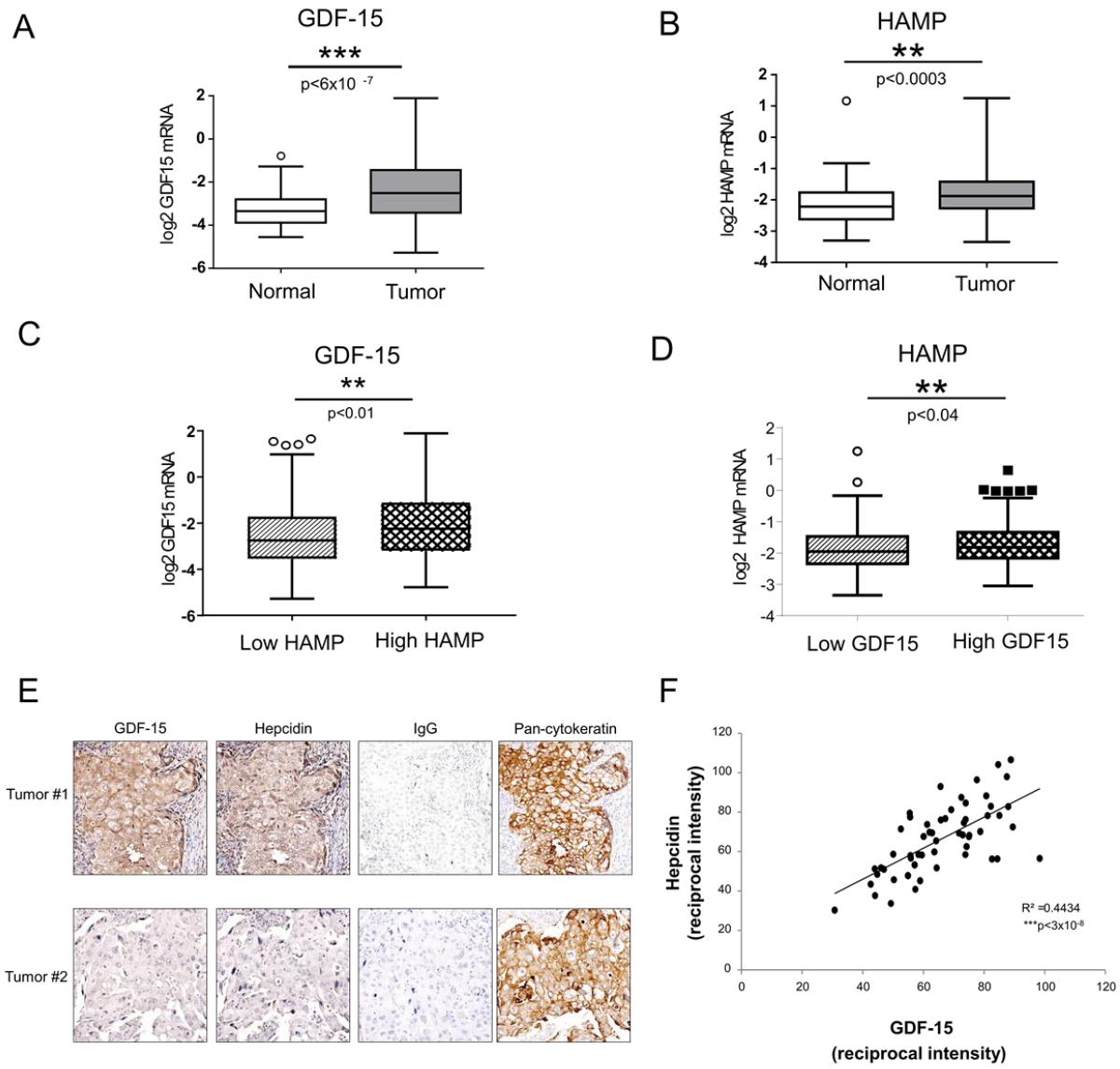
A
GDF-15
***
p<6x10 -7
log2 GDF15 mRNA
Normal
Tumor
B
HAMP
**
p<0.0003
log2 HAMP mRNA
Normal
Tumor
C
GDF-15
**
p<0.01
log2 GDF15 mRNA
Low HAMP
High HAMP
D
HAMP
**
p<0.04
log2 HAMP mRNA
Low GDF15
High GDF15
E
GDF-15
Hepcidin
IgG
Pan-cytokeratin
Tumor #1
Tumor #2
F
Hepcidin (reciprocal intensity)
GDF-15 (reciprocal intensity)
R² =0.4434
***p<3x10-8

Figure 3-7. Hepcidin and GDF-15 are increased and their expression is correlated in breast tumors. (A and B) Box plot with Tukey whisker of (A) GDF-15 and (B) HAMP mRNA expression (log2 transformed) in normal adjacent tissue (n=61) compared to primary tumor tissue (n=526) in the TCGA breast cancer dataset. (C) GDF15 transcripts in TCGA samples from breast cancer patients divided by HAMP expression (below and above the mean) shown as box and whisker plot. (D) HAMP transcripts in TCGA samples from breast cancer patients divided by GDF15 expression (below and above the mean) shown as box and whisker. (E) Representative images of immunohistochemical staining of tumor tissue from patients with invasive ductal carcinoma (IDC). Proteins stained are Hepcidin, GDF-15, Pan-Cytokeratin and IgG control. (F) Scatter plot displays quantification of staining of epithelial cells from tissues from 56 BRCA patients. A regression analysis was performed to examine correlation of staining intensities (R^2=0.4434 $p<3x10^{-8}$).

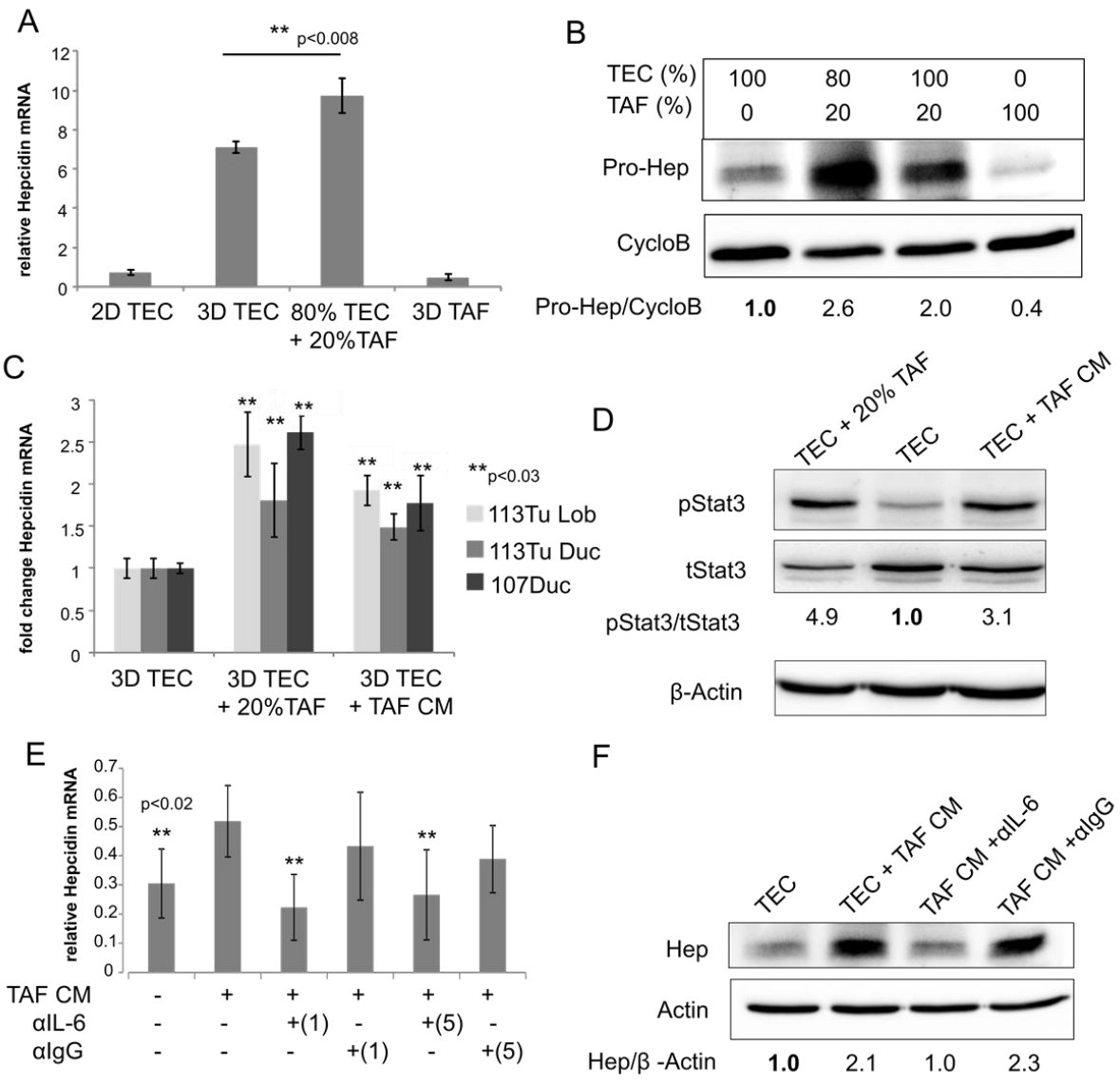
A
** p<0.008
relative Hepcidin mRNA
2D TEC
3D TEC
80% TEC + 20%TAF
3D TAF
B
TEC (%)
TAF (%)
100 80 100 0
0 20 20 100
Pro-Hep
CycloB
Pro-Hep/CycloB 1.0 2.6 2.0 0.4
C
fold change Hepcidin mRNA
**p<0.03
113Tu Lob
113Tu Duc
107Duc
3D TEC
3D TEC + 20%TAF
3D TEC + TAF CM
D
TEC + 20% TAF
TEC
TEC + TAF CM
pStat3
tStat3
pStat3/tStat3 4.9 1.0 3.1
β-Actin
E
relative Hepcidin mRNA
p<0.02
TAF CM - + + + + +
αIL-6 - - +(1) - +(5) -
αIgG - - - +(1) - +(5)
F
TEC
TEC + TAF CM
TAF CM +αIL-6
TAF CM +αIgG
Hep
Actin
Hep/β -Actin 1.0 2.1 1.0 2.3

Figure 3-8. IL-6 secreted by tumor-associated fibroblasts (TAFs) induces hepcidin in breast cancer spheroids. (A) RT-qPCR of hepcidin mRNA (normalized to Cyclophilin A) in patient 113Lobular cells. Samples were 100% 2D tumor epithelial cells (2D TEC), 100% tumor epithelial cell spheroids (3D TEC), spheroids composed of a mixture of 80% TEC and 20% irradiated TAFs, (80% TEC +20%TAF) and 100% irradiated TAF spheroids after 3 days of culture. (B) Western blot analysis of pro-hepcidin and Cyclophilin B for different TEC/TAF (%) combinations after 3 days of spheroid culture. (C) RT-qPCR of hepcidin mRNA (normalized to Cyclophilin A) and (D) western blot analysis of phosphorylated and total STAT3 of primary TEC spheroids alone, spheroids composed of a mixture of 80% TECs and 20%TAFs, or TEC spheroids exposed to conditioned media (CM) from TAFs for 4 days. For statistical analysis in (C) samples with 20% TAF or TAF CM were compared to their respective 3D TEC sample. (E) RT-qPCR of hepcidin mRNA (normalized to Cyclophilin A) of patient 113Lob spheroids after the addition of TAF CM and IL-6 neutralizing antibody (1=1μg/mL and 5=5μg/mL) for 4 days. Neutralizing antibody against IgG (1 and 5 μg/mL) was used as a control. For statistical analysis samples were compared to TAF CM sample. (F) Western blot analysis of pro-hepcidin and β-actin of patient 113Lob spheroids after the addition of TAF CM with or without 1μg/mL neutralizing antibodies against IL-6 or IgG for 4 days.

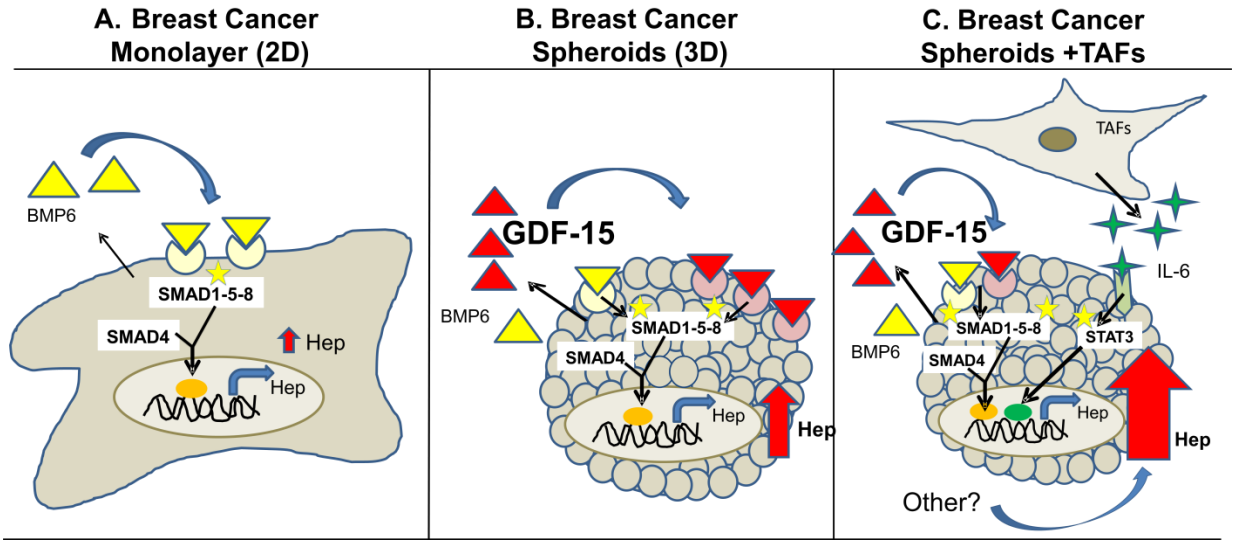

Figure 3-9. Working model of multiple modes of regulation of hepcidin in breast cancer spheroids.

Hepcidin expression is increased in breast cancer cells relative to non-cancer cells. (A) In MCF-7 cells grown as 2D monolayers, BMP6 plays a dominant role in the cancer-dependent increase in hepcidin through activation of a SMAD1-5-8 signaling pathway. (B) In breast cancer spheroids, spatial control of hepcidin synthesis is exerted by GDF-15, which augments SMAD 1-5-8 signaling to further increase hepcidin synthesis. (C) The microenvironment is an additional source for increased hepcidin in breast cancer cells, in part due to production of IL-6 by tumor-associated fibroblasts (TAFs).

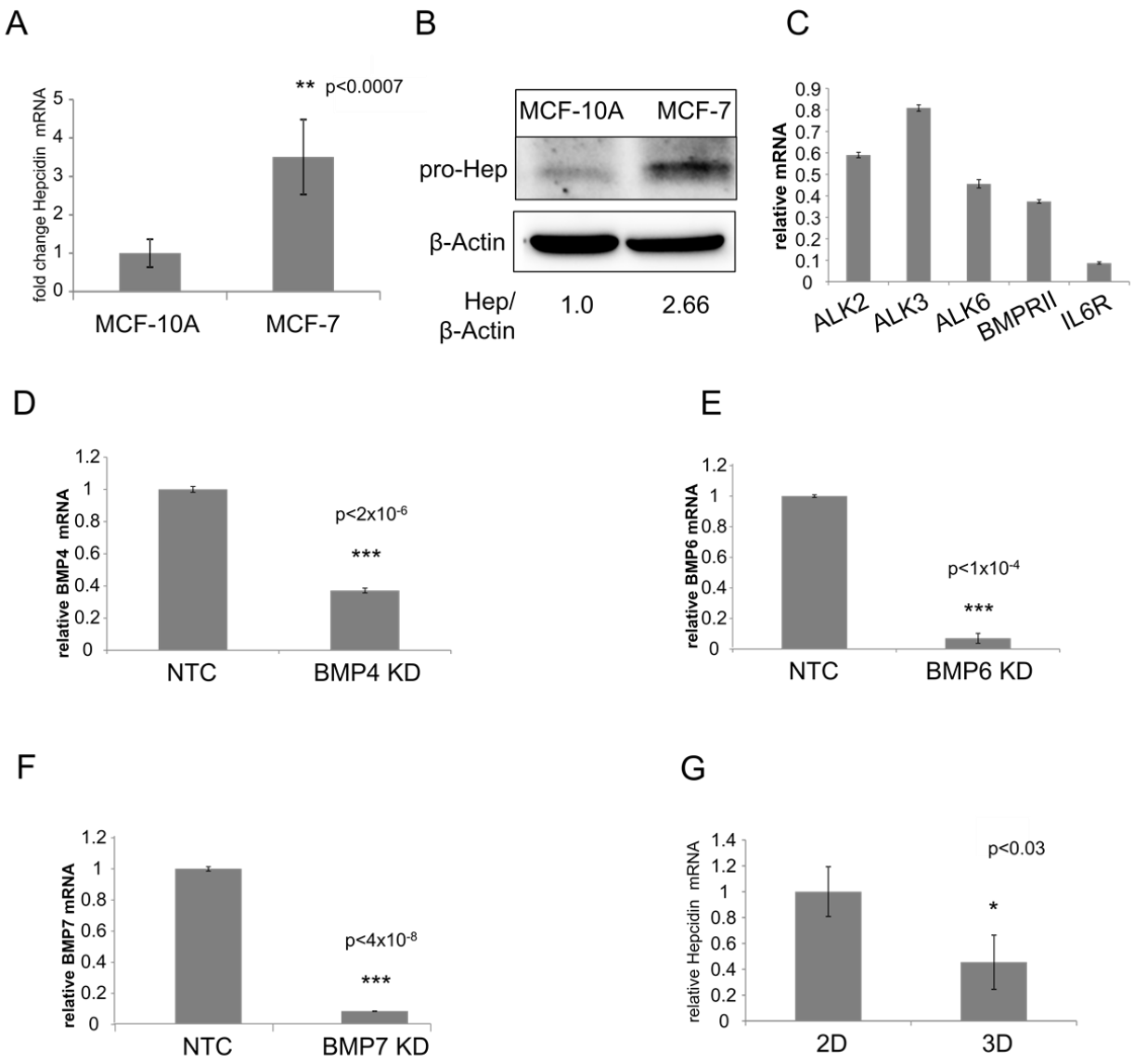

Supplementary Figure 3-S1. BMPs regulate hepcidin expression in breast cancer cells and induction of hepcidin in spheroids is specific to breast cancer spheroids.
(A) RT-qPCR of hepcidin mRNA (normalized to β-actin) and (B) western blot analysis of pro-hepcidin and β-actin in MCF-10A and MCF-7 monolayer cells. (C) RT-qPCR of ALK2, ALK3, ALK6, BMPRII and IL-6R mRNA (normalized to β-actin) in MCF-7 monolayer cells. (D-F) RT-qPCR of (D) BMP4 (E) BMP6 and (F) BMP7 mRNA following siRNA knock-down in MCF7 monolayer cells. Samples are normalized to β-Actin and are relative to non-targeting control (NTC). (G) RT-qPCR of hepcidin/Cyclophilin A in human mammary epithelial (HME) cell monolayer and spheroids.

Supplementary Table 3-S1. MCF-7 cells express higher transcript levels of BMP4, 6, and 7, but not BMP2 or IL-6 when compared to MCF-10A cells.

Ligand	MCF-10A	MCF-7
BMP2	9.92	1.01
BMP4	0.06	0.98
BMP6	0.73	1.51
BMP7	0.0009	1.00
IL-6	ND	ND

Relative mRNA transcripts from RT-qPCR of BMP2, BMP4, BMP6, BMP7 and IL-6 mRNA (normalized to β-actin) in MCF-7 and MCF-10A monolayer cells. (ND) Not detected.

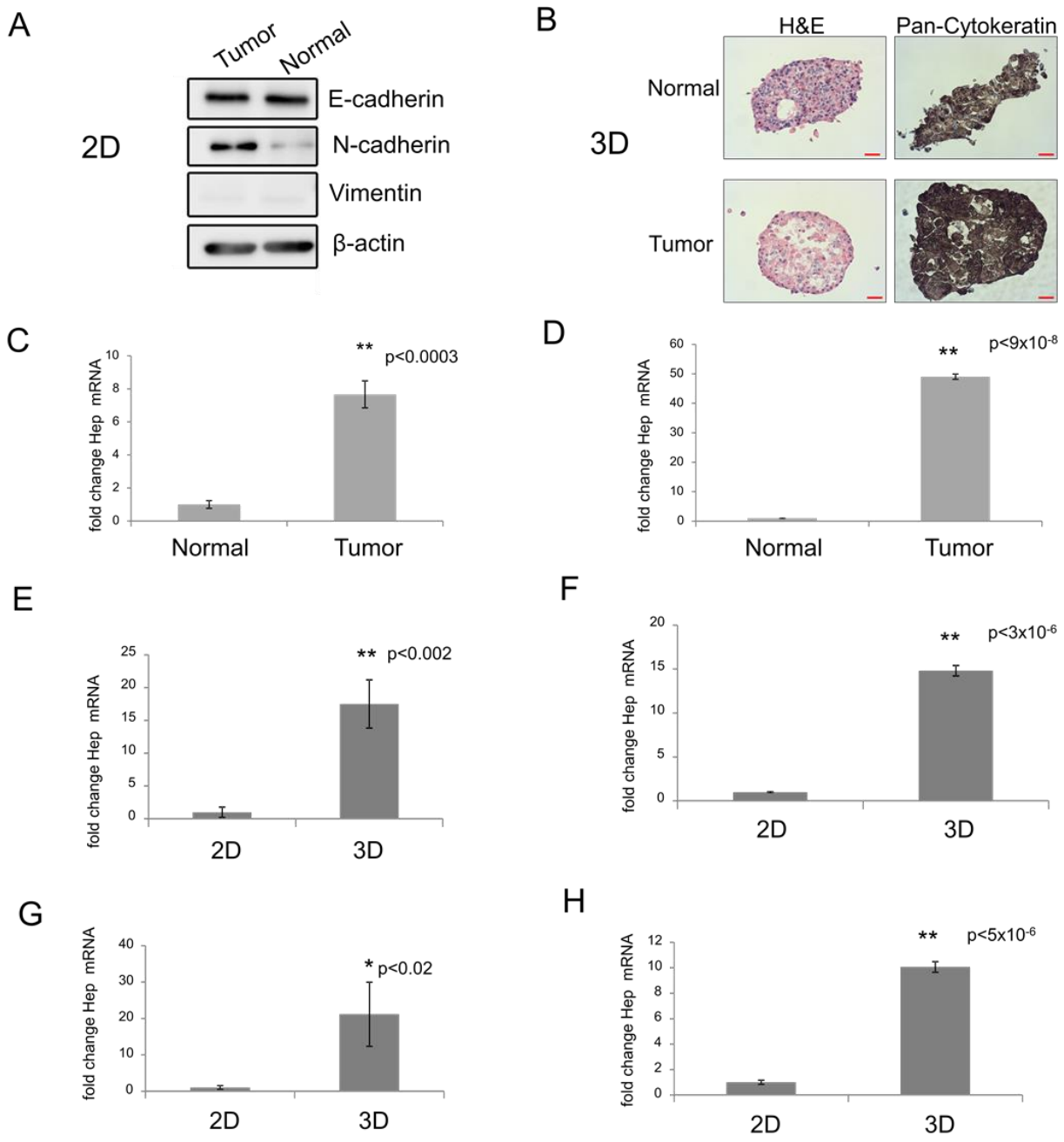

Supplementary Figure 3-S2. Primary patient cells retain epithelial characteristics and display hepcidin induction from 2D to 3D.

(A) Western blot analysis of patient 107 primary tumor and normal adjacent tissue for E-cadherin, N-cadherin, Vimentin and β-actin. (B) H&E and Immunohistochemistry staining of Pan-Cytokeratin AE 1/3 of patient 107 primary tumor and normal adjacent tissue spheroid sections. (C) RT-qPCR for hepcidin mRNA (normalized to β-actin) for patient 107 primary tumor and normal adjacent tissue monolayer cells. (D) RT-qPCR for hepcidin mRNA (normalized to Cyclophilin A) for patient 107 primary tumor and NAT spheroids. (E-H) RT-qPCR for hepcidin mRNA (normalized to Cyclophilin A) for monolayer vs spheroids from patient (E) 109Duc, (F) 129Duc, (G) 113Duc and (H) 113Lob tumor cells. Scale bar 100μm.

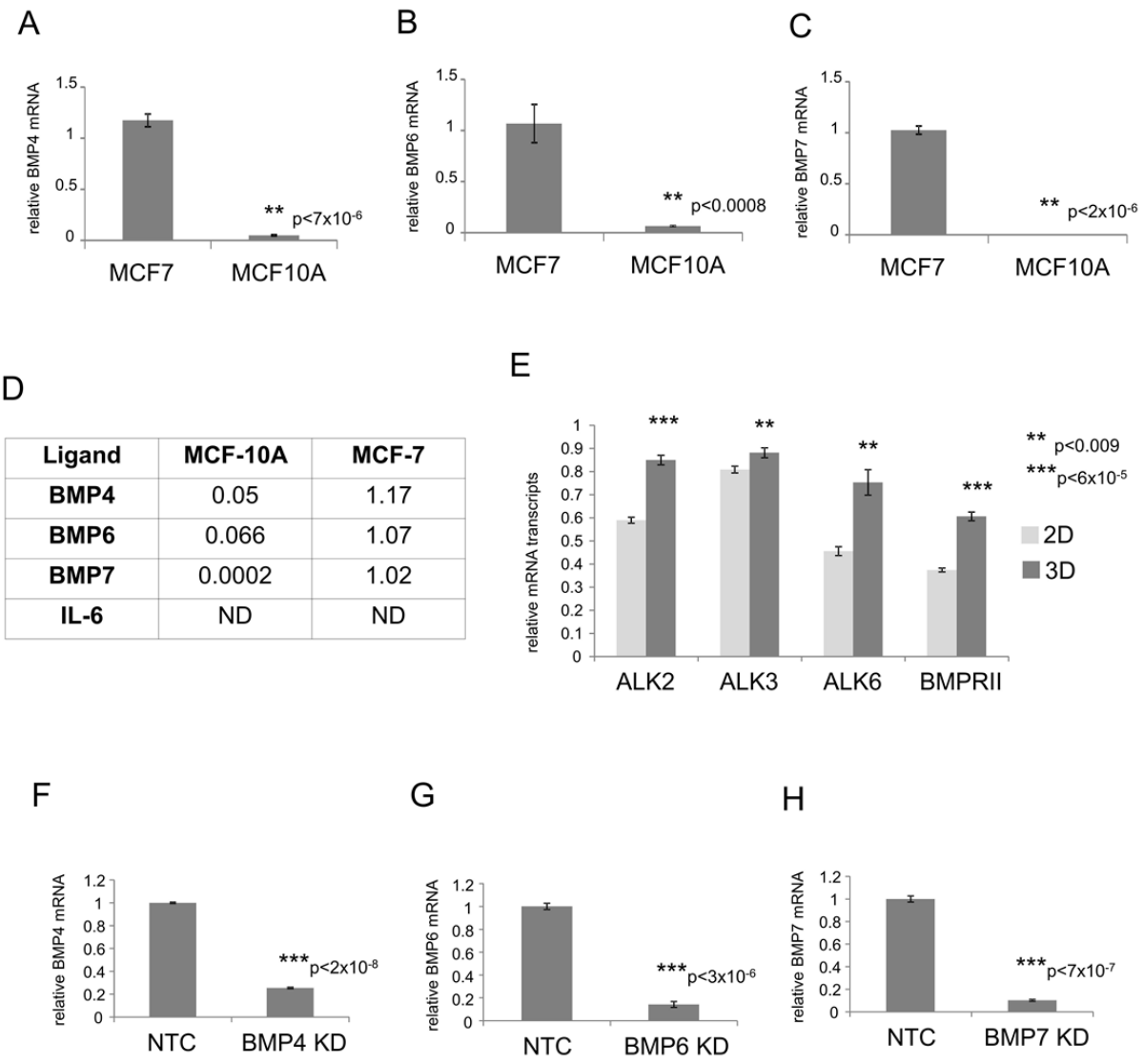

Ligand	MCF-10A	MCF-7
BMP4	0.05	1.17
BMP6	0.066	1.07
BMP7	0.0002	1.02
IL-6	ND	ND

Supplementary Figure 3-S3. BMPs are endogenously produced in BC spheroids and are elevated compared to non-tumor spheroids.

(A-C) RT-qPCR of (A) BMP4, (B) BMP6 and (C) BMP7 mRNA (normalized to Cyclophilin A) in MCF-7 and MCF-10A spheroids. (D) Relative mRNA transcript values from RT-qPCR of BMP4, BMP6, BMP7 and IL-6 mRNA (normalized to Cyclophilin A) in MCF-10A and MCF-7 spheroids. (E) RT-qPCR of ALK2, ALK3, ALK6, and BMPRII mRNA (normalized to Cyclophilin A) in MCF-7 monolayer and spheroids. (F-H) RT-qPCR of (F) BMP4, (G) BMP6 and (H) BMP7 mRNA of non-targeting control (NTC) and siRNA knock-down in MCF-7 spheroids. Samples are normalized to Cyclophilin A.

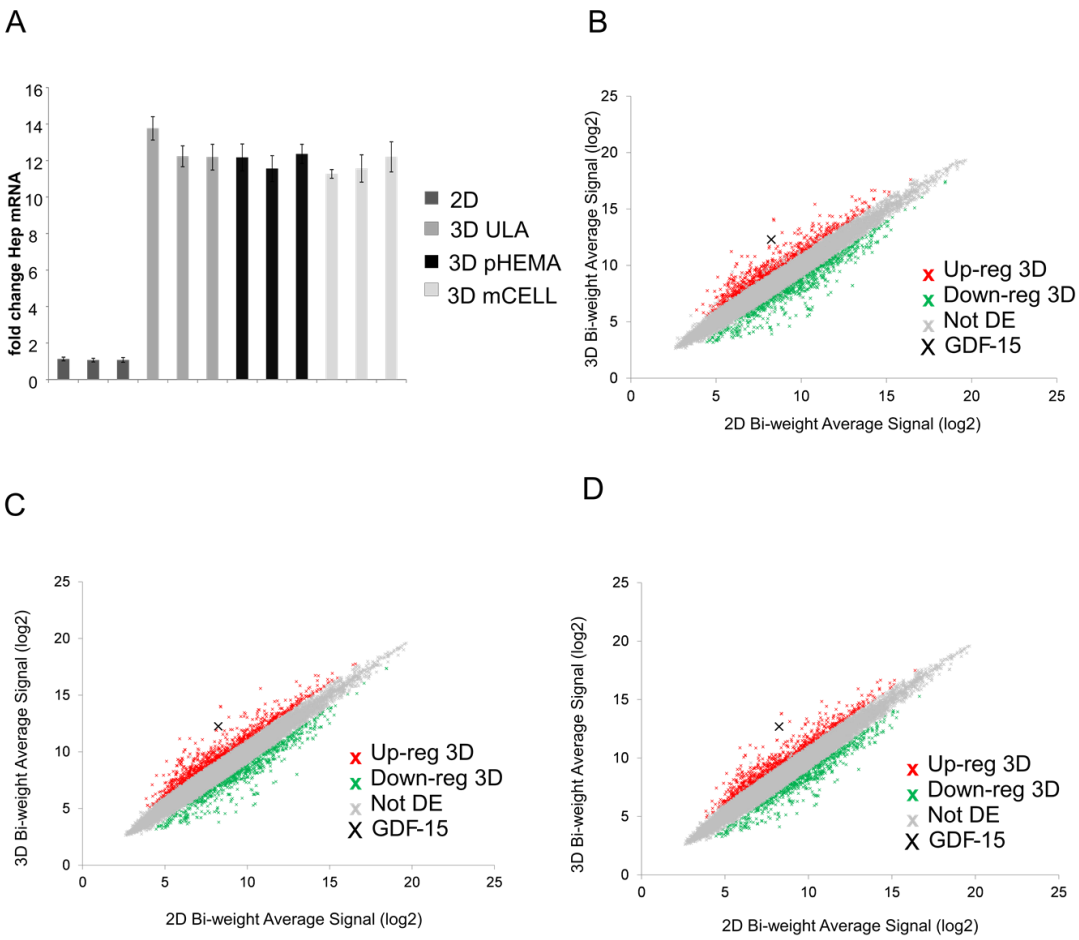

Supplementary Figure 3-S4. Hepcidin and GDF-15 are upregulated in MCF-7 cells grown as spheroids independent of the method used to induce spheroid formation.
(A) RT-qPCR of Hepcidin mRNA (normalized to Cyclophilin A) in replicate cultures of MCF-7 cells grown as monolayers (2D), ultra-low attachment (ULA) spheroids, poly-HEMA (pHEMA) spheroids, or methylcellulose (mCELL) spheroids submitted for microarray analysis. (B-D) Scatterplot of bi-weight average signals (log2) for all microarray transcript cluster IDs of 2D monolayer and (B) 3D polyHEMA (C) 3D ultra-low attachment and (D) 3D methylcellulose samples. Red represents genes up-regulated (up-reg) in 3D; green represents genes down-regulated (down-reg) in 3D; gray represents genes not differentially expressed (DE).

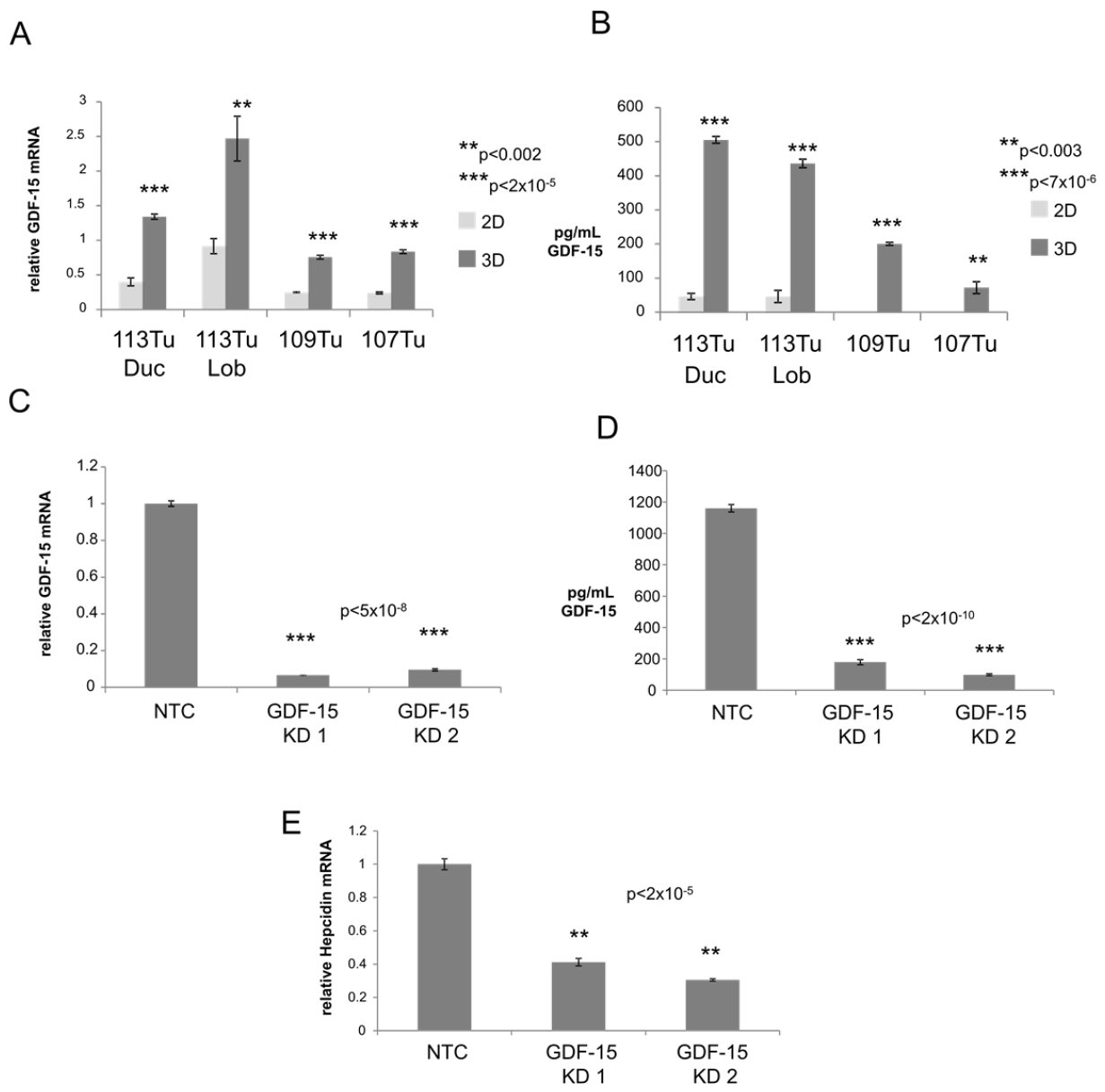

Supplementary Figure 3-S5. GDF-15 is induced in 3D culture of BC spheroids and depletion of GDF-15 results in significant reduction of hepcidin expression.
(A) RT-qPCR of GDF-15 mRNA(normalized to Cyclophilin A) in primary tumor monolayers vs. spheroids. (B) ELISA of secreted GDF-15 in primary tumor monolayers and spheroids. (C) RT-qPCR of GDF-15 mRNA (normalized to Cyclophilin A) and (D) GDF-15 ELISA following knock-down of GDF-15 using 2 different siRNAs (siRNA #1 and siRNA #2) compared to non-targeting control (NTC). (E) RT-qPCR of Hepcidin mRNA (normalized to Cyclophilin A) for NTC, GDF-15 siRNA#1 and siRNA#2.

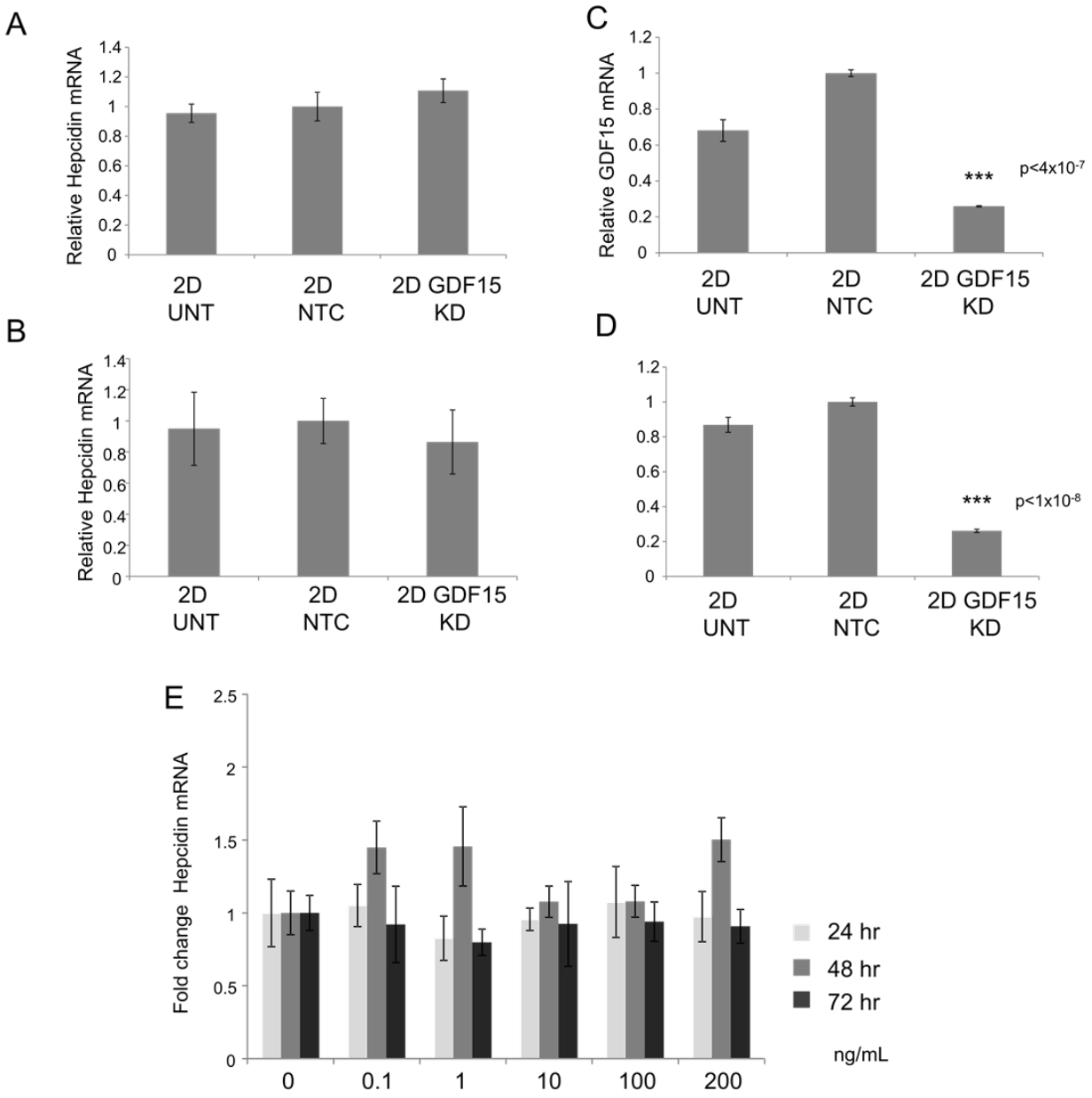

Supplementary Figure 3-S6. GDF-15 depletion does not affect hepcidin expression in MCF-7 monolayer cells.

(A-D) RT-qPCR of (A-B) Hepcidin mRNA (normalized to Cyclophilin A) and (C-D) GDF-15 mRNA (normalized to Cyclophilin A) following knock-down using non-targeting control (NTC) and GDF-15 (KD #1) siRNA for (A and C) 2 days or (B and D) 4 days in MCF-7 monolayer cells. For statistical analysis, samples were compared to non-targeting control. (E) RT-qPCR of Hepcidin mRNA (normalized to β-actin) following recombinant GDF-15 treatments for 24, 48 or 72 hours in MCF-7 monolayer cells.

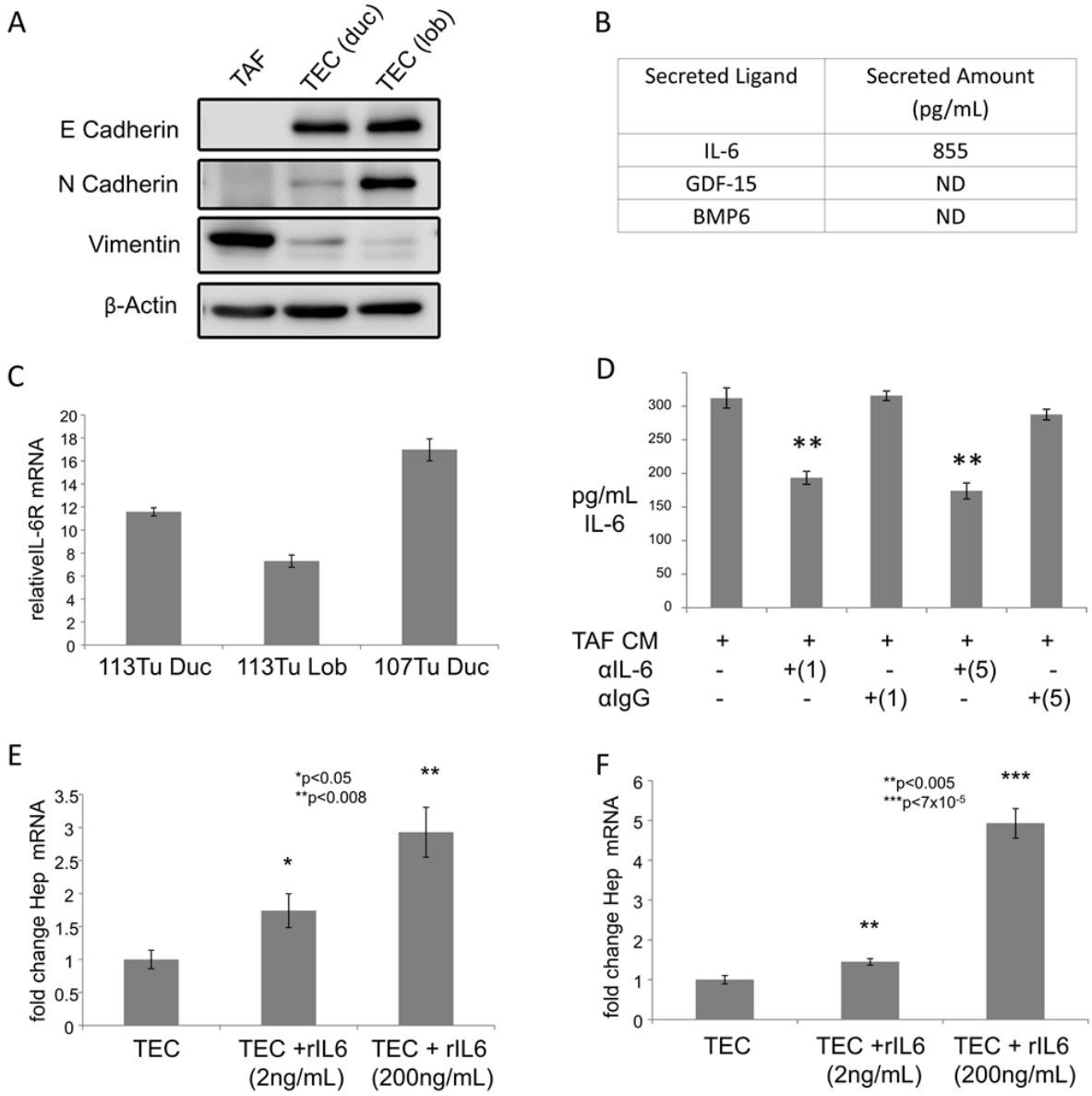

Secreted Ligand	Secreted Amount (pg/mL)
IL-6	855
GDF-15	ND
BMP6	ND

Supplementary Figure 3-S7. Characterization of tumor associated fibroblasts (TAFs) and their regulation of hepcidin by IL-6.

(A) Western blot analysis of patient 113 TAFs, TEC (ductal) and TEC (lobular) depicting expression of E-cadherin, N-cadherin, Vimentin and β-actin. (B) ELISA results of secreted IL-6, GDF-15 and BMP6 (pg/mL) from TAF conditioned media after 48 hours of secretion. ND=not detected based on ELISA minimum threshold (<23.4pg/mL for GDF-15, <150pg/ml for BMP6). (C) RT-qPCR of IL-6 receptor (IL-6R) mRNA (normalized to Cyclophilin A) for primary tumor cell spheroids. (D) IL-6 ELISA following neutralization of IL-6 or IgG (1=1μg/mL and 5=5μg/mL) in p113Tu lobular spheroids after 4 days. For statistical analysis, samples were compared to TAF conditioned media sample. (E-F) RT-qPCR of hepcidin mRNA (normalized to Cyclophilin A) after 3 days of recombinant IL-6 treatment in (E) patient 113TuLob or (F) patient 107TuDuc spheroids.

Supplementary Table 3-S2. Primer Sequences used for RT-qPCR.

Gene Name	Forward Primer Sequence	Reverse Primer Sequence
β-actin	TTGCCGACAGGATGCAGAAGGA	AGGTGGACAGCGAGGCCAGGAT
Cyclophilin A	CTGGACCCAACACAAATGGTT	CCACAATATTCATGCCTTCTTTCA
Hepcidin	CTGACCAGTGGCTCTGTTTTC	GAAGTGGGTGTCTCGCCTC
BMP2	CGCAGCTTCCACCATGAAGAA	CCTGAAGCTCTGCTGAGGTGATA
BMP4	AGGAGCTTCCACCACGAAGAAC	TGGAAGCCCCTTTCCCAATCAG
BMP6	GTGAACCTGGTGGAGTACGACAA	AGGTCAGAGTCTCTGTGCTGATG
BMP7	CAGCCTGCAAGATAGCCATT	GAGCAGGAAGAGATCCGATT
IL-6	AAATGCCAGCCTGCTGACGAAC	AACAACAATCTGAGGTGCCCATGCTA
IL-6R	CTCCTGCCAGTTAGCAGTCC	TCTTGCCAGGTGACACTGAG
STAT3	GGCATTCGGAAAGTATTGTCG	GGTAGGCGCCTCAGTCGTATC
GDF-15	GGTGTCGCTCCAGACCTATG	GGAACCTTGAGCCCATTCCA
ALK2	ACGATGGCTTCCACGTCTACCAG	ACAGTGTAATCTGGCGAGCCAC
ALK3	TGCTATTGCTCAGGGCACTGTC	TCGGCCTTTACCAACTTGCCG
ALK6	AGTGTCGGGACACTCCCATTC	TGAACCAGCTGGCTTCCTCTGTG
BMPRII	TGACACAACACCACTCAGTCCA	GCTGCTGCCTCCATCATGTTC

Chapter IV

Regulation of Hepcidin by the Extracellular Matrix

(Unpublished Data)

Abstract

The extracellular matrix (ECM) is commonly modified in breast cancer to support malignancy. Iron metabolism is also altered in breast cancer, where iron is retained to support cancer cells proliferative demands. Despite common contributions to breast cancer progression, no evidence exists to display a mechanistic link between the ECM an iron metabolism. Due to the fact that 3D spheroid culture can reflect the cell-ECM contacts present in breast tumors and hepcidin induction is elevated in spheroids as displayed in chapter three, we investigated a potential role of the ECM on regulation of hepcidin. The ECM, specifically collagen I and IV, was found to repress hepcidin spheroid induction at early time points in breast cancer spheroids. Mechanistically, collagen reduces levels and downstream activity of GDF-15, suggesting that collagen may act as a storage depot for potential release of ligands in times of cellular demand for increased iron. This reveals a novel relationship between the ECM and iron metabolism, potentially through tight control and release of positive regulators in times of hepcidin and subsequent iron demands.

Introduction

The extracellular matrix plays a vital role in maintaining normal breast architecture and is modified during breast cancer progression [144, 145]. The role of the ECM has been extensively studied in many cancers, including breast cancer [146-149]. Cancer cells can take advantage of the once organized and supportive integrity of the ECM, by breaking down and modifying the microenvironment to fuel its malignant potential [144, 150]. This has been shown to be a dynamic process in breast cancer. First, tumor cells break down their basement membrane ECM, which was once there to promote normal breast tissue architecture. Following this breakdown, breast cancer cells increase production of ECM resulting in increased breast density, mainly though deposition of collagen fibers [151]. Not only can this aberrant ECM production support tumor cell progression through direct signaling, but it has also been

observed that collagen fibers are positioned in a linear arrangement to aid in breast cancer cell migration and intravasation out of the primary tumor site [152-154].

3D spheroid culture has been praised for its ability to better recapitulate the cell-extracellular matrix (ECM) interactions present within tumors that monolayer culture is unable to model [81]. Studies have shown that 3D spheroid culture of cancer cells show an increased endogenous production of several matrix proteins, such as fibronectin, compared to monolayer culture [78]. It is believed that matrix protein production is increased in 3D culture to serve as a barrier to drug diffusion, resulting in increased chemoresistance [78]. Drug resistance has been repeatedly observed in 3D culture and better reflects the drug resistance of tumors [155-158]. Thus, the ECM and iron metabolism are both altered in spheroids compared to monolayer culture. Due to these concomitant changes, we wondered if any relationship might exist between the ECM and iron regulation, as both entities are known to contribute to breast cancer progression. Specifically, any potential role of the ECM in regulation of hepcidin has never been investigated.

Unlike MCF-7 breast cancer cells, which are known to spontaneously form spheroids in suspension culture, many other cancer cells require a 3D scaffold or exogenous ECM substrate, such as Matrigel™ (BD Biosciences), composed of mostly laminin and collagen IV, to assist with spheroid formation [79, 159, 160]. In this study, we first examine the effects of exogenous ECM on hepcidin expression by Matrigel addition. An effect on hepcidin would suggest that the ECM is an integral component in regulation of hepcidin within the tumor microenvironment and would provide a greater understanding of the crosstalk between the ECM and regulation of iron in breast cancer. Our findings highlight and important role of the ECM, specifically by collagen, in regulation of hepcidin. Mechanistically, collagen regulation of hepcidin may be a cell protective mechanism through storage of GDF-15 and potentially other positive regulators of hepcidin. This may involve a complex temporal relationship for iron sensing and release of positive regulators when a demand for hepcidin exists.

Results

Collagen negatively regulates hepcidin in breast cancer spheroids

In addition to stromal cells within the tumor microenvironment as we examined in chapter three, we also wondered if extracellular matrix (ECM) proteins could influence hepcidin expression, as a direct role of ECM proteins on breast tumorigenesis is evident [144]. To test this, we first cultured MCF-7 spheroids in the presence of Matrigel, either 2% supplemented in the media or cultured directly on pure Matrigel. We noted that 2% Matrigel resulted in more uniform, densely packed spheroids and those cultured on pure Matrigel were smaller and more numerous compared to our non-Matrigel spheroids (Figure 4-1A). All spheroids were viable as depicted by calcein-AM staining. We next examined hepcidin expression in these various spheroids and noticed a significant reduction of hepcidin in the presence of Matrigel compared to non-Matrigel containing spheroids (Figure 4-1B). Hepcidin transcript levels were reduced ~50% in Matrigel containing spheroids compared to the normal 3D spheroids, yet were still induced compared to monolayer cell levels. This led us to believe that the intrinsic properties of 3D culture results in induction in our Matrigel containing spheres compared to monolayer culture, yet something present in the Matrigel was limiting their full induction of hepcidin. Thus we hypothesized that something present in Matrigel may be negatively regulating hepcidin expression.

To test this, we examined the constituents of the growth factor reduced Matrigel we used in our experiments and found that according to the manufacturer (Corning), Matrigel is composed of 50% laminin, 30% collagen IV and 8% entactin as well as heparan sulfate proteoglycans. Thus we analyzed the effects of these proteins on hepcidin expression. We first started by exogenous addition of the two most highly abundant proteins in Matrigel, laminin and collagen IV, to our MCF-7 spheroids. We found that laminin had no effect on hepcidin expression, but addition of collagen IV resulted in significantly reduced hepcidin expression

compared to untreated spheroids at multiple concentrations (Figure 4-2 A and B). We next wondered if this effect was specific to collagen IV or was an effect of collagen in general. Thus, we treated MCF-7 spheroids with exogenous collagen I in addition to collagen IV and found both collagen proteins have a similar effect on reducing hepcidin expression in MCF-7 spheroids (Figure 4-2 C). To further support these results, we also treated our primary patient breast cancer spheroids with collagen I and IV and again saw the same negative effect on hepcidin expression, in which hepcidin was even more dramatically reduced in our patient spheroids (Figure 4-2 D and E). Overall we concluded that collagen I and IV negatively regulate hepcidin expression in breast cancer spheroids.

Collagen potentially sequesters GDF-15 for negative regulation of hepcidin

Next, we elucidated the mechanism by which collagen was negatively regulating hepcidin. It is known that the ECM can be a reservoir for growth factors and ligands and act as a storage depot of bioactive molecules for later use in times of cellular demand [161, 162]. Thus, collagen may be repressing hepcidin induction by sequestration of ligands that positively regulate hepcidin in spheroids, such as GDF-15, as modeled in Figure 4-5. Interestingly, previous literature suggests that prostate cancer cells secrete the unprocessed form of GDF-15 and that it associates with the ECM for extracellular storage of GDF-15 [163]. Thus we hypothesized that collagen is initially sequestering GDF-15 extracellularly and preventing GDF-15 from binding to spheroid cells and triggering its downstream signal cascade for hepcidin induction. To test this, we first treated MCF-7 spheroids with collagen I or IV and found that levels of secreted GDF-15 in the media of spheroids was reduced in spheroids containing collagen compared to spheroids without collagen (Figure 4-3A). Additionally, since our previous work in chapter three suggests that GDF-15 regulates hepcidin via signaling through SMAD1-5-8, we checked activity of this pathway in the presence of collagen I or IV. We found that in the presence of collagen, pSMAD1-5-8 was reduced and again resulted in decreased hepcidin

expression (Figure 4-3B). Overall, this suggests that collagen could be mediating its effect of reducing hepcidin expression through initial sequestration of GDF-15 and subsequent reduction of SMAD1-5-8 activity, which is modeled in Figure 4-4.

Discussion

In this study, we found that exogenous ECM, either by Matrigel, collagen I or collagen IV addition, results in reduced hepcidin expression compared to spheroids not treated with exogenous ECM (Figure 4-1 and 4-2). Additionally, we found that secreted GDF-15 was reduced in the presence of collagen I or IV and that its downstream activation through pSMAD1-5-8 was also reduced (Figure 4-3). Thus, we postulated that collagen may be sequestering and binding GDF-15, as a similar mechanism has been previously described in prostate cancer cells [163]. However, in that study they showed that GDF-15 was secreted from prostate cancer cells in its precursor form and that this inactive form was sequestered and binding to the ECM for extracellular storage [163]. Thus it's postulated that once the cancer cells require GDF-15, it could be cleaved extracellularly where it becomes free to dissociate from the ECM and trigger its signaling cascade on neighboring cancer cells or be secreted into serum for maintaining systemic levels of GDF-15. In our study, our detection methods for analyzing GDF-15 (by ELISA method) can detect both the precursor as well as the active forms, so it would be worthwhile to determine what form (precursor or mature) of GDF-15 is predominantly being secreted from MCF-7 spheroids. In addition to which form is being secreted, we would next want to examine a potential physical binding between GDF-15 and collagen. Although GDF-15 was previously found to be generally associated with the ECM, a direct binding between GDF-15 and collagen has not been identified [163].

Furthermore, our experiments were conducted very short term, where the spheroid may not need the excess GDF-15 currently being stored in the ECM. It would be interesting to determine if the levels of active GDF-15, and subsequent pSMAD1-5-8 signaling would increase

over time when GDF-15 would be needed for positive regulation of hepcidin (and thus increasing intracellular iron). If levels of active GDF-15 increase over time, one would also expect levels of hepcidin to increase over time as well. If this is a dynamic process and GDF-15 and its subsequent signaling are increasing over time, it would be interesting to determine what is responsible for this shift from bound to unbound (or inactive to active) GDF-15. If it is binding as a precursor, one may presume that GDF-15 would be cleaved by ECM associated pro-convertases such as PC6 or PACE4 or matrix metalloproteinases (MMPs) such as MMP14 or MMP26, both of which were previously found to cleave and activate GDF-15 [164-166]. It is plausible that low iron is sensed in spheroid cells, leading to up-regulation of a cleavage factor for extracellular cleavage of GDF-15, which would result in its activation. Upon cleavage, the GDF-15 would be free to trigger its downstream signaling pathway for increased hepcidin expression, leading to increased intracellular iron.

In addition to further characterization between the direct relationship between collagen and GDF-15, we would also want to examine potential relationships between collagen and other positive regulators of hepcidin, such as the BMPs, as BMP2 and collagen binding has been previously observed [167]. Since our data demonstrates that GDF-15 and BMPs utilize the same pathway through pSMAD1-5-8 activation, it is possible that levels of BMPs are also decreased by addition of collagen and this contributes to the decrease in hepcidin observed in spheroids treated with collagen. It would also be interesting to determine if collagen has the same effect on decreasing hepcidin in monolayer culture of MCF-7 breast cancer cells. This would enable us to determine if this negative effect on hepcidin by collagen is an effect specific to 3D structures, or a general effect of collagen scaffolds through ligand sequestration in either dimension. Overall, this study demonstrated a dynamic connection between the ECM and hepcidin and although there is still much to be elucidated, this is the first study to reveal a relationship between the ECM and iron metabolism in breast cancer. Both the ECM and iron

metabolism are well characterized as contributors to breast cancer progression, thus establishing a connection between them would prove extremely impactful.

Materials and Methods

Cell Line Culture

MCF-7 cells were obtained from the Wake Forest University Comprehensive Cancer Center Tissue Culture Core facility and verified by ATCC cell authentication testing service. MCF-7 cells were cultured in Dulbecco's minimal essential medium (DMEM)–F12 (Gibco) supplemented with 10% FBS (Benchmark) and were maintained at 37°C in a humidified atmosphere containing 5% CO2.

Spheroid Culture

24 hours before spheroid plating, U-bottom 96-Well Polystyrene Round Bottom Microwell Plates (Fischer Scientific) were coated with Poly(2-hydroxyethyl methacrylate) (polyHEMA) (Sigma). Briefly, 2.4g of polyHEMA (Sigma) was dissolved in 20mL of 70% EtOH to make a 10X stock. A 1X solution was prepared with 70%EtOH and 30ul per well was added. Plates were left in laminar flow hood overnight to ensure EtOH evaporation. To generate spheroids, cells were passaged from monolayer cultures and cells were seeded at 8,000 cells/well in polyHEMA coated plates in corresponding normal growth media. In some experiments, spheroids were plated with supplementation of 2% Matrigel™ Membrane Matrix; Growth Factor Reduced (Corning) in normal growth media. For 3D Matrigel spheroids, 100ul of pure Matrigel was placed on non-polyHEMA coated U-bottom plates and was placed into 37°C incubator to allow for Matrigel solidification. Subsequently, 8,000 cells/well were plated directly onto Matrigel coated plates in normal growth media with the supplementation of 2% Matrigel. To examine spheroid viability, 2uM calcein-AM was added to spheroid wells and live spheroids were imaged using a fluorescent inverted microscope (Zeiss Axio Vert.A1).

Real-time qPCR.

RNA was isolated and purified from cells using High Pure RNA Isolation Kit (Roche Diagnostics) following the manufacturer's instructions. Oligo(dT) primer was used in cDNA synthesis. Briefly, 200–400 ng of RNA was reverse transcribed in a total volume of 50 µl with a reverse transcription reagents kit (Applied Biosystems). To make a standard curve, serial dilutions of RNA from one sample were added to the RT reaction. Aliquots (2 µl) of cDNA were added to a 18 µl reaction mixture containing 10 µlof 2× SYBR® Green PCR Master Mix (BioRad) and 400 nm primers. The reaction included primer sequences specific to hepcidin, GDF-15 or Cyclophilin A depending on the experiments described See Supplemental Table 3-S2 for primer sequences. Absence of DNA contamination was confirmed by performing PCR from cDNA without reverse transcriptase.

Western Blots

Samples were lysed in 1X RIPA buffer in the presence of protease and phosphatase inhibitors (Roche Diagnostics, Basel, Switzerland), were reduced with 10 mM β-mercaptoethanol and proteins separated by SDS-PAGE. Western blots were probed with antibodies to phospho-Smad-1/5/8 (Cell Signaling), hepcidin (Fitzgerald), or β-actin (Abcam). Western blots were quantified with Image J. Hepcidin blots were quantified by normalization to β-actin.

ELISA analysis for secreted GDF-15

GDF-15 was measured in conditioned growth media using a GDF-15 Human ELISA kit from R&D systems and following manufacturers' protocol. Recombinant GDF-15 (R&D systems) was used as a positive control.

Extracellular Matrix Protein Addition

Before spheroid plating, the addition of 1, 5, 10, or 20 ug/mL of mouse laminin (Corning), mouse collagen 1 (MD Biosciences) or Cultrex mouse collagen 4 (R&D systems) was added to cell suspension. Unless otherwise noted, spheroids were harvested after 3 days of ECM treatment.

Statistical analysis

Statistical analyses were performed using Excel and are reported as the mean ± standard deviation. Error bars represent standard deviation. Unless otherwise noted, significant differences between control and treatment groups were determined using two-tailed unpaired Student's t tests.

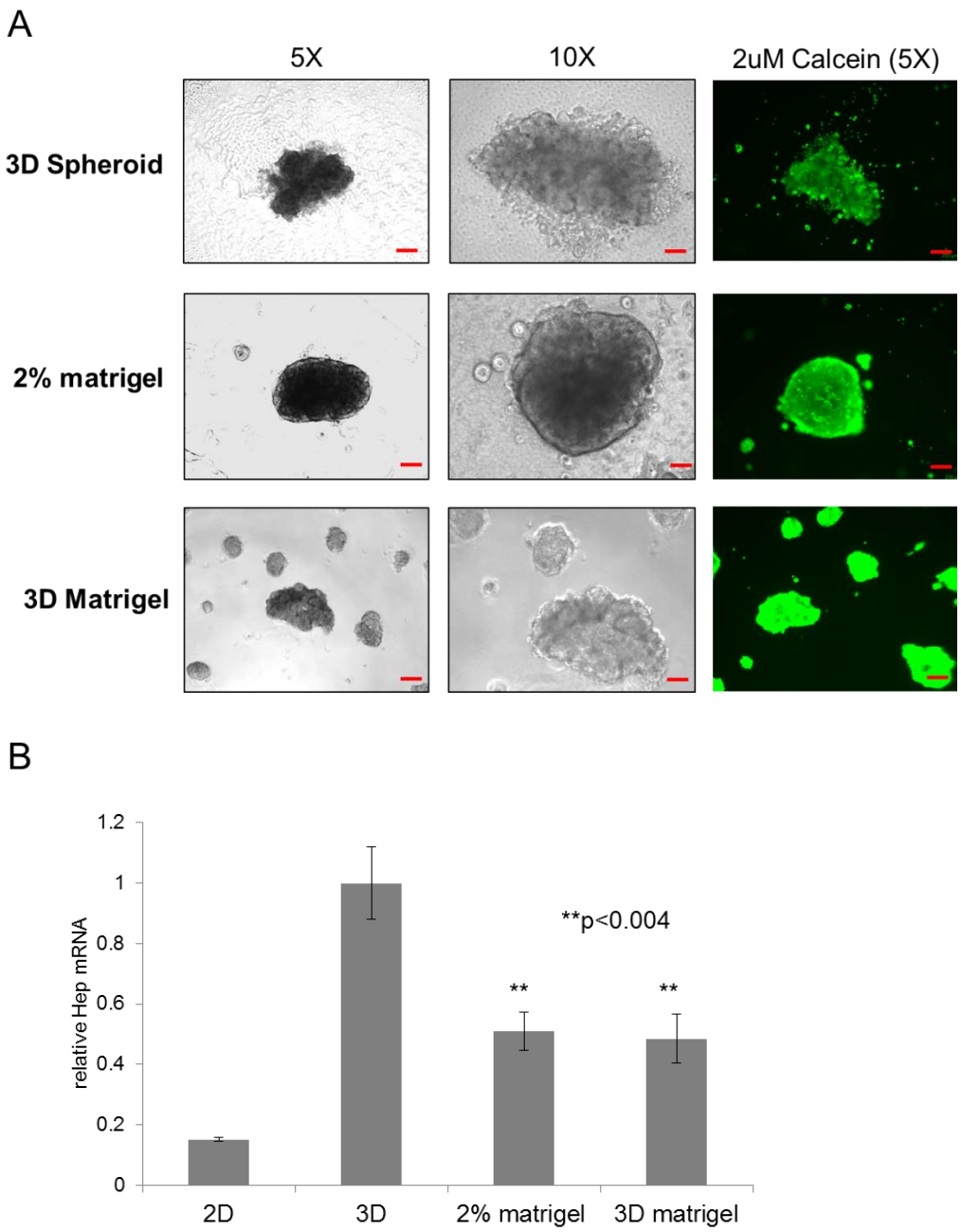

Figure 4-1. Addition of Matrigel to breast cancer spheroids limits hepcidin spheroid induction.

(A) Representative images of MCF-7 spheroids without Matrigel (top row; 3D spheroid), with 2% Matrigel supplemented in the media (middle row; 2% Matrigel) or embedded into pure Matrigel with the addition of 2% Matrigel supplemented in the media (bottom row; 3D Matrigel) at 5X and 10X magnification. (B) RT-qPCR of hepcidin (normalized to Cyclophilin A) for MCF-7 cells grown in 2D, 3D spheroid, 3D spheroid +2% Matrigel, or 3D pure Matrigel for three days. Scale bar=200uM (5X), 100uM (10X)

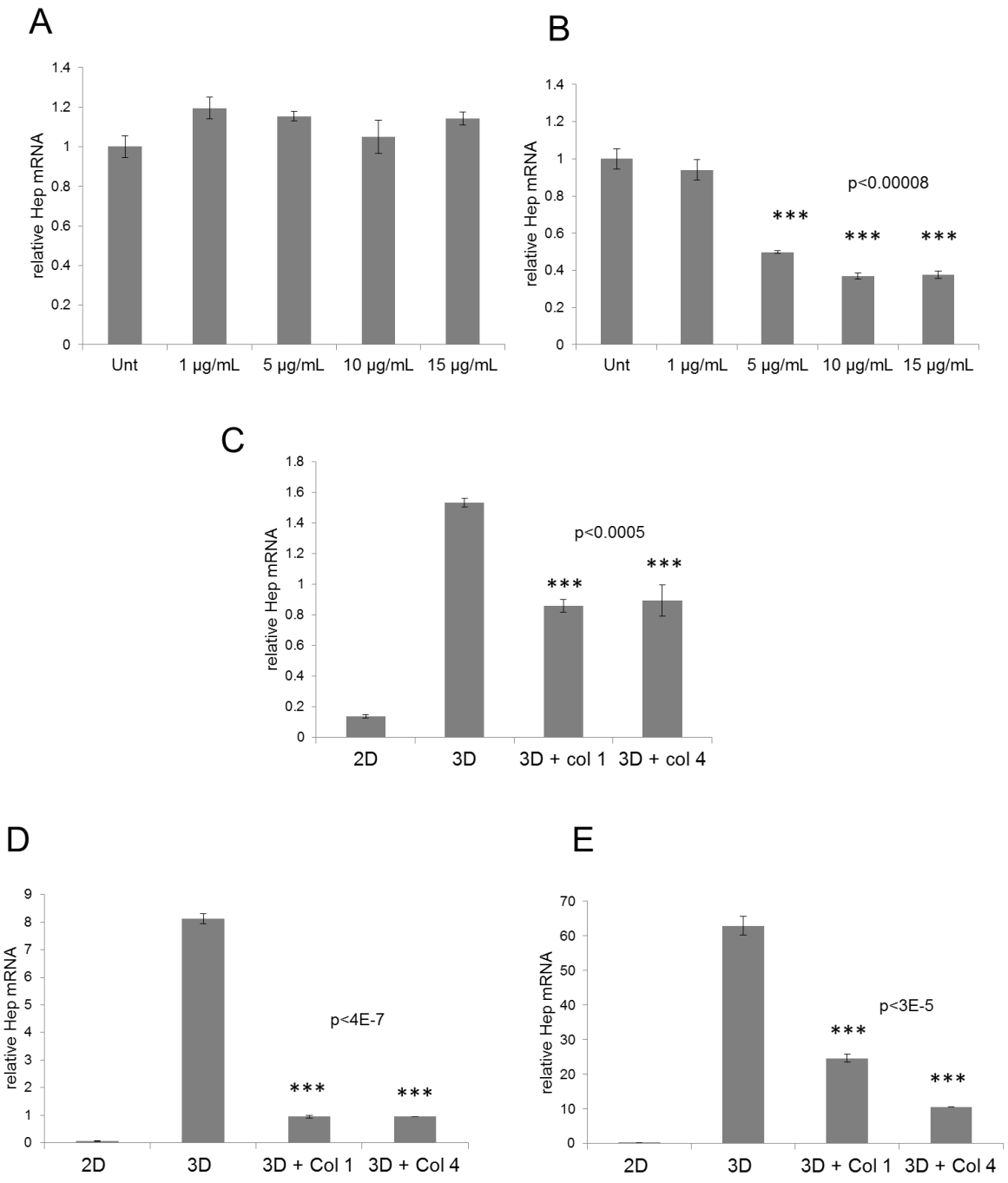

Figure 4-2. Collagen 1 and 4, not laminin, represses hepcidin induction in breast cancer spheroids.

(A) RT-qPCR of hepcidin (normalized to Cyclophilin A) following laminin addition to MCF-7 spheroids for 3 days. (B) RT-qPCR of hepcidin (normalized to Cyclophilin A) following addition of collagen I addition to MCF-7 spheroids for 3 days. (C-E) RT-qPCR of hepcidin (normalized to Cyclophilin A) following addition of 10ug/mL collagen I or collagen IV for 3 days in (C) MCF-7 spheroids, (D)p107Tu spheroids, and (E)p129Tu spheroids.

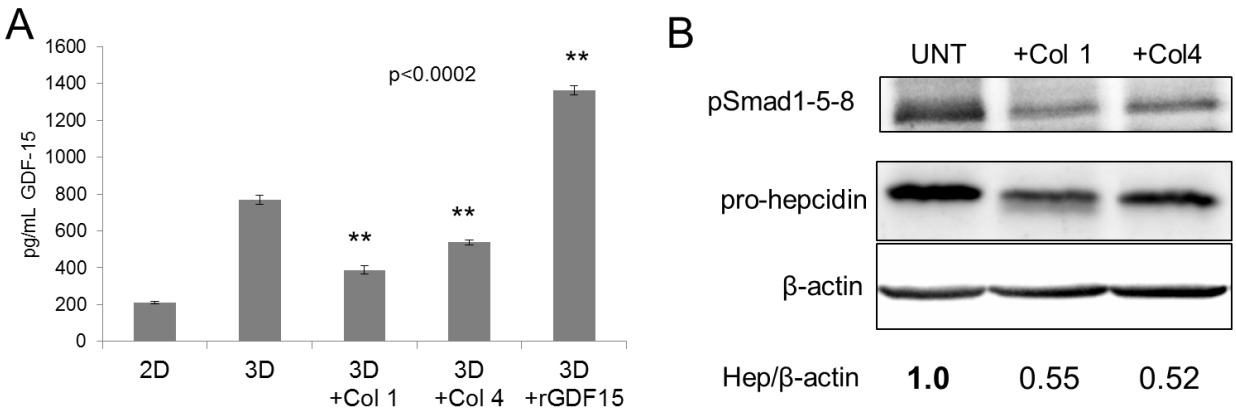

Figure 4-3. Addition of collagen results in decreased GDF-15 secretion and p-SMAD1-5-8 activity.

(A) Secreted GDF-15, as detected by ELISA after the addition of 10ug/mL collagen 1, 10ug/mL collagen 4 or 1000pg/mL recombinant human GDF-15 (as a control) for 3 days to MCF-7 spheroids. (B) Western blot analysis of pSmad1-5-8, pro-hepcidin, and β-actin following addition of collagen 1 or collagen 4 to MCF-7 spheroids for 3 days.

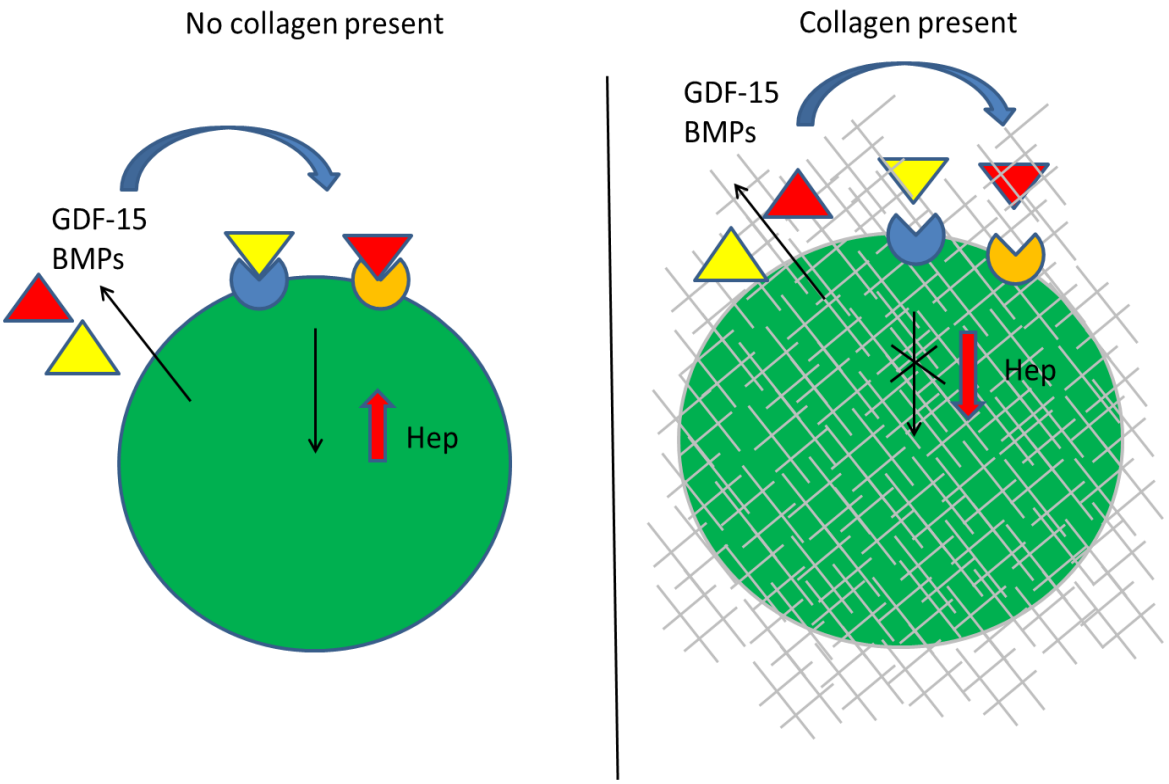

Figure 4-4. A proposed model for GDF-15 and/or BMP sequestration by collagen in breast cancer spheroids.
In the presence of collagen, GDF-15 and/or BMPs is sequestered and stored in an ECM reservoir, preventing its ability to bind and induce a signaling cascade for induction of hepcidin in the nucleus.

Chapter V:

Further Characterization of Spheroid Iron Metabolism

(Unpublished Data)

Abstract

Iron metabolism is altered in breast cancer to favor accumulation of intracellular iron for continuous cancer cell proliferation. Hepcidin, a peptide hormone that reduces iron export by binding to and degrading the mammalian iron export protein, ferroportin (FPN), is increased in breast cancer and is vastly induced by 3D spheroid culture. Due to the nutrient and oxygen gradients within spheroids, we hypothesized that hepcidin expression could be altered based on modifying these metabolic parameters. We found that modulation of spheroid metabolic parameters directly correlates with hepcidin expression, where hepcidin expression increases with more metabolic stress through modulation of spheroid size and nutrients. Furthermore, depletion of hepcidin results in decreased spheroid size, suggesting that hepcidin contributes to intracellular spheroid iron and subsequent cellular growth. Additionally, other genes that control iron metabolism are altered in breast cancer spheroids to favor intracellular iron accumulation. Thus targeting increased iron globally, through iron chelation or iron-dependent cell death mechanisms, may be the most effective treatment strategy to target iron addicted breast tumors.

Introduction

In chapter 3, we observed that hepcidin is induced, simply by culturing cells in 3D, suggesting that something intrinsic about spheroid culture is regulating hepcidin. Overall, we found that GDF-15 was majorly responsible for this induction of hepcidin, but it still remains to be known how the metabolic properties of spheroids directly influence hepcidin (and GDF-15). It is well established that spheroid culture results in nutrient and oxygen gradients, with plentiful resources towards the outside of the sphere and decreasing resources towards the spheroid core [168]. Thus we hypothesize that as the spheroid increases in size and as nutrients become deprived, hepcidin will increase to retain intracellular iron desperately needed as nutrients become limited. Additionally, as a result of increased iron, we hypothesize that depletion of hepcidin will limit spheroid growth, as iron efflux will be enhanced. This would

coincide with a previous study that found hepcidin depletion in breast cancer xenografts reduced tumor growth [28].

In addition to hepcidin induction observed in breast cancer spheroids, other proteins that control iron metabolism would be expected to be altered concomitantly with hepcidin, with the overall goal of increasing intracellular iron. Breast cancer spheroids would best achieve this goal by increasing iron uptake and storage by transferrin receptor (TFR1) and Ferritin (FT) respectively, and further reduce iron efflux by basal reduction of surface Ferroportin (FPN). All of these proteins are altered in breast cancer, but have never been shown to be further altered in spheroid culture of breast cancer cells [6]. As previously mentioned, as spheroids grow, iron becomes a limited nutrient and proteins that regulate intracellular iron would need to be altered to favor accumulation of iron for growth.

Iron is an essential nutrient for tumor cell growth and has long been thought of as an attractive target to halt cancer cell proliferation [169]. Since our data from chapter 3 demonstrates that hepcidin and ferritin are altered in spheroids to promote increased intracellular iron, spheroids may be even more susceptible to changes in iron than their own 2D counterparts, and better recapitulate iron metabolism present in breast tumors *in vivo*. Thus, utilization of breast cancer spheroids may be an attractive model to assess the effects of iron modulators for potential breast cancer therapies. We hypothesize that breast cancer spheroids are be susceptible to cell death by iron depletion. Additionally, as spheroid cells have enhanced iron-retaining phenotype, treatment of these spheroids with agents that induce ferroptosis, an iron-dependent type of cell death by accumulation of lipid ROS, may unveil a new strategy to selectively kill cancer cells with excess iron [170].

Results

Increased spheroid size and serum starvation increases hepcidin in MCF-7 cells

Due to the fact that hepcidin is induced in spheroids, most likely as a result the nutrient barriers that occur when cells are cultured in 3D, we wondered if altering the size and nutrients of spheroid culture would further impact hepcidin expression. To test this, we first cultured MCF-7 spheroids of different sizes, simply by altering the number of cells plated. Since most of our experiments have utilized 8,000 cells/spheroid at time of plating, we wondered if reducing or increasing the number of cells would impact hepcidin expression, as the nutrient gradient would be lessened the smaller the spheroid. As expected, hepcidin expression is increased with increasing cell number at time of spheroid plating (Figure 5-1 A and B). Thus, we can conclude that by reducing the spheroid size, the fewer amounts of cells are nutrient deprived and subsequently, the spheroid has less of a need for hepcidin induction for the goal of iron retention.

In addition to altering spheroid size, we also wondered if serum starvation would also impact hepcidin expression in spheroids, as iron would be severely depleted in serum-deprived conditions. To test this, we cultured MCF-7 spheroids in their normal growth media with 0% FBS and examined hepcidin expression. We found that serum starvation (0% FBS) of spheroids further induces hepcidin to a greater extent from monolayer culture (~34 fold) compared to induction observed from spheroids cultured in the presence of serum (10% FBS) from monolayer culture (~24 fold) (Figure 5-1 C). We next wondered if induction of hepcidin by serum starvation was specific for spheroids or if this could also be observed in monolayer culture. Thus, we cultured MCF-7 cells for 3 days in their normal growth media containing 10% FBS or normal growth media containing 0% FBS and examined hepcidin expression. Consistent with what we observed in spheroids, serum starvation resulted in increased hepcidin expression (Figure 5-1D). This suggests that serum starvation results in increased hepcidin expression in monolayers and spheroids, although a direct mechanism for this regulation

remains to be elucidated. It is plausible that hepcidin induction present in normal spheroids compared to monolayers may be regulated by nutrient deprivation sensing mechanisms, similar to mechanisms that regulate increased hepcidin during serum starvation.

Depletion of spheroid hepcidin levels results in decreased spheroid size

Next, we wondered what the physiological consequences of hepcidin induction would be in spheroids. Since hepcidin is induced and we previously showed that ferritin expression was increased in spheres compared to monolayer culture (Figure 3-3), we would expect this increased iron to be functional and facilitate spheroid growth. To test this, we depleted hepcidin in spheroids utilizing a siRNA knock-down (KD) approach and found that reducing hepcidin expression (~90% effective) resulted in a significant reduction in spheroid size after 5 days of KD (Figure 5-2). This suggests that hepcidin directly contributes to spheroid size and or/growth, most likely though its role in limiting iron export and increasing intracellular iron necessary for cell proliferation.

Other genes that control iron metabolism are altered in breast cancer spheroids

In addition to hepcidin, which was mainly the focus of this thesis, we also wondered if spheroid culture impacted other proteins that control cellular iron metabolism. We hypothesized that additional iron related genes would be altered in spheroids to favor intracellular iron within spheroids. We first examined FPN mRNA expression to see if any changes occurred at the mRNA level. Despite regulation of FPN by IRP post-transcriptionally, and by hepcidin post-translationally via direct binding, there is some evidence of FPN regulation at the transcriptional level, although mechanisms that control this regulation remain partially known [171]. Basal levels of FPN transcript are reduced in breast cancer cells compared to non-tumor breast epithelial cells [7]. Thus we hypothesized that spheroids, in attempt to retain cellular iron, may have reduced FPN transcript as a first line of defense. We found that compared to monolayer MCF-7 cells, MCF-7 spheroids have significantly reduced FPN transcript (Figure 5-3A).

In addition to reducing iron export, we also hypothesized that iron import would be increased in spheroids, again favoring accumulation of intracellular iron to overcome nutrient deprivation present in spheroids. Thus we examined expression of transferrin receptor (TFR1), the cell surface receptor responsible for transferrin-mediated iron uptake, and found a significant increase in TFR1 mRNA in MCF-7 spheroids compared to monolayer culture (Figure 5-3B).

Lastly, despite our previous findings that ferritin, the iron storage protein that is a surrogate marker for intracellular iron, was increased in spheroid culture (Figure 3-3E), we wondered if this was also true at the mRNA level. Ferritin was previously found to be transcriptionally regulated by oxidative stress [172], thus we hypothesized that as a result of spheroid culture ferritin mRNA expression may be increased. We found a significant increase in both Ferritin H and L subunit transcripts in MCF-7 spheroids compared to monolayer culture (Figure 5-3C and D). This may be a direct result of oxidative stress, although future studies would elucidate the mechanistic reasoning behind transcriptional elevation of ferritin H and L. Taken together, all of these alterations in genes that control iron metabolism suggest accumulation of intracellular iron to overcome nutrient limitations present in spheroids in order for spheroids to remain viable and proliferate.

Spheroids are sensitive to iron deprivation and erastin mediated ferroptotic cell death

Due to the combination of altered genes that control iron metabolism in spheroids, we hypothesized that spheroids would be sensitive to sudden changes in iron. To test this, we first treated spheroids with the iron chelator Deferoxamine (DFO) and assessed its effect on spheroid viability by calcein and propidium iodide (PI) staining for live and dead cells respectively. We noticed that treatment with DFO, either during spheroid plating or treatment 24 hours after spheroid plating, resulted in a significant increase in cell death and an astounding effect of total disruption of spheroid structures (Figure 5-4). Therefore, we concluded that iron is essential for maintaining spheroid structure.

Due to the fact that spheroids have altered genes to favor accumulation of intracellular iron and are sensitive to chelation of iron, we next wondered if this excess iron retained by breast cancer spheroids might enhance their susceptibility to agents that induce ferroptosis. Ferroptosis is a newly discovered form of cell death distinguished by its dependence on iron [170]. To test this, we treated spheroids with erastin, a small molecule that induces ferroptosis or erastin in combination with ferrostatin-1, a specific inhibitor of erastin mediated ferroptotic cell death [170]. After staining with calcein and PI, we observed a dramatic increase in cell death upon erastin treatment that could be rescued in the presence of ferrostatin-1 (Figure 5-5). This suggests that MCF-7 spheroids are sensitive to erastin mediated ferroptotic cell death.

Discussion

In this chapter, we further characterized iron metabolism in spheroids and other potential differences in proteins that control iron metabolism between monolayer and spheroid culture. Although chapter 3 focused on regulation for hepcidin induction in breast cancer spheroids, we wanted to further characterize hepcidin induction and the physiological effects of this increase. Thus, we started by examining how alterations to spheroid culture influenced hepcidin expression. We first concluded that hepcidin expression increases with increasing spheroid size and that this increase plateaus around 8,000-16,000 cells (Figure 5-1A and B). This corresponds to spheroid literature that larger spheroids (<500uM) have oxygen and nutrient gradients present, whereas smaller spheres have more access to those essentials [168]**.** Thus, one could postulate that as the spheroid increases in size, the more that iron becomes limited and hepcidin becomes induced to retain intracellular iron already present within those spheroid cells. Furthermore, we also observed that serum starvation has the ability to further induce hepcidin in both monolayer and spheroid cultures (Figure 5-1C and D). Without fetal bovine serum, which has an abundance of iron, cells must alter the proteins that control iron metabolism to ensure that any iron present within the cells does not escape. Thus, upon serum

deprivation, cells up-regulate hepcidin to prevent iron export. Since GDF-15 was found to regulate hepcidin induction in breast cancer spheroids, it would be interesting to determine if GDF-15 also regulates hepcidin under different iron alterations, such as serum starvation. If there is a direct connection between iron levels and GDF-15, we would want to determine how iron directly regulates GDF-15 mechanistically to elicit an effect on hepcidin. A previous publication indicated a direct connection between iron and GDF-15, but no mechanistic connection was elucidated [173].

In addition to further characterization of hepcidin in spheroids, we also concluded that depletion of hepcidin in breast cancer spheroids results in decreased spheroid size (Figure 5-2). Although we would need to determine if hepcidin reduction resulted in a decrease in the labile iron pool, this suggests that hepcidin plays a role in spheroid growth. Simultaneously with this thesis, a group published that depletion of hepcidin in MDA-MB-231 breast cancer cells resulted in a significant reduction in tumor growth [28]. Taken together, these data confirm that hepcidin would be an attractive molecular target for reducing breast cancer progression.

Furthermore, we began to characterize other proteins that control iron metabolism in breast cancer spheroids. Although we only examined proteins at the mRNA level, their patterns of expression all favored accumulation of intracellular iron, consistent with our results on hepcidin (Figure 5-3). Transferrin Receptor was increased, indicating that iron import may be upregulated in 3D. Ferritin mRNA was also upregulated in 3D, consistent with increased ferritin protein in patient tumor spheroids, shown in Figure 3-3. We also noted that despite tumor cells having limited ferroportin expression to start, there seemed to be a decrease in ferroportin mRNA in spheroids, again suggesting further reduced iron export in breast cancer spheroids.

It is interesting to note that these changes were observed at the mRNA level, where most known regulation of TFR1, FT, and FPN occurs post-transcriptionally. Iron regulatory proteins (IRP) 1 and 2 are master regulators of cellular iron homeostasis whose main function is to increase iron uptake when iron levels are low and decrease iron uptake when iron levels are

high [6]. Thus, TFR1, FT and FPN have iron responsive elements (IREs) in the untranslated (UTR) of their mRNAs that are bound by IRPs for post-transcriptional regulation. For example, when iron is low, IRPs bind to IREs in the 5' UTR of FT and FPN mRNAs, which inhibits their translation and thus inhibits iron storage and efflux. Additionally, IRPs bind to the IRE in the 3' UTR of TFR1 mRNA, resulting in its stabilization and translation of TFR1 to increase iron import. Thus, iron directly regulates TFR1, FT and FPN post-transcriptionally, so it is evident that some other mechanism exists to alter these iron regulatory genes at the transcriptional level. This regulation warrants investigation to determine the IRP-independent pathways that control these genes.

Additionally, we would want to observe expression of TFR1 and FPN at the protein level in spheroids to determine if the changes present at the mRNA level are consistent at the protein level, as we saw in the case of FTH and FTL. If these changes are consistent, this would demonstrate that there are global changes in iron metabolism in breast cancer spheroids, all of which favor accumulation of intracellular iron and potentially contribute to tumor cell progression.

Global changes in iron, by chelation of iron with DFO in spheroids, demonstrated that iron is clearly essential for maintaining spheroid structures (Figure 5-4). Thus, altering proteins that control iron metabolism to promote accumulation of intracellular iron seems to be essential for overcoming spheroid nutrient gradients and maintaining tumor growth and progression. Interestingly, we may be able to take advantage of this increased iron present in spheroids to kill tumor cells by ferroptosis (Figure 5-5). It would be interesting to see if tumor spheroids are more sensitive to ferroptotic cell death compared to non-tumor spheroids, as their levels of iron would be much greater and render them more susceptible to ferroptotic inducing agents. Ferroptosis may prove to be an advantageous way to selectively kill tumor cells that have selfishly increased their iron levels for continuous cell growth and tumor progression.

Materials and Methods

Cell Line Culture

MCF-7 cells were obtained from the Wake Forest University Comprehensive Cancer Center Tissue Culture Core facility and verified by ATCC cell authentication testing service. MCF-7 cells were cultured in Dulbecco's minimal essential medium (DMEM)–F12 (Gibco) supplemented with 10% FBS (Benchmark) and were maintained at 37°C in a humidified atmosphere containing 5% CO2.

Spheroid Culture

24 hours before spheroid plating, U-bottom 96-Well Polystyrene Round Bottom Microwell Plates (Fischer Scientific) were coated with Poly(2-hydroxyethyl methacrylate) (polyHEMA) (Sigma). Briefly, 2.4g of polyHEMA (Sigma) was dissolved in 20mL of 70% EtOH to make a 10X stock. A 1X solution was prepared with 70%EtOH and 30ul per well was added. Plates were left in laminar flow hood overnight to ensure EtOH evaporation. To generate spheroids, cells were passaged from monolayer cultures and cells were seeded at 8,000 cells/well in polyHEMA coated plates in corresponding normal growth media unless otherwise noted. In some experiments, 2000, 4000 and 16,000 cells were also used to generate spheroids and some spheroids were cultured without serum as specified. Live spheroids were imaged using a fluorescent inverted microscope (Zeiss Axio Vert.A1).

Real-time qPCR.

RNA was isolated and purified from cells using High Pure RNA Isolation Kit (Roche Diagnostics) following the manufacturer's instructions. Oligo(dT) primer was used in cDNA synthesis. Briefly, 200–400 ng of RNA was reverse transcribed in a total volume of 50 µl with a reverse transcription reagents kit (Applied Biosystems). To make a standard curve, serial dilutions of RNA from one sample were added to the RT reaction. Aliquots (2 µl) of cDNA were added to a

18 µl reaction mixture containing 10 µlof 2× SYBR® Green PCR Master Mix (BioRad) and 400 nm primers. The reaction included primer sequences specific to hepcidin, ferroportin, transferrin receptor, Ferritin H, Ferritin L and Cyclophilin A depending on the experiments described. See Supplemental Table 3-S2 for primer sequences. Absence of DNA contamination was confirmed by performing PCR from cDNA without reverse transcriptase.

DFO and Erastin Treatment

8000 MCF-7 cells were seeded in 96-well ultra-low attachment plates for spheroid formation and treated with deferoxamine mesylate (Sigma), erastin (Selleckchem, Houston, TX, USA) or ferrostatin-1 (Selleckchem) either during spheroid plating or 24 hours after spheroid formation. Puromycin was used as a positive control of cell death. To examine spheroid viability, 2µM calcein-AM (Life Technologies) and 4µM propidium iodide (PI) (Life Technologies) was added to spheroid wells and live spheroids were imaged using a fluorescent inverted microscope (Zeiss Axio Vert.A1).

siRNA Knock-down

All reagents were obtained from GE Dharmacon (Lafayette, CO, USA). ON-TARGETplus human SMARTpools were used for siHAMP(cat#: L-014014-00-0010) and siNTC (cat#: D-001810-10-05) were used for knockdown experiments. Transfections were performed in MCF-7 cells according to the manufacturer's recommendations using Dharmafect #1 (T-2001) transfection reagent and normal growth media without serum. Knock-down was performed in monolayer culture for 24 hours before trypansization of cells and subsequent spheroid plating. Effect on spheroid size was determined from imaging 3 spheroids for each condition after 6 days of KD (5 days as spheroids). Hep KD efficiency was confirmed at this time-point by RT-qPCR.

Statistical Analysis

Statistical analyses were performed using Excel and are reported as the mean ± standard deviation. Error bars represent standard deviation. Unless otherwise noted, significant differences between control and treatment groups were determined using two-tailed unpaired Student's t tests.

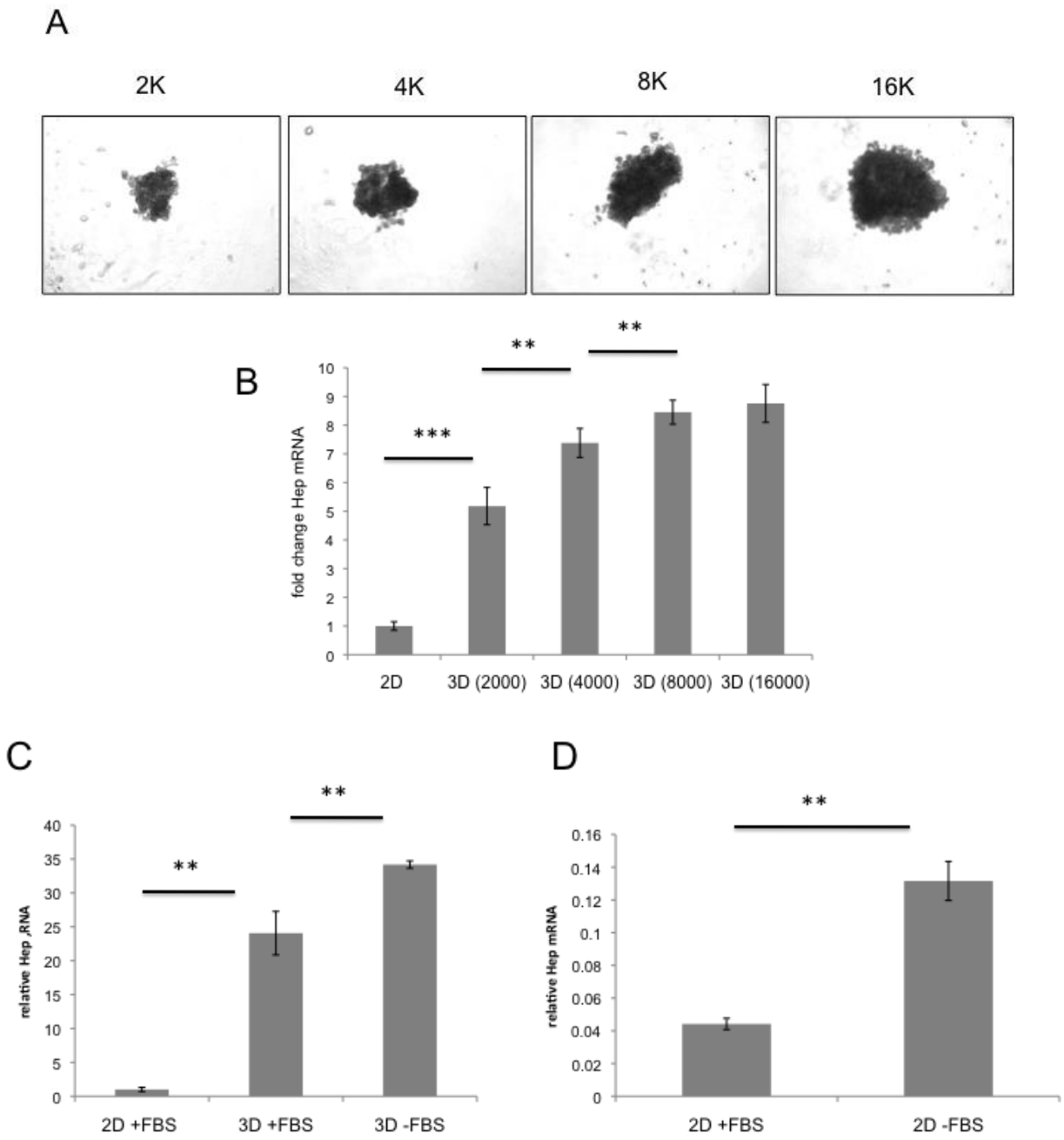

Figure 5-1.Hepcidin expression is further increased with increasing spheroid size or serum starvation.

(A) Representative images of spheroids cultured at initial seeding densities of 2000, 4000, 8000 o 16,000 MCF-7 cells respectively after 7 days in culture. (B). RT-qPCR of hepcidin mRNA (normalized to Cyclophilin A) of spheroids with varying seeding densities after 7 days in culture. (C) RT-qPCR of hepcidin mRNA (normalized to Cyclophilin A) of MCF-7 cells grown as monolayers or spheroids in normal growth medium (containing 10% FBS) or spheroids grown in medium containing no serum (0%FBS) after 7 days in culture. (D) RT-qPCR of hepcidin mRNA (normalized to β-actin) in MCF-7 cells grown in medium containing no serum or 10% serum for 3 days.

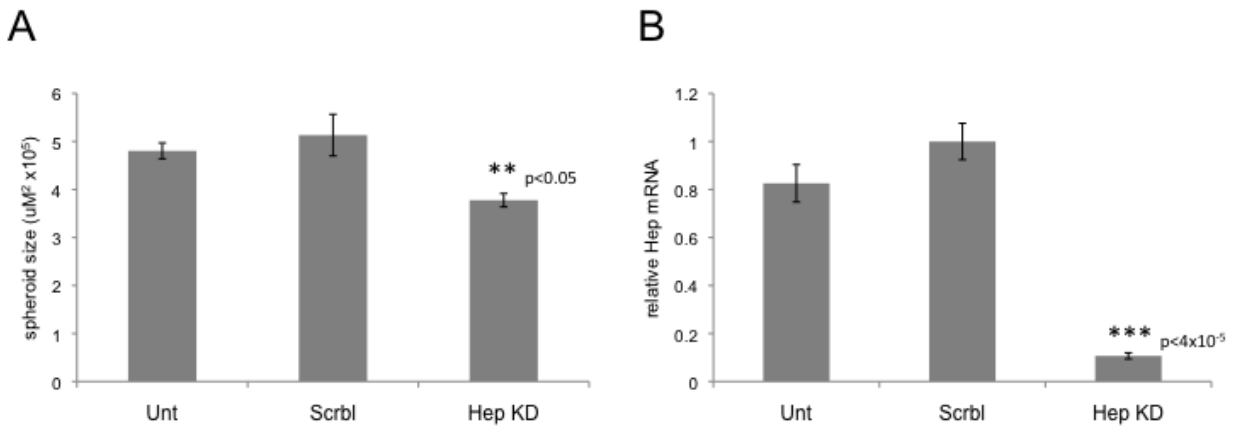

Figure 5-2. Hepcidin knock-down results in decreased spheroid size.
(A) Spheroid area as measured from images acquired after knock-down (KD) of hepcidin (Hep) or scramble (Scrbl) non-targeting control following 6 days of KD or untreated spheroids (Unt). (B) RT-qPCR of of UNT, NTC and Hep siRNAs after 6 days in MCF-7 spheroids to display knock-down efficiency.

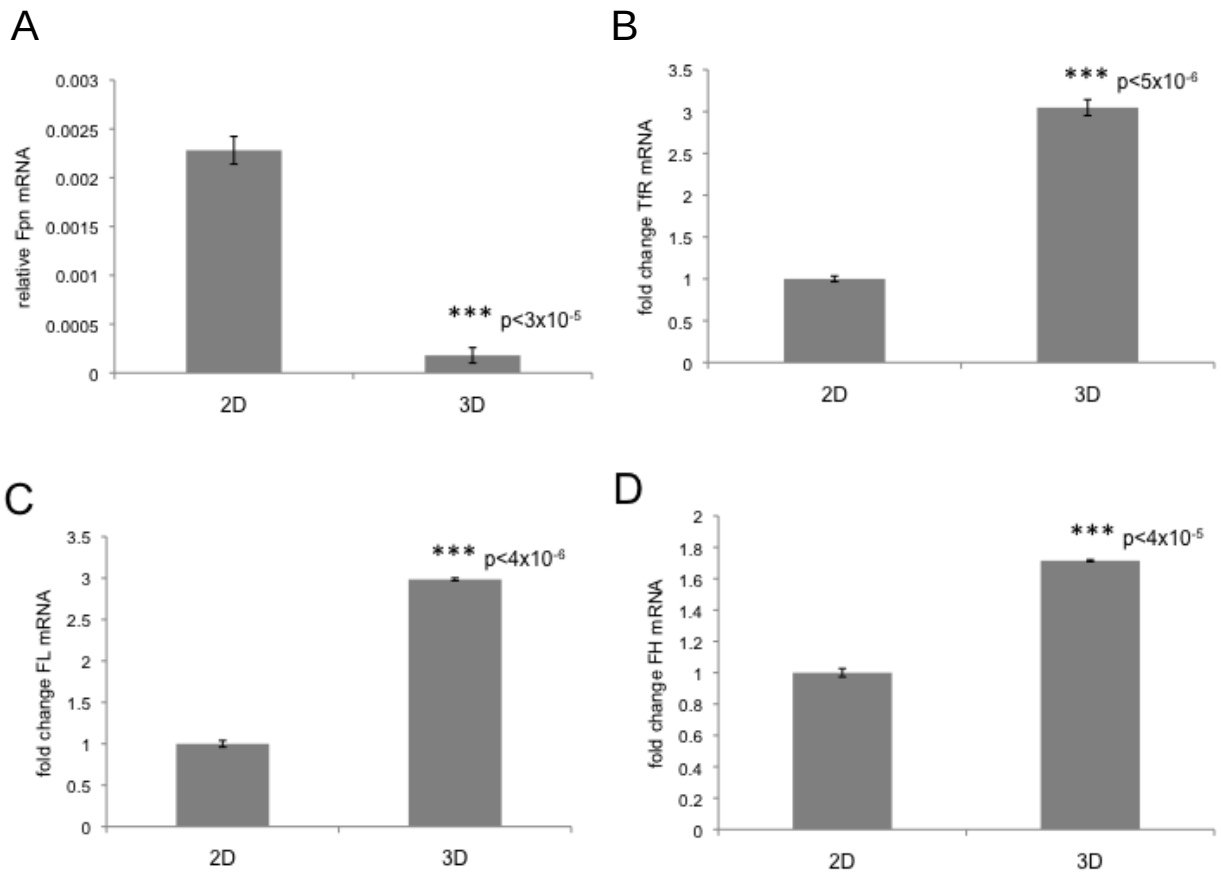

Figure 5-3. Other iron related genes favor accumulation of intracellular iron in MCF-7 spheroids.

RT-qPCR of (A) Ferroportin (B) Transferrin Receptor (C) Ferritin L and (D) Ferritin H mRNA (all normalized to Cyclophilin A) for MCF-7 monolayer and spheroids after 3 days in culture.

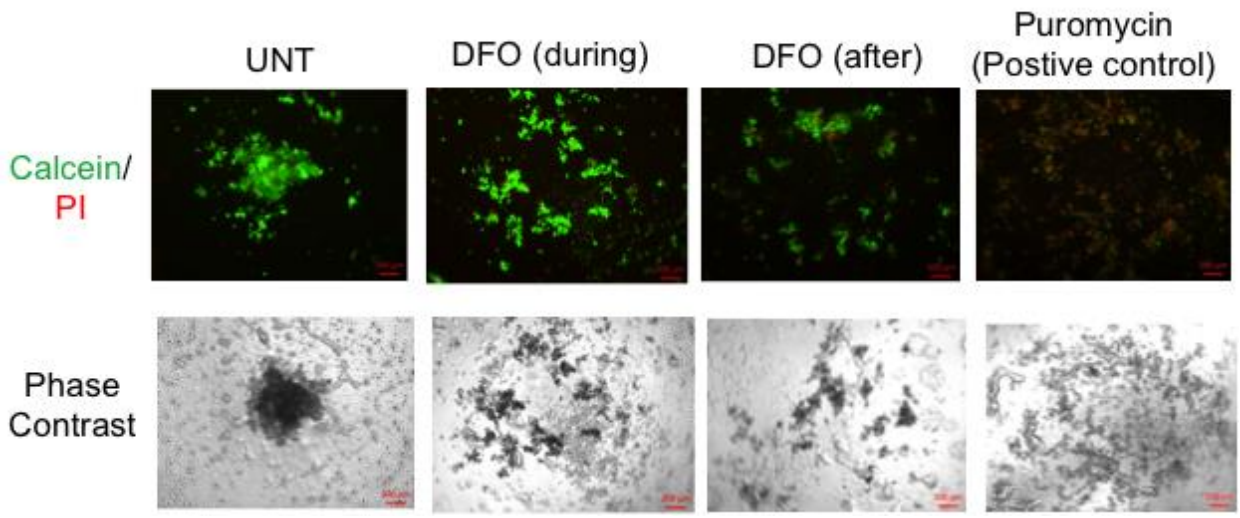

Figure 5-4. Iron chelation results in disruption of spheroid structures.
Calcein (2uM) and Propidium Iodide (PI) (4uM) staining (top row) and corresponding phase contrast images (bottom row) of MCF-7 spheroids after 5 days of no treatment (UNT) or addition of 100uM DFO treatment (added during spheroid plating or added 24 hours after spheroid plating). Puromycin was used as a positive control for spheroid cell death.

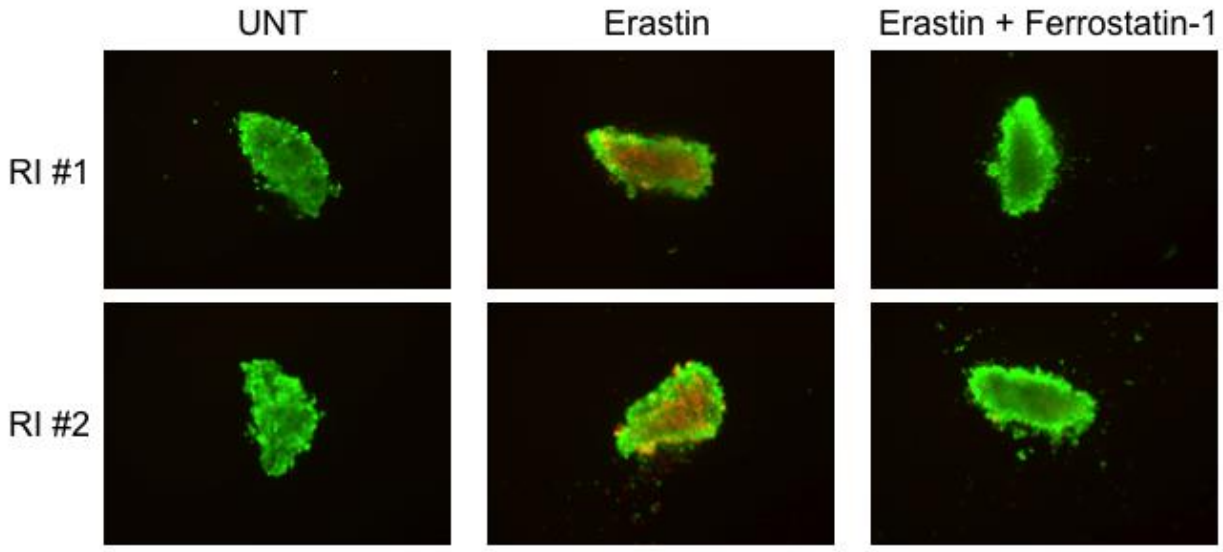

Figure 5-5. Spheroids are sensitive to erastin via ferroptosis mediated cell death. Representative images (RI) from untreated MCF-7 spheroids (UNT), spheroids treat with 50uM erastin, or spheroids treated with 50uM erastin in addition to 2uM ferrostatin for rescue. Treatments were completed 24 hours after spheroids were plated. Spheroids were harvested 48 hours following treatment.

Chapter VI: Conclusions and Future Directions

Conclusions & Future Directions

Hepcidin was originally discovered in the liver for control of systemic iron homeostasis [37]. Our lab was among the first to reveal that hepcidin is conserved in peripheral tissues, including the breast epithelium, for control of cellular iron homeostasis [7]. Although hepcidin regulation has been extensively studied in the liver, the mechanisms that regulate hepcidin in breast cancer cells remained unknown, until now. Ultimately, in this thesis we found that hepcidin is regulated by a complex network of protein molecules and spatial cues, consisting of changes at the cellular, dimensional and microenvironmental levels during breast cancer progression. Revealing these mechanisms that regulate hepcidin in breast cancer now provides novel targets for the ultimate goal of decreasing cancer cell iron and preventing the detrimental effects that arise from its excess. Based on the chapters in this thesis we arrive at 3 main conclusions and provide directions for which this research can continue.

A. Positive regulation of hepcidin in breast cancer involves BMPs, GDF-15 and IL-6 (Chapters 2 and 3)

Through investigation of the pathways that control positive regulation of hepcidin in breast cancer, we uncovered a dynamic network of positive regulators, including BMPs, IL-6 and GDF-15. We utilized various *in vitro* culture systems to uncover these molecular players in regulation of hepcidin. First, utilizing traditional monolayer culture, we found that the main positive regulators of hepcidin in the liver were conserved in the breast (Chapter 2). Specifically, these included BMP4, BMP6, BMP7 and IL-6. Interestingly, all of the breast cancer cell lines we examined displayed varied preferences and response by these ligands in regulation of hepcidin. Specifically, different breast cancer cells had varied basal expression of BMPs/IL-6 as well as varied response to perturbation of these ligands. However, at least one of these ligands was conserved for regulation of hepcidin in monolayer culture (Figure 2-2 through 2-7 and Figure 3-1). Additionally, induction of hepcidin by all of these ligands was shown to be

functional, as treatment of T47-D breast cancer cells with BMPs or IL-6 resulted in decreased FPN membrane staining (Figure 2-9). Furthermore, treatment of normal human mammary epithelial (HME) cells with IL-6 resulted in hepcidin induction (Figure 2-8). This suggests that IL-6 mediated regulation of hepcidin is conserved in normal breast cells. This would infer that if an extracellular source of IL-6 was present, hepcidin could be increased in the non-malignant breast for local degradation of FPN, leading to accumulation of intracellular iron and potential increased proliferation and iron mediated DNA damaging events. It is possible that increased hepcidin in non-tumorigenic cells could be an early transformation event. In the next conclusion, we will discuss the potential exogenous sources of IL-6 from the microenvironment. Taken together, our data demonstrates that BMPs and IL-6 are conserved regulators of hepcidin in breast tissue and these ligands are elevated in breast cancer cells for increased basal hepcidin expression. Thus, these ligands and their downstream signaling pathways would be attractive molecular targets for reduction of hepcidin and ultimately intracellular iron in breast cancer cells.

In addition to traditional monolayer culture, we also utilized three-dimensional culture systems of both established cancer cell lines as well as primary patient breast cells to elucidate hepcidin regulation in breast cancer (Chapter 3). 3D culture was performed to better recapitulate breast tumor architecture and metabolism, in order to capture the full spectrum of hepcidin regulation. Serendipitously, we found that hepcidin was drastically induced by spheroid culture of breast cancer lines and primary cells compared to monolayer culture, suggesting novel regulation of hepcidin through spatial cues (Figure 3-2, Figure 3-3 and Supplementary Figure 2-S2). Ultimately, we found only a modest contribution of BMPs/IL-6 in this induction between dimensions (Figure 3-4), but instead revealed GDF-15 as the main dimensional regulator of hepcidin in breast cancer spheroids (Figure 3-6). Although we still have yet to understand what regulates GDF-15 in breast cancer spheroids, we found that GDF-15 directly regulates hepcidin induction through a conserved BMP signaling pathway involving

activation of downstream signal mediators, including SMAD1-5-8 and SMAD4 (Figure 3-6). It would be interesting to extend these studies to *in vivo* systems, to determine if depletion of GDF-15 in breast tumor xenografts in mice results in decreased breast tumor SMAD signaling, hepcidin expression, tumor iron and an overall reduction of tumor growth. Furthermore, previous studies have found that GDF-15 up-regulates IL-6 to promote tumorigenesis in prostate cancer cells[174]. It would be interesting to determine if such crosstalk exists in breast tumor spheroids between GDF-15 and IL-6 and/or BMPs, for further (or perhaps synergistic) positive control of hepcidin in breast cancer.

In addition to the regulators identified in this study, it is possible that additional regulators remain unknown for tight regulation of hepcidin in breast cancer. Although GDF-15 played a big role in hepcidin induction in spheroid culture of breast cancer cells, there were several other genes that were up-regulated in our microarray analysis completed in chapter 3. Although many of these genes are most likely correlated with hepcidin induction in spheroids, it is possible that some of these up-regulated genes play a role, either indirect or direct, in regulation of hepcidin induction in breast cancer spheroids. Previous studies have linked hypoxia with regulation of hepcidin [64, 66-68]. It is known that spheroids have increased hypoxia, due to oxygen gradients [168]. Although changes in HIF occur at the protein level and were not detected by the microarray, other hypoxia target genes, such as VEGF, were increased in MCF-7 spheroids compared to monolayer. This supports the idea of a hypoxic environment in these spheroids and that this hypoxia could contribute to hepcidin induction in breast cancer spheroids. This potential regulatory mechanism could be explored through modulation of HIF proteins.

In addition to hypoxia, another potential relationship between spheroid literature and hepcidin could be relevant. It is known that spheroid culture of breast cancer cells enhances a stem-like cell population, where cells in the spheroid core take on a less proliferative and more quiescent-like state. In the breast, these cells are characterized molecularly by low CD24 expression and high CD44 expression [175]. We found that CD44 was ~8-9 fold increased in

breast cancer spheroids compared to monolayer as expected from the literature. Thus, a correlation exists between increased hepcidin and stem like cells in spheroids. Interestingly, our lab and others have previously found that tumor initiating cells or cancer stem cells have an enhanced iron seeking phenotype[29, 176, 177]. Furthermore, a recent study suggested that GDF-15 plays a role in the maintenance of breast cancer stem-like cells [135]. Thus, it would be interesting to determine if a mechanistic connection exists between GDF-15, hepcidin and stem cells. It is possible that hepcidin is induced by GDF-15 in spheroids as a result of the increased iron demands of stem like cells.

Overall, positive regulation of hepcidin seems to be majorly controlled by BMPs, GDF-15 and IL-6 in breast tumors. Although additional regulators may exist and would have to be further characterized, the identification of these factors in regulation of hepcidin in breast cancer cells provides molecular targets for reduction of hepcidin in breast tumors. As these regulators are all secreted proteins, targeted antibodies would be a great strategy for inhibiting the activation of pathways that contribute to in increased hepcidin expression and breast tumor growth.

B. Regulation of hepcidin by the microenvironment

(Chapters 3 and 4)

In addition to regulation of hepcidin by the tumor epithelial cells themselves, we also wondered if the tumor microenvironment may play a role in hepcidin regulation, as evidence supports a significant role of the microenvironment in breast cancer progression [178]. These experiments included investigation into the role of stromal cells, specifically tumor associated fibroblasts (TAFs) (Chapter 3), as well as the extracellular matrix (ECM) (Chapter 4) in regulation of hepcidin in breast cancer.

We first examined the potential regulation of hepcidin by stromal cells within the tumor microenvironment. We began by isolating and propagating TAFs from breast cancer patients, and subsequently performed co-culture experiments with various tumor epithelial cells.

Following co-culture, we examined the potential multi-cellular regulation of hepcidin in breast cancer, as TAFs have been well characterized to contribute to breast cancer progression through direct signaling to TECs [179]. Interestingly, we found that TAFs further contribute to hepcidin expression and that this was mediated by paracrine regulation involving secretion of IL-6 by TAFs (Figure 3-8).

Since these experiments were conducted using TAFs from only one patient, it would be interesting to determine if other TAFs have a similar effect on hepcidin, mediated by IL-6. Furthermore, we would also like to investigate the effect of non-tumor breast fibroblasts on hepcidin regulation in TECs. It would also be worthwhile to conduct *in vivo* co-culture experiments and analyze TAF effect on hepcidin, tumor iron and tumor growth over time. Since MCF-7 and primary patient cells are slow growing as tumor xenografts, they would be a good model cell line to conduct such co-culture *in vivo* experiments. Furthermore, although GDF-15 was not secreted by this specific patients' TAFs used for this thesis, other studies have identified TAF derived GDF-15 in prostate cancer, in which this TAF produced GDF-15 contributed to tumorigenesis at both a local and systemic level [139]. Thus, we would like to extend these studies through use of additional patient TAFs. Ultimately, these studies support a pro-tumorigenic role of TAFs in breast cancer, which is in part due to paracrine production of IL-6 for increased production of hepcidin in breast TECs.

It would also be interesting to isolate additional stromal cells, such as adipocytes and macrophages from the tumor microenvironment and asses their contribution to hepcidin regulation and iron metabolism in breast TECs. Interestingly, studies have found hepcidin production from adipose tissue, which could potentially degrade FPN on TECs for increased iron retention [180]. Furthermore, tumor associated macrophages, which have increased iron stores, could act iron donors, where their iron stores could directly transfer iron to TECs for subsequent tumor growth [181]. The contribution by these additional stromal cells to hepcidin and iron metabolism deserves investigation in the context of breast tumors.

In addition to stromal cells, this thesis identified a novel dynamic role of the extracellular matrix (ECM) in regulation of hepcidin in breast cancer spheroids. We first concluded that Matrigel repressed the induction of hepcidin in breast cancer spheroids, and subsequently identified collagen as the main ECM protein responsible for this reduction of hepcidin at early time points (Figure 4-1 and Figure 4-2). Ultimately, one of the potential mechanisms by which collagen represses hepcidin was found to be through sequestration of GDF-15, as its presence in the media and downstream signaling through pSMAD1-5-8 was reduced in the presence of collagen (Figure 4-3). Although the exact dynamics and specifics of this effect have yet to be characterized, we hypothesize that collagen acts as a storage depot for GDF-15. When tumor cells require increased iron, GDF-15 would be released from collagen for activation of the downstream signaling pathway for induction of hepcidin. Thus, in the future we hope to further characterize this interaction between collagen and GDF-15 and how their association tightly regulates hepcidin expression over time in breast cancer spheroids. In addition, we would like to examine additional contribution of the ECM, such as fibronectin or vimentin on hepcidin expression and other players of iron metabolism, as these ECM proteins have also been attributed to progression of breast cancer [145]. In this thesis, we have only just begun to understand the complex relationship between the extracellular matrix and iron metabolism in breast cancer and hope to continue to elucidate this relationship in the future.

Overall, the data in this thesis was the first to provide scientific evidence between the tumor microenvironment in regulation of hepcidin. The role of the microenvironment is emerging in progression of tumors, especially of the breast. Thus, when developing new treatment strategies, components of the microenvironment, such as stromal cells and ECM must be considered, especially for targeting iron metabolism.

C. Global iron metabolism alterations in breast cancer spheroids

(Chapters 3 and 5)

Due to the fact that hepcidin was induced simply by three-dimesnsional culture, we hypothesized that this effect may be due to nutrient and oxygen gradients present within spheroids. Thus, we postulated that hepcidin expression could be altered based on modifying these metabolic parameters. Through modulation of spheroid nutrients and size, we found a direct correlation with hepcidin expression (Figure 5-1). Hepcidin expression increased with depleted iron via serum starvation and larger nutrient gradients due to size limitations. Furthermore, depletion of hepcidin results in decreased spheroid size (Figure 5-2), suggesting that hepcidin contributes to intracellular spheroid iron and subsequent cellular growth, consistent with hepcidin depletion in breast tumor xenografts [28].

In addition to our investigation into hepcidin expression and the regulatory pathways that control its expression in breast cancer, we also examined other changes in iron metabolism and the effects of iron perturbation in breast cancer spheroids. Since there are many proteins that control cellular iron metabolism, we postulated that in addition to hepcidin, other iron related proteins would be altered to favor enhanced iron retention in breast cancer spheroids. Indeed, we found alteration of other genes that control iron metabolism. Specifically, we found increased TFR1 mRNA in MCF-7 spheroids (Figure 5-3), which would promote spheroid iron uptake. Additionally, we found increased Ferritin H and L mRNA and protein (Figure 3-3 and Figure 5-3), suggesting that iron stores are enhanced in spheroids. Lastly, we found decreased FPN mRNA in spheroids (Figure 5-3), implying that FPN is basally reduced transcriptionally, before hepcidin mediated FPN degradation occurs at the post-translational level. Although these changes between monolayer and spheroid culture would need to be confirmed at the protein level for FPN and TFR1, all of these modifications are consistent with a pattern of increased iron retention in breast cancer spheroids. Overall, this suggests that breast cancer

spheroids alter several iron metabolism genes to attain enhanced spheroid iron for survival and growth.

Due to these dimensional changes in iron metabolism genes to promote enhanced spheroid iron acquisition, we postulated that global perturbation of the iron would be detrimental to spheroid viability. Thus, when spheroid iron was chelated, spheroid cell death was observed and spheroid formation was completely disrupted (Figure 5-4). This supports the hypothesis of spheroid demand for iron for growth and further displays a role of iron for tumor architectural maintenance. Overall, this supports therapeutic intervention by targeting genes that control iron metabolism for the goal of reducing iron within breast tumors.

As this thesis has alluded to, future directions of this project hope to target regulatory mechanisms that control hepcidin. However, due to the dynamic regulation of hepcidin involving TECs and the microenvironment, in addition to alteration of several other genes that control iron metabolism, future treatment strategies to deplete tumors of iron may have to take on a more global approach. It is possible that selective targeting of hepcidin in breast tumors may only work temporarily, before other iron metabolism proteins become altered to compensate and increase intracellular iron levels for continued growth. Thus, more general strategies of targeting enhanced spheroid iron may have to be explored.

One potential iron targeting therapy in cancer would be through ferroptosis, a newly discovered form of non-apoptotic cell death that is dependent on iron [170]. Mechanistically, cell death by ferroptosis is caused by iron-mediated accumulation of lipid ROS [182]. Induction of ferroptosis by small molecules, such as erastin, reduced ovarian tumor mass *in vivo* and was also found to selectively kill ovarian cancer tumor initiating cells compared to non-cancer stem cells, as labile iron is higher in the tumor initiating cells compared to non-cancer stem cells[29]. In this thesis, we successfully induced ferroptotic cell death in breast cancer spheroids (Figure 5-5), suggesting that enhanced iron presence in spheroids can be targeted by ferroptosis inducing agents. We would also want to extend our investigation of ferroptosis to non-tumor

breast spheroids, as one would hypothesize that lower iron present in non-tumor spheroids would render them less susceptible to death by ferroptosis. Together, this data demonstrates that that breast cancer spheroids would be a good model system to further explore this treatment strategy and suggests that enhanced iron seeking phenotype present in breast tumors may be targeted via ferroptosis.

References

1. Siegel, R.L., K.D. Miller, and A. Jemal, *Cancer Statistics, 2017.* CA Cancer J Clin, 2017. **67**(1): p. 7-30.
2. Berry, D.A., *Breast cancer screening: controversy of impact.* Breast, 2013. **22 Suppl 2**: p. S73-6.
3. Bleyer, A. and H.G. Welch, *Effect of three decades of screening mammography on breast-cancer incidence.* N Engl J Med, 2012. **367**(21): p. 1998-2005.
4. Liu, X., et al., *ROCK inhibitor and feeder cells induce the conditional reprogramming of epithelial cells.* Am J Pathol, 2012. **180**(2): p. 599-607.
5. Guo, J., et al., *Ferroptosis: A Novel Anti-Tumor Action for Cisplatin.* Cancer Res Treat, 2017.
6. Torti, S.V. and F.M. Torti, *Iron and cancer: more ore to be mined.* Nat Rev Cancer, 2013. **13**(5): p. 342-55.
7. Pinnix, Z.K., et al., *Ferroportin and iron regulation in breast cancer progression and prognosis.* Sci Transl Med, 2010. **2**(43): p. 43ra56.
8. Tesfay, L., et al., *Hepcidin regulation in prostate and its disruption in prostate cancer.* Cancer Res, 2015. **75**(11): p. 2254-63.
9. Raha, A.A., et al., *The systemic iron-regulatory proteins hepcidin and ferroportin are reduced in the brain in Alzheimer's disease.* Acta Neuropathol Commun, 2013. **1**: p. 55.
10. Manz, D.H., et al., *Iron and cancer: recent insights.* Ann N Y Acad Sci, 2016. **1368**(1): p. 149-61.
11. Stevens, R.G., et al., *Body iron stores and the risk of cancer.* N Engl J Med, 1988. **319**(16): p. 1047-52.
12. Stevens, R.G., et al., *Moderate elevation of body iron level and increased risk of cancer occurrence and death.* Int J Cancer, 1994. **56**(3): p. 364-9.
13. Nelson, R.L., *Iron and colorectal cancer risk: human studies.* Nutr Rev, 2001. **59**(5): p. 140-8.
14. Kabat, G.C., et al., *Dietary iron and haem iron intake and risk of endometrial cancer: a prospective cohort study.* Br J Cancer, 2008. **98**(1): p. 194-8.
15. Mursu, J., et al., *Dietary supplements and mortality rate in older women: the Iowa Women's Health Study.* Arch Intern Med, 2011. **171**(18): p. 1625-33.
16. Bradbear, R.A., et al., *Cohort study of internal malignancy in genetic hemochromatosis and other chronic nonalcoholic liver diseases.* J Natl Cancer Inst, 1985. **75**(1): p. 81-4.
17. Milman, N., et al., *Clinically overt hereditary hemochromatosis in Denmark 1948-1985: epidemiology, factors of significance for long-term survival, and causes of death in 179 patients.* Ann Hematol, 2001. **80**(12): p. 737-44.
18. Hsing, A.W., et al., *Cancer risk following primary hemochromatosis: a population-based cohort study in Denmark.* Int J Cancer, 1995. **60**(2): p. 160-2.
19. Osborne, N.J., et al., *HFE C282Y homozygotes are at increased risk of breast and colorectal cancer.* Hepatology, 2010. **51**(4): p. 1311-8.
20. Edgren, G., et al., *Donation frequency, iron loss, and risk of cancer among blood donors.* J Natl Cancer Inst, 2008. **100**(8): p. 572-9.
21. Huang, X., *Does iron have a role in breast cancer?* The lancet oncology, 2008. **9**(8): p. 803-807.
22. Lederman, H.M., et al., *Deferoxamine: a reversible S-phase inhibitor of human lymphocyte proliferation.* Blood, 1984. **64**(3): p. 748-53.
23. Inoue, S. and S. Kawanishi, *Hydroxyl radical production and human DNA damage induced by ferric nitrilotriacetate and hydrogen peroxide.* Cancer Res, 1987. **47**(24 Pt 1): p. 6522-7.
24. Yang, D.C., et al., *Expression of transferrin receptor and ferritin H-chain mRNA are associated with clinical and histopathological prognostic indicators in breast cancer.* Anticancer Res, 2001. **21**(1B): p. 541-9.

25. Miller, L.D., et al., *An iron regulatory gene signature predicts outcome in breast cancer.* Cancer Res, 2011. **71**(21): p. 6728-37.
26. Daniels, T.R., et al., *The transferrin receptor and the targeted delivery of therapeutic agents against cancer.* Biochim Biophys Acta, 2012. **1820**(3): p. 291-317.
27. Brooks, D., et al., *Phase Ia trial of murine immunoglobulin A antitransferrin receptor antibody 42/6.* Clin Cancer Res, 1995. **1**(11): p. 1259-65.
28. Zhang, S., et al., *Disordered hepcidin-ferroportin signaling promotes breast cancer growth.* Cell Signal, 2014. **26**(11): p. 2539-50.
29. Basuli, D., et al., *Iron addiction: a novel therapeutic target in ovarian cancer.* Oncogene, 2017.
30. Tanno, T., et al., *Hepcidin, anaemia, and prostate cancer.* BJU Int, 2011. **107**(4): p. 678-9.
31. Lamy, P.J., A. Durigova, and W. Jacot, *Iron homeostasis and anemia markers in early breast cancer.* Clin Chim Acta, 2014. **434**: p. 34-40.
32. Mei, S., et al., *Hepcidin and GDF15 in anemia of multiple myeloma.* Int J Hematol, 2014. **100**(3): p. 266-73.
33. Tisi, M.C., et al., *Anemia in diffuse large B-cell non-Hodgkin lymphoma: the role of interleukin-6, hepcidin and erythropoietin.* Leuk Lymphoma, 2014. **55**(2): p. 270-5.
34. Abd Elmonem, E., et al., *Hepcidin mRNA level as a parameter of disease progression in chronic hepatitis C and hepatocellular carcinoma.* J Egypt Natl Canc Inst, 2009. **21**(4): p. 333-42.
35. Maccio, A., et al., *The role of inflammation, iron, and nutritional status in cancer-related anemia: results of a large, prospective, observational study.* Haematologica, 2015. **100**(1): p. 124-32.
36. Krause, A., et al., *LEAP-1, a novel highly disulfide-bonded human peptide, exhibits antimicrobial activity.* FEBS Lett, 2000. **480**(2-3): p. 147-50.
37. Park, C.H., et al., *Hepcidin, a urinary antimicrobial peptide synthesized in the liver.* J Biol Chem, 2001. **276**(11): p. 7806-10.
38. Valore, E.V. and T. Ganz, *Posttranslational processing of hepcidin in human hepatocytes is mediated by the prohormone convertase furin.* Blood Cells Mol Dis, 2008. **40**(1): p. 132-8.
39. Pigeon, C., et al., *A new mouse liver-specific gene, encoding a protein homologous to human antimicrobial peptide hepcidin, is overexpressed during iron overload.* J Biol Chem, 2001. **276**(11): p. 7811-9.
40. Nicolas, G., et al., *Lack of hepcidin gene expression and severe tissue iron overload in upstream stimulatory factor 2 (USF2) knockout mice.* Proc Natl Acad Sci U S A, 2001. **98**(15): p. 8780-5.
41. Nemeth, E., et al., *Hepcidin regulates cellular iron efflux by binding to ferroportin and inducing its internalization.* Science, 2004. **306**(5704): p. 2090-3.
42. Preza, G.C., et al., *Cellular catabolism of the iron-regulatory peptide hormone hepcidin.* PLoS One, 2013. **8**(3): p. e58934.
43. Donovan, A., et al., *The iron exporter ferroportin/Slc40a1 is essential for iron homeostasis.* Cell Metab, 2005. **1**(3): p. 191-200.
44. Ward, D.G., et al., *Increased hepcidin expression in colorectal carcinogenesis.* World J Gastroenterol, 2008. **14**(9): p. 1339-45.
45. Miyazono, K., Y. Kamiya, and M. Morikawa, *Bone morphogenetic protein receptors and signal transduction.* J Biochem, 2010. **147**(1): p. 35-51.
46. Chen, D., et al., *Signal transduction and biological functions of bone morphogenetic proteins.* Front Biosci, 2004. **9**: p. 349-58.
47. Wang, R.H., et al., *A role of SMAD4 in iron metabolism through the positive regulation of hepcidin expression.* Cell Metab, 2005. **2**(6): p. 399-409.
48. Xia, Y., et al., *Hemojuvelin regulates hepcidin expression via a selective subset of BMP ligands and receptors independently of neogenin.* Blood, 2008. **111**(10): p. 5195-204.

49. Andriopoulos, B., Jr., et al., *BMP6 is a key endogenous regulator of hepcidin expression and iron metabolism.* Nat Genet, 2009. **41**(4): p. 482-7.
50. Meynard, D., et al., *Lack of the bone morphogenetic protein BMP6 induces massive iron overload.* Nat Genet, 2009. **41**(4): p. 478-81.
51. Roetto, A., et al., *Mutant antimicrobial peptide hepcidin is associated with severe juvenile hemochromatosis.* Nat Genet, 2003. **33**(1): p. 21-2.
52. Lee, P.L., et al., *Genetic abnormalities and juvenile hemochromatosis: mutations of the HJV gene encoding hemojuvelin.* Blood, 2004. **103**(12): p. 4669-71.
53. Feder, J.N., et al., *A novel MHC class I-like gene is mutated in patients with hereditary haemochromatosis.* Nat Genet, 1996. **13**(4): p. 399-408.
54. Camaschella, C., et al., *The gene TFR2 is mutated in a new type of haemochromatosis mapping to 7q22.* Nat Genet, 2000. **25**(1): p. 14-5.
55. Goswami, T. and N.C. Andrews, *Hereditary hemochromatosis protein, HFE, interaction with transferrin receptor 2 suggests a molecular mechanism for mammalian iron sensing.* J Biol Chem, 2006. **281**(39): p. 28494-8.
56. Ganz, T., *The role of hepcidin in iron sequestration during infections and in the pathogenesis of anemia of chronic disease.* Isr Med Assoc J, 2002. **4**(11): p. 1043-5.
57. Nemeth, E., et al., *Hepcidin, a putative mediator of anemia of inflammation, is a type II acute-phase protein.* Blood, 2003. **101**(7): p. 2461-3.
58. Gabay, C., *Interleukin-6 and chronic inflammation.* Arthritis Res Ther, 2006. **8 Suppl 2**: p. S3.
59. Mayeur, C., et al., *The type I BMP receptor Alk3 is required for the induction of hepatic hepcidin gene expression by interleukin-6.* Blood, 2014. **123**(14): p. 2261-8.
60. Pinto, J.P., et al., *Erythropoietin mediates hepcidin expression in hepatocytes through EPOR signaling and regulation of C/EBPalpha.* Blood, 2008. **111**(12): p. 5727-33.
61. Ashby, D.R., et al., *Erythropoietin administration in humans causes a marked and prolonged reduction in circulating hepcidin.* Haematologica, 2010. **95**(3): p. 505-8.
62. Kautz, L., et al., *Identification of erythroferrone as an erythroid regulator of iron metabolism.* Nat Genet, 2014. **46**(7): p. 678-84.
63. Tanno, T., et al., *High levels of GDF15 in thalassemia suppress expression of the iron regulatory protein hepcidin.* Nat Med, 2007. **13**(9): p. 1096-101.
64. Haase, V.H., *Hypoxic regulation of erythropoiesis and iron metabolism.* Am J Physiol Renal Physiol, 2010. **299**(1): p. F1-13.
65. Peyssonnaux, C., et al., *Regulation of iron homeostasis by the hypoxia-inducible transcription factors (HIFs).* Journal of Clinical Investigation, 2007. **117**(7): p. 1926-1932.
66. Mastrogiannaki, M., et al., *HIF-2alpha, but not HIF-1alpha, promotes iron absorption in mice.* J Clin Invest, 2009. **119**(5): p. 1159-66.
67. Volke, M., et al., *Evidence for a lack of a direct transcriptional suppression of the iron regulatory peptide hepcidin by hypoxia-inducible factors.* PLoS One, 2009. **4**(11): p. e7875.
68. Silvestri, L., A. Pagani, and C. Camaschella, *Furin-mediated release of soluble hemojuvelin: a new link between hypoxia and iron homeostasis.* Blood, 2008. **111**(2): p. 924-31.
69. Finberg, K.E., et al., *Mutations in TMPRSS6 cause iron-refractory iron deficiency anemia (IRIDA).* Nat Genet, 2008. **40**(5): p. 569-71.
70. Silvestri, L., et al., *The serine protease matriptase-2 (TMPRSS6) inhibits hepcidin activation by cleaving membrane hemojuvelin.* Cell Metab, 2008. **8**(6): p. 502-11.
71. Yanagita, M., et al., *USAG-1: a bone morphogenetic protein antagonist abundantly expressed in the kidney.* Biochem Biophys Res Commun, 2004. **316**(2): p. 490-500.
72. Yang, Q., et al., *17beta-Estradiol inhibits iron hormone hepcidin through an estrogen responsive element half-site.* Endocrinology, 2012. **153**(7): p. 3170-8.

73. Ikeda, Y., et al., *Estrogen regulates hepcidin expression via GPR30-BMP6-dependent signaling in hepatocytes.* PLoS One, 2012. **7**(7): p. e40465.
74. do Amaral, J.B., et al., *MCF-7 cells as a three-dimensional model for the study of human breast cancer.* Tissue Eng Part C Methods, 2011. **17**(11): p. 1097-107.
75. Bissell, M.J., et al., *Tissue structure, nuclear organization, and gene expression in normal and malignant breast.* Cancer Res, 1999. **59**(7 Suppl): p. 1757-1763s; discussion 1763s-1764s.
76. Kenny, P.A., et al., *The morphologies of breast cancer cell lines in three-dimensional assays correlate with their profiles of gene expression.* Mol Oncol, 2007. **1**(1): p. 84-96.
77. Martin, K.J., et al., *Prognostic breast cancer signature identified from 3D culture model accurately predicts clinical outcome across independent datasets.* PLoS One, 2008. **3**(8): p. e2994.
78. Longati, P., et al., *3D pancreatic carcinoma spheroids induce a matrix-rich, chemoresistant phenotype offering a better model for drug testing.* BMC Cancer, 2013. **13**: p. 95.
79. Ivascu, A. and M. Kubbies, *Rapid generation of single-tumor spheroids for high-throughput cell function and toxicity analysis.* J Biomol Screen, 2006. **11**(8): p. 922-32.
80. Edmondson, R., et al., *Three-dimensional cell culture systems and their applications in drug discovery and cell-based biosensors.* Assay Drug Dev Technol, 2014. **12**(4): p. 207-18.
81. Weigelt, B. and M.J. Bissell, *Unraveling the microenvironmental influences on the normal mammary gland and breast cancer.* Semin Cancer Biol, 2008. **18**(5): p. 311-21.
82. Schmeichel, K.L. and M.J. Bissell, *Modeling tissue-specific signaling and organ function in three dimensions.* J Cell Sci, 2003. **116**(Pt 12): p. 2377-88.
83. Zhang, F., et al., *Effect of fibroblasts on breast cancer cell mammosphere formation and regulation of stem cell-related gene expression.* Int J Mol Med, 2011. **28**(3): p. 365-71.
84. Kaur, G. and J.M. Dufour, *Cell lines: Valuable tools or useless artifacts.* Spermatogenesis, 2012. **2**(1): p. 1-5.
85. Domcke, S., et al., *Evaluating cell lines as tumour models by comparison of genomic profiles.* Nat Commun, 2013. **4**: p. 2126.
86. Burdall, S.E., et al., *Breast cancer cell lines: friend or foe?* Breast Cancer Res, 2003. **5**(2): p. 89-95.
87. Kuilman, T., et al., *The essence of senescence.* Genes Dev, 2010. **24**(22): p. 2463-79.
88. Donovan, A., et al., *Positional cloning of zebrafish ferroportin1 identifies a conserved vertebrate iron exporter.* Nature, 2000. **403**(6771): p. 776-81.
89. Kamai, T., et al., *Increased serum hepcidin-25 level and increased tumor expression of hepcidin mRNA are associated with metastasis of renal cell carcinoma.* BMC Cancer, 2009. **9**: p. 270.
90. Ganz, T. and E. Nemeth, *The hepcidin-ferroportin system as a therapeutic target in anemias and iron overload disorders.* Hematology Am Soc Hematol Educ Program, 2011. **2011**: p. 538-42.
91. Nicolas, G., et al., *The gene encoding the iron regulatory peptide hepcidin is regulated by anemia, hypoxia, and inflammation.* J Clin Invest, 2002. **110**(7): p. 1037-44.
92. Babitt, J.L., et al., *Modulation of bone morphogenetic protein signaling in vivo regulates systemic iron balance.* J Clin Invest, 2007. **117**(7): p. 1933-9.
93. Wrighting, D.M. and N.C. Andrews, *Interleukin-6 induces hepcidin expression through STAT3.* Blood, 2006. **108**(9): p. 3204-9.
94. Truksa, J., P. Lee, and E. Beutler, *Two BMP responsive elements, STAT, and bZIP/HNF4/COUP motifs of the hepcidin promoter are critical for BMP, SMAD1, and HJV responsiveness.* Blood, 2009. **113**(3): p. 688-95.
95. Alarmo, E.L., et al., *A comprehensive expression survey of bone morphogenetic proteins in breast cancer highlights the importance of BMP4 and BMP7.* Breast Cancer Res Treat, 2007. **103**(2): p. 239-46.

96. Ndlovu, M.N., et al., *Hyperactivated NF-{kappa}B and AP-1 transcription factors promote highly accessible chromatin and constitutive transcription across the interleukin-6 gene promoter in metastatic breast cancer cells.* Mol Cell Biol, 2009. **29**(20): p. 5488-504.
97. Alarmo, E.L., et al., *Bone morphogenetic protein 7 expression associates with bone metastasis in breast carcinomas.* Ann Oncol, 2008. **19**(2): p. 308-14.
98. Montesano, R., *Bone morphogenetic protein-4 abrogates lumen formation by mammary epithelial cells and promotes invasive growth.* Biochem Biophys Res Commun, 2007. **353**(3): p. 817-22.
99. Sasser, A.K., et al., *Interleukin-6 is a potent growth factor for ER-alpha-positive human breast cancer.* FASEB J, 2007. **21**(13): p. 3763-70.
100. Selander, K.S., et al., *Inhibition of gp130 signaling in breast cancer blocks constitutive activation of Stat3 and inhibits in vivo malignancy.* Cancer Res, 2004. **64**(19): p. 6924-33.
101. Elenbaas, B., et al., *Human breast cancer cells generated by oncogenic transformation of primary mammary epithelial cells.* Genes Dev, 2001. **15**(1): p. 50-65.
102. Path, G., et al., *Human breast adipocytes express interleukin-6 (IL-6) and its receptor system: increased IL-6 production by beta-adrenergic activation and effects of IL-6 on adipocyte function.* J Clin Endocrinol Metab, 2001. **86**(5): p. 2281-8.
103. Adams, E.F., B. Rafferty, and M.C. White, *Interleukin 6 is secreted by breast fibroblasts and stimulates 17 beta-oestradiol oxidoreductase activity of MCF-7 cells: possible paracrine regulation of breast 17 beta-oestradiol levels.* Int J Cancer, 1991. **49**(1): p. 118-21.
104. Aboussekhra, A., *Role of cancer-associated fibroblasts in breast cancer development and prognosis.* Int J Dev Biol, 2011. **55**(7-9): p. 841-9.
105. Kartikasari, A.E., et al., *Secretion of bioactive hepcidin-25 by liver cells correlates with its gene transcription and points towards synergism between iron and inflammation signaling pathways.* Biochim Biophys Acta, 2008. **1784**(12): p. 2029-37.
106. Soule, H.D., et al., *A human cell line from a pleural effusion derived from a breast carcinoma.* J Natl Cancer Inst, 1973. **51**(5): p. 1409-16.
107. Arman, A. and P.E. Auron, *Interleukin 1 (IL-1) induces the activation of Stat3.* Adv Exp Med Biol, 2003. **534**: p. 297-307.
108. Caldenhoven, E., et al., *Activation of the STAT3/acute phase response factor transcription factor by interleukin-5.* J Biol Chem, 1995. **270**(43): p. 25778-84.
109. Yang, C.H., A. Murti, and L.M. Pfeffer, *STAT3 complements defects in an interferon-resistant cell line: evidence for an essential role for STAT3 in interferon signaling and biological activities.* Proc Natl Acad Sci U S A, 1998. **95**(10): p. 5568-72.
110. Garcia, R., et al., *Constitutive activation of Stat3 by the Src and JAK tyrosine kinases participates in growth regulation of human breast carcinoma cells.* Oncogene, 2001. **20**(20): p. 2499-513.
111. Schafer, Z.T., et al., *Antioxidant and oncogene rescue of metabolic defects caused by loss of matrix attachment.* Nature, 2009. **461**(7260): p. 109-13.
112. Coloff, J.L., et al., *Differential Glutamate Metabolism in Proliferating and Quiescent Mammary Epithelial Cells.* Cell Metab, 2016. **23**(5): p. 867-80.
113. Saias, L., et al., *Cell-Cell Adhesion and Cytoskeleton Tension Oppose Each Other in Regulating Tumor Cell Aggregation.* Cancer Res, 2015. **75**(12): p. 2426-33.
114. Liu, X., et al., *Conditional reprogramming and long-term expansion of normal and tumor cells from human biospecimens.* Nat Protoc, 2017. **12**(2): p. 439-451.
115. Nieman, M.T., et al., *N-cadherin promotes motility in human breast cancer cells regardless of their E-cadherin expression.* J Cell Biol, 1999. **147**(3): p. 631-44.
116. Torti, F.M. and S.V. Torti, *Regulation of ferritin genes and protein.* Blood, 2002. **99**(10): p. 3505-16.

117. Hentze, M.W., et al., *Identification of the iron-responsive element for the translational regulation of human ferritin mRNA.* Science, 1987. **238**(4833): p. 1570-3.
118. Arosio, P. and S. Levi, *Cytosolic and mitochondrial ferritins in the regulation of cellular iron homeostasis and oxidative damage.* Biochim Biophys Acta, 2010. **1800**(8): p. 783-92.
119. Theil, E.C., T. Tosha, and R.K. Behera, *Solving Biology's Iron Chemistry Problem with Ferritin Protein Nanocages.* Acc Chem Res, 2016. **49**(5): p. 784-91.
120. Picard, V., et al., *Role of ferritin in the control of the labile iron pool in murine erythroleukemia cells.* J Biol Chem, 1998. **273**(25): p. 15382-6.
121. Yu, M., et al., *Expression profiling during mammary epithelial cell three-dimensional morphogenesis identifies PTPRO as a novel regulator of morphogenesis and ErbB2-mediated transformation.* Mol Cell Biol, 2012. **32**(19): p. 3913-24.
122. Francia, G., et al., *Gene expression analysis of tumor spheroids reveals a role for suppressed DNA mismatch repair in multicellular resistance to alkylating agents.* Mol Cell Biol, 2004. **24**(15): p. 6837-49.
123. Riedl, A., et al., *Comparison of cancer cells in 2D vs 3D culture reveals differences in AKT-mTOR-S6K signaling and drug responses.* J Cell Sci, 2017. **130**(1): p. 203-218.
124. Bootcov, M.R., et al., *MIC-1, a novel macrophage inhibitory cytokine, is a divergent member of the TGF-beta superfamily.* Proc Natl Acad Sci U S A, 1997. **94**(21): p. 11514-9.
125. Welsh, J.B., et al., *Large-scale delineation of secreted protein biomarkers overexpressed in cancer tissue and serum.* Proc Natl Acad Sci U S A, 2003. **100**(6): p. 3410-5.
126. Yalcin, M.M., et al., *GDF-15 and Hepcidin Levels in Nonanemic Patients with Impaired Glucose Tolerance.* J Diabetes Res, 2016. **2016**: p. 1240843.
127. Yilmaz, H., et al., *Can Serum Gdf-15 be Associated with Functional Iron Deficiency in Hemodialysis Patients?* Indian J Hematol Blood Transfus, 2016. **32**(2): p. 221-7.
128. Winand, F.J., et al., *GDF15 and Hepcidin as Prognostic Factors in Patients with Prostate Cancer.* Journal of Molecular Biomarkers & Diagnosis, 2014. **05**(06).
129. Debnath, J. and J.S. Brugge, *Modelling glandular epithelial cancers in three-dimensional cultures.* Nat Rev Cancer, 2005. **5**(9): p. 675-88.
130. Horning, J.L., et al., *3-D tumor model for in vitro evaluation of anticancer drugs.* Mol Pharm, 2008. **5**(5): p. 849-62.
131. Nath, S. and G.R. Devi, *Three-dimensional culture systems in cancer research: Focus on tumor spheroid model.* Pharmacol Ther, 2016. **163**: p. 94-108.
132. Fairlie, W.D., et al., *MIC-1 is a novel TGF-beta superfamily cytokine associated with macrophage activation.* J Leukoc Biol, 1999. **65**(1): p. 2-5.
133. Schober, A., et al., *Expression of growth differentiation factor-15/ macrophage inhibitory cytokine-1 (GDF-15/MIC-1) in the perinatal, adult, and injured rat brain.* J Comp Neurol, 2001. **439**(1): p. 32-45.
134. Park, Y.J., H. Lee, and J.H. Lee, *Macrophage inhibitory cytokine-1 transactivates ErbB family receptors via the activation of Src in SK-BR-3 human breast cancer cells.* BMB Rep, 2010. **43**(2): p. 91-6.
135. Sasahara, A., et al., *An autocrine/paracrine circuit of growth differentiation factor (GDF) 15 has a role for maintenance of breast cancer stem-like cells.* Oncotarget, 2017. **8**(15): p. 24869-24881.
136. Hanahan, D. and L.M. Coussens, *Accessories to the crime: functions of cells recruited to the tumor microenvironment.* Cancer Cell, 2012. **21**(3): p. 309-22.
137. Allinen, M., et al., *Molecular characterization of the tumor microenvironment in breast cancer.* Cancer Cell, 2004. **6**(1): p. 17-32.
138. Whiteside, T.L., *The tumor microenvironment and its role in promoting tumor growth.* Oncogene, 2008. **27**(45): p. 5904-12.

139. Bruzzese, F., et al., *Local and systemic protumorigenic effects of cancer-associated fibroblast-derived GDF15.* Cancer Res, 2014. **74**(13): p. 3408-17.
140. Cooke, K.S., et al., *A fully human anti-hepcidin antibody modulates iron metabolism in both mice and nonhuman primates.* Blood, 2013. **122**(17): p. 3054-61.
141. Wilkinson, J.t., et al., *Ferritin regulation by oxidants and chemopreventive xenobiotics.* Adv Enzyme Regul, 2003. **43**: p. 135-51.
142. Nguyen, D., *Quantifying chromogen intensity in immunohistochemistry via reciprocal intensity.* 2013.
143. *Comprehensive molecular portraits of human breast tumours.* Nature, 2012. **490**(7418): p. 61-70.
144. Bissell, M.J. and W.C. Hines, *Why don't we get more cancer? A proposed role of the microenvironment in restraining cancer progression.* Nature medicine, 2011. **17**(3): p. 320-329.
145. Oskarsson, T., *Extracellular matrix components in breast cancer progression and metastasis.* Breast, 2013. **22 Suppl 2**: p. S66-72.
146. Streuli, C.H., N. Bailey, and M.J. Bissell, *Control of mammary epithelial differentiation: basement membrane induces tissue-specific gene expression in the absence of cell-cell interaction and morphological polarity.* J Cell Biol, 1991. **115**(5): p. 1383-95.
147. Petersen, O.W., et al., *Interaction with basement membrane serves to rapidly distinguish growth and differentiation pattern of normal and malignant human breast epithelial cells.* Proc Natl Acad Sci U S A, 1992. **89**(19): p. 9064-8.
148. Streuli, C.H., et al., *Laminin mediates tissue-specific gene expression in mammary epithelia.* J Cell Biol, 1995. **129**(3): p. 591-603.
149. Ohbayashi, M., et al., *Effect of interleukins response to ECM-induced acquisition of drug resistance in MCF-7 cells.* Exp Oncol, 2008. **30**(4): p. 276-82.
150. Sternlicht, M.D., et al., *The stromal proteinase MMP3/stromelysin-1 promotes mammary carcinogenesis.* Cell, 1999. **98**(2): p. 137-46.
151. Alowami, S., et al., *Mammographic density is related to stroma and stromal proteoglycan expression.* Breast Cancer Res, 2003. **5**(5): p. R129-35.
152. Fang, M., et al., *Collagen as a double-edged sword in tumor progression.* Tumour Biol, 2014. **35**(4): p. 2871-82.
153. Conklin, M.W., et al., *Aligned collagen is a prognostic signature for survival in human breast carcinoma.* Am J Pathol, 2011. **178**(3): p. 1221-32.
154. Han, W., et al., *Oriented collagen fibers direct tumor cell intravasation.* Proc Natl Acad Sci U S A, 2016. **113**(40): p. 11208-11213.
155. Olive, P.L. and R.E. Durand, *Drug and radiation resistance in spheroids: cell contact and kinetics.* Cancer Metastasis Rev, 1994. **13**(2): p. 121-38.
156. Kim, H., Y. Phung, and M. Ho, *Changes in global gene expression associated with 3D structure of tumors: an ex vivo matrix-free mesothelioma spheroid model.* PLoS One, 2012. **7**(6): p. e39556.
157. Li, C.L., et al., *Survival advantages of multicellular spheroids vs. monolayers of HepG2 cells in vitro.* Oncol Rep, 2008. **20**(6): p. 1465-71.
158. Harma, V., et al., *A comprehensive panel of three-dimensional models for studies of prostate cancer growth, invasion and drug responses.* PLoS One, 2010. **5**(5): p. e10431.
159. Kleinman, H.K., et al., *Isolation and characterization of type IV procollagen, laminin, and heparan sulfate proteoglycan from the EHS sarcoma.* Biochemistry, 1982. **21**(24): p. 6188-93.
160. Manuel Iglesias, J., et al., *Mammosphere formation in breast carcinoma cell lines depends upon expression of E-cadherin.* PLoS One, 2013. **8**(10): p. e77281.
161. Yue, B., *Biology of the extracellular matrix: an overview.* J Glaucoma, 2014. **23**(8 Suppl 1): p. S20-3.

162. Bonnans, C., J. Chou, and Z. Werb, *Remodelling the extracellular matrix in development and disease.* Nat Rev Mol Cell Biol, 2014. **15**(12): p. 786-801.
163. Bauskin, A.R., et al., *The propeptide mediates formation of stromal stores of PROMIC-1: role in determining prostate cancer outcome.* Cancer Res, 2005. **65**(6): p. 2330-6.
164. Tsuji, A., et al., *Secretory proprotein convertases PACE4 and PC6A are heparin-binding proteins which are localized in the extracellular matrix. Potential role of PACE4 in the activation of proproteins in the extracellular matrix.* Biochim Biophys Acta, 2003. **1645**(1): p. 95-104.
165. Abd El-Aziz, S.H., et al., *Cleavage of growth differentiation factor 15 (GDF15) by membrane type 1-matrix metalloproteinase abrogates GDF15-mediated suppression of tumor cell growth.* Cancer Sci, 2007. **98**(9): p. 1330-5.
166. Li, S., et al., *Maturation of growth differentiation factor 15 in human placental trophoblast cells depends on the interaction with Matrix Metalloproteinase-26.* J Clin Endocrinol Metab, 2014. **99**(11): p. E2277-87.
167. Laub, M., M. Chatzinikolaidou, and H.P. Jennissen, *Aspects of BMP-2 binding to receptors and collagen: Influence of cell senescence on receptor binding and absence of high-affinity stoichiometric binding to collagen.* Materialwissenschaft und Werkstofftechnik, 2007. **38**(12): p. 1019-1026.
168. Cui, X., et al., *A mechanistic study on tumour spheroid formation in thermosensitive hydrogels: experiments and mathematical modelling.* RSC Advances, 2016. **6**(77): p. 73282-73291.
169. Crielaard, B.J., T. Lammers, and S. Rivella, *Targeting iron metabolism in drug discovery and delivery.* Nat Rev Drug Discov, 2017. **16**(6): p. 400-423.
170. Dixon, S.J., et al., *Ferroptosis: an iron-dependent form of nonapoptotic cell death.* Cell, 2012. **149**(5): p. 1060-72.
171. Marro, S., et al., *Heme controls ferroportin1 (FPN1) transcription involving Bach1, Nrf2 and a MARE/ARE sequence motif at position -7007 of the FPN1 promoter.* Haematologica, 2010. **95**(8): p. 1261-8.
172. Tsuji, Y., et al., *Coordinate transcriptional and translational regulation of ferritin in response to oxidative stress.* Mol Cell Biol, 2000. **20**(16): p. 5818-27.
173. Lakhal, S., et al., *Regulation of growth differentiation factor 15 expression by intracellular iron.* Blood, 2009. **113**(7): p. 1555-63.
174. Tsui, K.H., et al., *Growth differentiation factor-15 upregulates interleukin-6 to promote tumorigenesis of prostate carcinoma PC-3 cells.* J Mol Endocrinol, 2012. **49**(2): p. 153-63.
175. Sheridan, C., et al., *CD44+/CD24- breast cancer cells exhibit enhanced invasive properties: an early step necessary for metastasis.* Breast Cancer Res, 2006. **8**(5): p. R59.
176. Schonberg, D.L., et al., *Preferential Iron Trafficking Characterizes Glioblastoma Stem-like Cells.* Cancer Cell, 2015. **28**(4): p. 441-55.
177. Mai, T.T., et al., *Salinomycin kills cancer stem cells by sequestering iron in lysosomes.* Nat Chem, 2017. **advance online publication**.
178. Place, A.E., S. Jin Huh, and K. Polyak, *The microenvironment in breast cancer progression: biology and implications for treatment.* Breast Cancer Res, 2011. **13**(6): p. 227.
179. Mao, Y., et al., *Stroma Cells in Tumor Microenvironment and Breast Cancer.* Cancer metastasis reviews, 2013. **32**(0): p. 303-315.
180. Bekri, S., et al., *Increased adipose tissue expression of hepcidin in severe obesity is independent from diabetes and NASH.* Gastroenterology, 2006. **131**(3): p. 788-96.
181. Alkhateeb, A.A., B. Han, and J.R. Connor, *Ferritin stimulates breast cancer cells through an iron-independent mechanism and is localized within tumor-associated macrophages.* Breast Cancer Res Treat, 2013. **137**(3): p. 733-44.

182. Dixon, S.J. and B.R. Stockwell, *The role of iron and reactive oxygen species in cell death.* Nat Chem Biol, 2014. **10**(1): p. 9-17.